# EFFECT OF AGED AND CONTAMINATED LUBRICANT ON WEAR PERFORMANCE OF ZDDP-CONTAINING LUBRICANT BY ARTIFICIAL AGEING WITH ETHANOL

KRITIN CHONVASIN

A THESIS REPORT SUBMITTED IN PARTIAL FULFILLMENT
OF THE REQUIREMENTS FOR THE DEGREE OF
MASTER OF ENGINEERING IN AUTOMOTIVE ENGINEERING
INTERNATIONAL COLLEGE
KING MONGKUT'S INSTITUTE OF TECHNOLOGY LADKRABANG
ACADEMIC YEAR 2018

KMITL-2018-IC-M-004-013

# EFFECT OF AGED AND CONTAMINATED LUBRICANT ON WEAR PERFORMANCE OF ZDDP-CONTAINING LUBRICANT BY ARTIFICIAL AGEING WITH ETHANOL

**KRITIN CHONVASIN**

**A THESIS REPORT SUBMITTED IN PARTIAL FULFILLMENT**
**OF THE REQUIREMENTS FOR THE DEGREE OF**
**MASTER OF ENGINEERING IN AUTOMOTIVE ENGINEERING**
**INTERNATIONAL COLLEGE**
**KING MONGKUT'S INSTITUTE OF TECHNOLOGY LADKRABANG**
**ACADEMIC YEAR 2018**
**KMITL-2018-IC-M-004-013**

| | |
|---|---|
| THESIS TITLE | **EFFECT OF AGED AND CONTAMINATED LUBRICANT ON WEAR PERFORMANCE OF ZDDP-CONTAINING LUBRICANT BY ARTIFICIAL AGEING WITH ETHANOL** |
| STUDENT NAME | Mr. Kritin Chonvasin |
| STUDENT ID | 58610002 |
| DEGREE | Master of Engineering |
| PROGRAME | Automotive Engineering |
| ADVISOR | Dr.Chi-na Benyajati |
| CO-ADVISOR | Asst.Prof.Dr.Preechar Karin |
| CO-ADVISOR | Prof.Katsunori Hanamura |

## ABSTRACT

Lubricant oils generally contain an anti-wear additive that would form into a protective film to protect the rubbed surfaces, resulting in wear reduction. However, the performance of such additive has been observed to be limited with a presence of contamination in the lubricant such as ethanol, or combustion products, etc. This research focused on the effect of ZDDP and aging of lubricant on a tribological performance especially wear. In this work, lubricated-sliding wear tests were conducted with different lubricant samples using a tribometer with a ball-on-disc configuration. The test model lubricants were comprised of base stock of Group II mineral base oil and synthetic, PAO6,and base stocks with addition of ZDDP. Furthermore, in order to take into account of real engine conditions, the model lubricants were artificially deteriorated by an oxidation process, i.e. ageing, prior to the wear tests. Apart from a normal ageing process with air, another group of test lubricant was also aged with ethanol to study the effect of leaked fuel on tribological performance of lubricants. The experimental results consisted of wear scar depth measurement on steel disc specimens from various test model lubricants. When operating temperature was increased, a better wear performance was observed with ZDDP-containing lubricants. In addition, aged lubricants were found to result in a better wear performance than non-aged lubricants. It could be attributed to all aged lubricants (with air and with air and ethanol) having an overall higher viscosity than those of non-aged lubricants. However, it was observed that there was an increase in wear depth for all aged ZDDP-containing lubricants at a higher operating temperature. This was in contrast with the results from the case of non-aged lubricants. It was proposed that there could a ZDDP depletion during the artificial aging process employed in this study.

**ACKNOWLEDGEMENT**

Without the contribution of many people, this thesis would not have been existed. It owes the existence to the supports and inspirations from a lot of people.

To my thesis advisor Dr.Chi-na Benyajati of National Metal and Material Technology Center (MTEC) and co-advisor Asst.Prof.Dr.Preechar Karinof International College at King Mongkut's Institute of Technology Ladkrabang, I would like to express my deepest gratitude for the encouragement and supervisionthrough all obstacles and challenges since the beginning until the end of my study.

I also want to express my gratitude to all lecturers for yoursupport and guidance to me for the whole two years. Also, I would like to thank all my friends who always be there to support and motivate me as always. Moreover, I also would love to express my gratitude to all respondents who contribute their information and time on this study. And I do believe the study could not been done without their input.

Finally, I must express my very greatest gratitude to my parents and all relatives for providing me with unfailing support and continuous motivation throughout my years of study. This accomplishment would not have been possible without them.

Kritin Chonvasin

## TABLE OF CONTENTS

## LIST OF TABLES

**Table** **Page**

## LIST OF FIGURES

**Figure** **Page**

## LIST OF SYMBOLS

| | |
|---|---|
| $R'$ | **THE REDUCED RADIUS OF CURVATURE** |
| $R_x$ | **THE REDUCED RADIUS OF CURVATURE IN THE X DIRECTION** |
| $R_y$ | **THE REDUCED RADIUS OF CURVATURE IN THE Y DIRECTION** |
| $R_{ax}$ | **THE REDUCED RADIUS OF CURVATURE OF BODY A IN THE X DIRECTION** |
| $R_{ay}$ | **THE REDUCED RADIUS OF CURVATUREOF BODY A IN THE Y DIRECTION** |
| $R_{bx}$ | **THE REDUCED RADIUS OF CURVATURE OF BODY B IN THE X DIRECTION** |
| $R_{by}$ | **THE REDUCED RADIUS OF CURVATURE OF BODY B IN THE Y DIRECTION** |
| $E'$ | **THE REDUCED YOUNG'S MODULUS** |
| $\nu_A$ | **THE POISSON'S RATIOS OF THE CONTACTING BODIES A** |
| $\nu_B$ | **THE POISSON'S RATIOS OF THE CONTACTING BODIES B** |
| $E_A$ | **THE YOUNG'S MODULUS OF THE CONTACTING BODIES A** |
| $E_B$ | **THE YOUNG'S MODULUS OF THE CONTACTING BODIES B** |
| $h_c$ | **THE CENTRAL FILM THICKNESS** |
| $h_0$ | **THE MINIMUM FILM THICKNESS** |
| $U$ | **THE ENTRAINING SURFACE VELOCITY** |
| $\eta_0$ | **THE VISCOSITY AT ATMOSPHERIC PRESSURE OF THE LUBRICANT** |
| $\alpha$ | **THE PRESSURE-VISCOSITY COEFFICIENT** |
| $W$ | **THE CONTACT LOAD** |
| $k$ | **THE ELLIPTICITY PARAMETER** |

$P_{max}$ **MAXIMUM HERTZIAN CONTACT PRESSURE**

P **APPLIED LOAD**

ω **SPINDLE SPEED**

r **THE CENTER DISTANCE BETWEEN A CENTER OF LOWER SPECIMEN HOLDER AND CENTER OF BALL HOLDER**

$V_L$ **WEAR VOLUME OF DISC SPECIMEN**

$M_L$ **MASS LOSS OF DISC SPECIMEN**

D **DENSITY OF DISC SPECIMEN**

## LIST OF DEFINITIONS

| | |
|---|---|
| ZDDP | **ZINC DIALKYLDITHIOPHOSPHATE** |
| PAO6 | **POLY-ALPHA-OLEFIN 6** |
| NSTDA | **NATIONAL SCIENCE AND TECHNOLOGY DEVELOPMENT AGENCY** |
| TISTR | **THAILAND INSTITUTE OF SCIENTIFIC ANDTECHNOLOGY RESEARCH** |
| TAN | **TOTAL ACID NUMBER** |
| FTIR | **FOURIER-TRANSFORM INFRARED SPECTROSCOPY** |
| EHL | **ELASTOHYDRODYNAMIC LUBRICATION** |
| PFPE | **POLY-FLUORINATED POLYETHER** |
| ASTM | **AMERICAN SOCIETY FOR TESTING AND MATERIALS** |
| SEM | **SCANNING ELECTRON MICROSCOPE** |
| OM | **OPTICAL MICROSCOPE** |
| AISI | **AMERICAN IRON AND STEEL INSTITUTE** |
| GC-MS | **GAS CHOMATOGRAPHY -MASS SPECTROMETRY** |
| ICP-OES | **INDUCTIVELY COUPLED-PLASMA OPTICAL EMISSION SPECTROMETRY** |
| XRF | **X-RAY FLUORESCENCE** |
| PAI | **PEAK AREA INCREASE** |
| COF | **COEFFICIENT OF FRICTION** |

# CHAPTER 1

# INTRODUCTION

## 1.1 Research Background

Nowadays, the general engine components there have several moving couple parts interactive against with each other, i.e. the couple of piston ring and cylinder liner, the couple of valve train and camshaft and the couple of connecting rod and crankshaft. While moving couple parts interactive against each other the heat is generated between contacts of two counter-parts hence the temperature inside their contact is raised resulted in the reduction of viscosity which would cause more severe lubrication condition with more asperities contact and can cause lubricating oil deficiency. Owing to more asperities contact condition, it could be attributed to can cause metal wear, i.e. abrasive wear; adhesive wear and fatigue wear presence inside or above the surface of the material. As the wear dilemma which mention earlier, the anti-wear additive is introduced. The most of ordinary engine oil used Zinc Dialkyldithiophosphate (ZDDP), as an anti-wear additive which is a protective film for the rubbed surfaces, resulting in wear and friction reduction. The greatest wear reduction occurs when a thermal film was formed by the friction of the surface in a ZDDP containing oil to generate tribofilm. Tribofilm is a protective film which was formed by spontaneous decomposition of the additive on a worn surface because of the only small amount of iron is found in the film [1]. ZDDP is formed by reaction of one or more alcohol with phosphorus-pentasulfide to give appropriate dialkyldithiophosphoric acid and then the acid was neutralized by the addition of zinc oxide to give the product of ZDDP [31]. Besides, ZDDP is effective to wear reduction

at moderate loads and temperatures nevertheless, for high loads and high temperatures application s of ZDDP might increase wear beyond that of base oil [29]. However, the performance of such additive has been observed to be limited with a presence of contamination in the lubricant such as ethanol. Ethanol is an alternative fuel for a gasoline engine. The effect of ethanol contaminates with lubricating oil have conducted in various researches. Costa and Spikes [38] have investigated the impact of ethanol on the formation of anti-wear tribofilms from engine lubricants. The result showed that ethanol reduced the rate of formation of the tribofilm very remarkably and the final thickness of tribofilm was less than ethanol-free lubricants. Moreover, ethanol can cause oxidation of lubricant, resulting in the formation of deposits and sludge [39]. Artificial ageing means applied severe conditions to the lubricating oil sample to expedite lubricant deterioration at a very short-term scale [32]. This thesis focused on the effect of ZDDP on tribological performance of lubricating oils, the effect of aged lubricant with oxidation, and additional ethanol on tribological performance of lubricating oils. In this thesis, lubricated-sliding wear tests were conducted with different lubricant samples using a tribometer with ball-on-disc configuration. The test model lubricants, Group II mineral base stock, PAO6, Group II mineral base stock and PAO6, added with 1.2% wt of ZDDP consecutively. Furthermore, in order to take into account the real engine conditions, the lubricant samples were artificially deteriorated by an oxidation process, i.e. ageing, prior to wearing test. Moreover, apart from a normal ageing process with air, another group of the test lubricants were also aged with ethanol to study the effect of leaked fuel contaminated with lubricant.

## 1.2 Research objectives

1.2.1 To investigate the effect of ZDDP on tribological performance of lubricants.

1.2.2 To investigate the ageing characteristic of lubricants by an artificial alteration in the laboratory with oxidation, and the addition of ethanol.

1.2.3 To study the effect of aged lubricants on the tribological performance of lubricants.

## 1.3 Scope of works

1.3.1 Group II base stock and PAO6 base stock were mixed with ZDDP at the constant composition of 1.2 % by weight per weight to investigate the effect of ZDDP. Another group of lubricants are not mixed with ZDDP

1.3.2 Before the tribological test, all the disc specimens were polished to archive surface roughness about 0.003-0.004 micron and surface like mirror.

1.3.3 All of the tribological tests were performed on tribometer with ball-on-disc configuration.

## 1.4 Thesis outlines

The research methodology this thesis are divided into 6 chapters following:

Chapter 1 will be describing a research background, research objectives, scope of works and expectedresults.

Chapter 2 illustrates a fundamental of lubrication, lubricants and their additives, and the oxidation of lubricants.

Chapter3 discusses the experimental apparatuses and experimental approaches.

Chapter 4 discusses the results of NSTDA tribology experiment.

Chapter 5 discusses the results of ageing characteristic and results of TISTR tribology experiment.

Chapter 6 concludes the results and suggests.

## 1.5 Expected results

1.5.1 Wear performance of ZDDP-containing lubricants will be better than the lubricants without ZDDP.

1.5.2 Four efficient bulk properties of test lubricant i.e. viscosity, Total Acid Number (TAN) and oxidation value (FTIR) will be increased when ageing with oxidation and addition of ethanol. Besides, the sludge will occur after aged with ZDDP-containing lubricants.

1.5.3 Aged lubricants will give a lower wear performance than non-aged lubricants.

1.5.4 Sludge formation form aged lubricants will scuff or rub on metal surfaces which leads to more wear than non-aged lubricants.

# CHAPTER 2

# LITERATURE REVIEW

## 2.1Fundamental of lubrication

### 2.1.1 Introduction

The lubricant is a substance was introduced between two moving surfaces to reduce friction, minimize wear, distribute heat, remove contaminants and improve efficiency. In addition, a lubricant is formed a protective fluid film that keeps both rubbing surfaces separated, resulting in wear reduction.

### 2.1.2 Lubrication regime

2.1.2.1 Boundary lubrication

Boundary lubrication occurs when one of the essential factors that influence full-fluid film formation between contacting surfaces are deficient. In addition, boundary lubrication is the lubrication regime with the most asperity contact between the surfaces occurring due to the presence of a thin fluid film.

2.1.2.1.1 Low temperature-low load lubrication mechanisms

At low speed, a thin layer of liquid with an anomalously high viscosity can form on the contacting surface. Furthermore, linear molecules of hydrocarbon align themselves normally to the contacting surfaces to form a lubricating, protective layer as shown in Figure 1. Beside the molecules are polar the opposite ends are attracted to form pairs of molecules which are subsequently incorporated into a viscous surface layer [1].

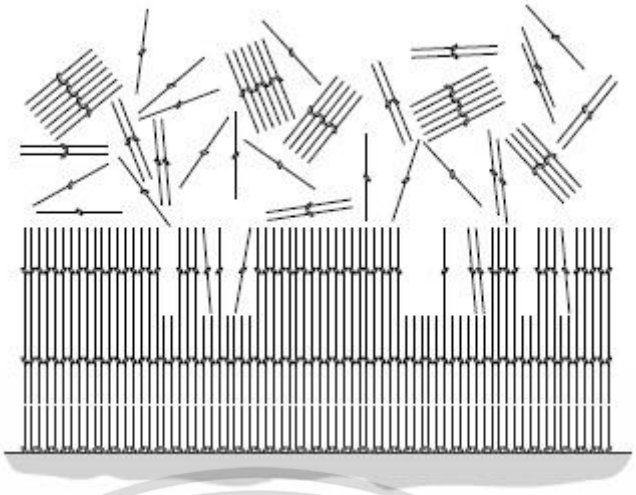

**Figure 1.**Low temperature, low load mechanism of lubrication [1].

2.1.2.1.2 Low temperature-high load lubrication mechanisms

It is generally known as "adsorption lubrication". In addition, adsorption on the metallic surface of organic polar molecules produces low friction, mono-molecular layer on the surface as shown in Figure 2. Beside The polarity of the adsorbate is essential to the lubrication mechanism. Polarity means that a molecule is asymmetrical with a different chemical affinity at either end of the molecule. For example, one end of a molecule which is the carboxyl group of a fatty acid, -COOH is strongly attracted to the metallic surface while the other end which is an alkyl group, -CH3 is repellant to almost any other substance. Adsorption can divide into two basic categories: "physisorption" and "chemisorption". Physisorption or physical adsorption is a classical form of adsorption. Molecules of adsorbate may attach or detach from a surface without irreversible changes to the surface or the adsorbate. In physisorption, van der Waals or dispersion forces provide the bonding between substrate and adsorbate as illustrated in Figure 3 [1]. Chemisorption or chemical adsorption is an irreversible form of adsorption which involves some degree of chemical bonding between adsorbate and substrate as illustrated in Figure 4. There was a major finding of adsorption lubrication [2]; the more polar an additive the better

the lubrication and higher molecular weight compounds have better durability and frictional behaviour.

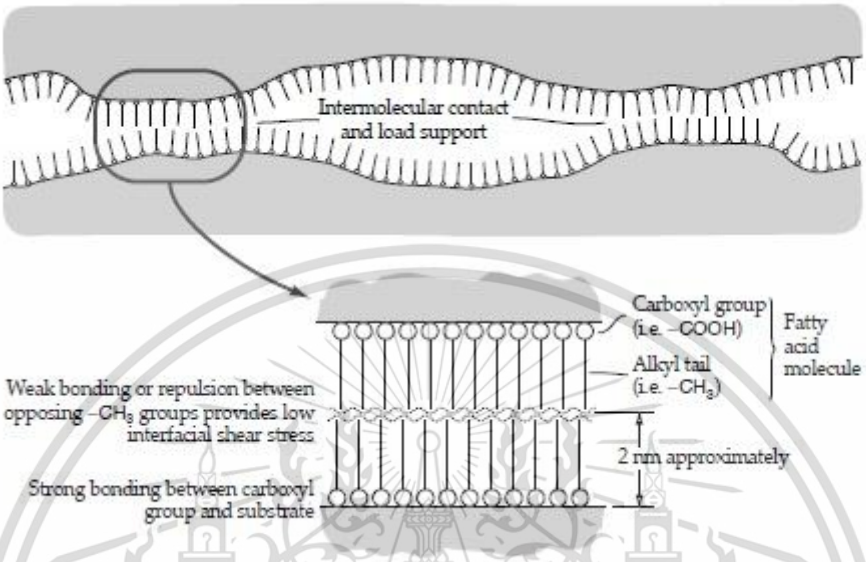


**Figure 2.** Low friction mono-molecular layer of adsorbed organic polar molecules on metallic surfaces [1].

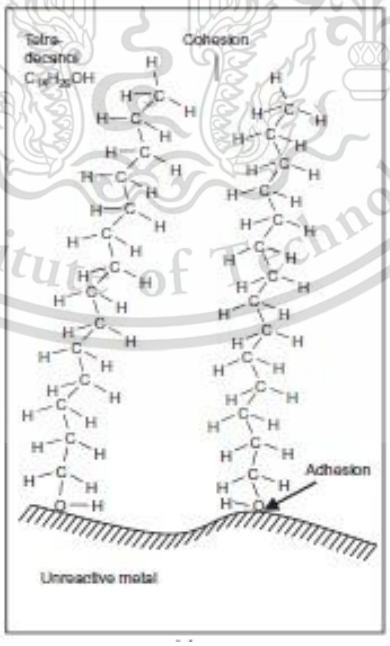


**Figure 3.**Schematic illustration of physisorption [2].

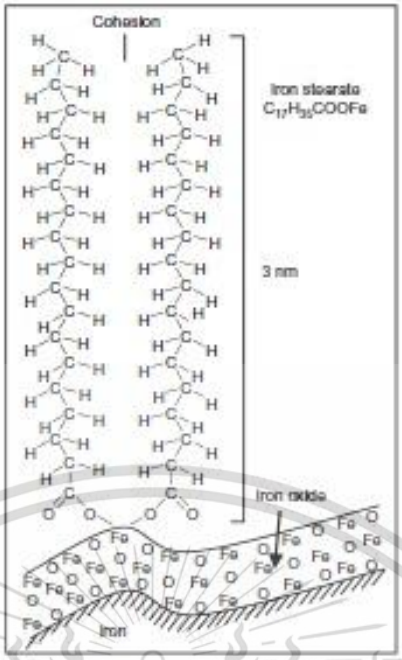


**Figure 4.**Mechanism of chemisorption [2].

2.1.2.1.3 High temperature-medium load lubrication mechanisms

Two basic mechanisms were involved in high-temperature lubrication at medium loads comprise of chain matching and formation of thick films of soapy or amorphous material. Chain matching is an improvement of lubricant properties which occurs when the chain lengths of the solute fatty acid and the solvent hydrocarbon are equal. Furthermore, chain matching occurs, a thin layer with an ordered structure forms on the metallic surface. If the chain length does not match or equal, then the coherent surface structure cannot form, and the properties of the surface liquid remain like those of the disordered state of bulk fluid as shown in Figure 5. Soap layers are formed by the reaction between a metal hydroxide and a fatty acid which results in soap plus water. Moreover, soap formation promoted by the heat and mechanical agitation of sliding contact. The formation of the soap layer on steel surface is shown in Figure 6. Amorphous layers, phosphate-containing iron and zinc in steel sliding contact when ZDDP was used as an anti-wear additive, are the process of sliding involves grinding which can reduce the thickness of any interposed

object; a crystal lattice can be dismantled into an amorphous assembly of atom and molecules. The process of amorphization of interposed material can be illustrated by a bubble raft analogue of a crystal lattice. An example of a bubble raft model of a sliding interface is shown in Figure 7 [1], each bubble represents an atom and when closely packed, the bubble assembly to a crystal lattice.

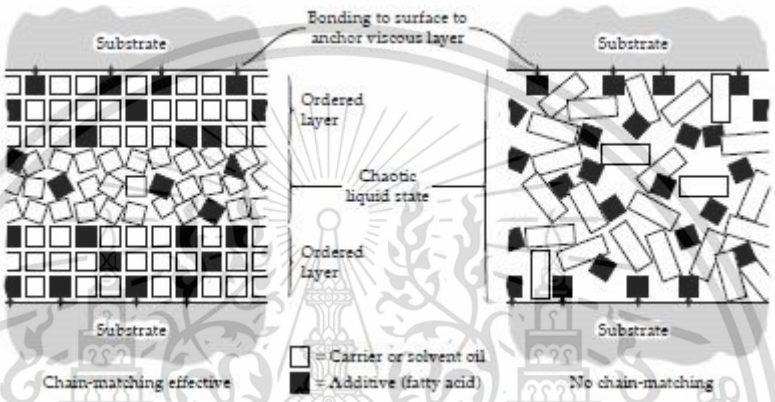


**Figure 5.** Model of chain matching [1].

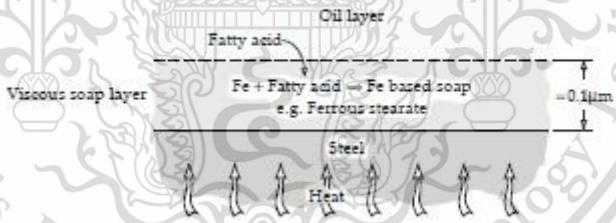


**Figure 6.** Formation of a viscous soap layer on steel by a reaction between iron and a fatty acid in lubricating oil [1].

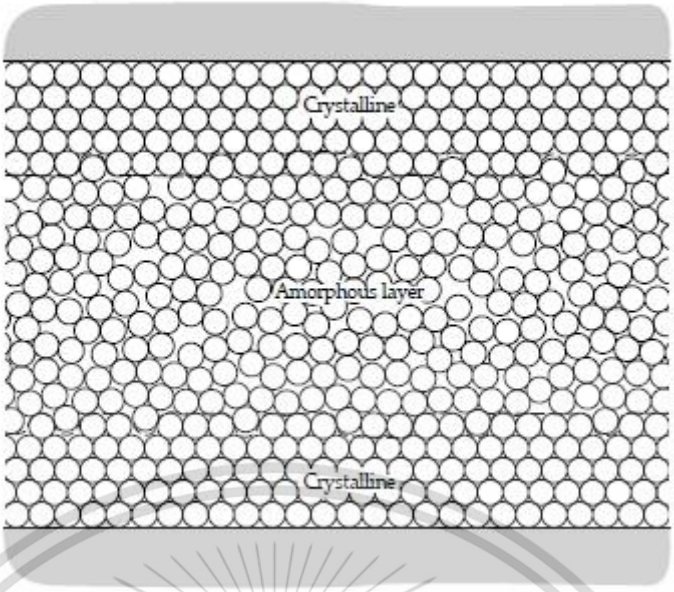


**Figure 7.**Bubble raft analogy of crystal/amorphous structure of the material separating sliding surfaces [1].

2.1.2.1.4 High temperature-high load lubrication mechanisms

It generally is known as lubrication by sacrificial reaction film or "Extreme Pressure lubrication" this mechanism takes place in lubricated contacts in which loads and speeds are high enough to result in high transient friction temperature.When transient friction temperature is high, sufficient to cause desorption of available adsorption lubricants. When desorption of adsorbed lubricants occurs, another lubricant mechanism based on the sacrificial film is usually the most effective mean available of preventing seizure or scuffing. The model of lubrication by sacrificial film between two surfaces is illustrated in Figure 8 [1].

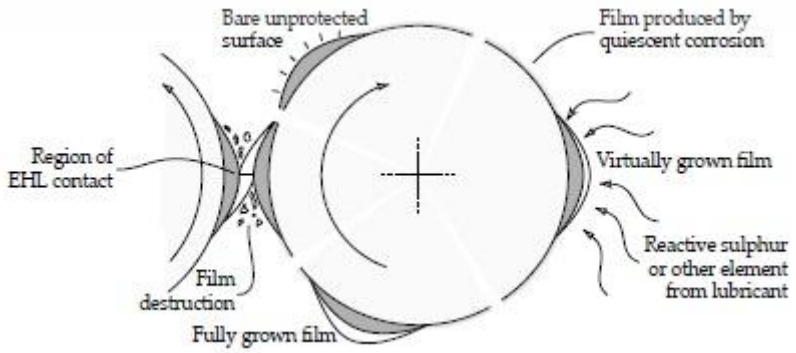

**Figure 8.** Model of lubricant by sacrificial film [1].

2.1.2.1.5 Scuffing phenomena and modeling

Scuffing is gross damage characterized by the formation of local welds between surfaces. In addition, scuffing occurs when the temperature in the contact reaches a critical value independent of sliding speed, load and bulk lubricant temperature. Furthermore, scuffing depends on roughening of surfaces by plastic flow with or without material transfer [3]. The EHL-based model of scuffing by Lee and Cheng [4] in Figure 9 based on the collapse of EHL film when a critical temperature at the inlet of the contact reached the viscosity suddenly fall causing EHL film to collapse promoting scuffing. Moreover, the effect of micro-EHL film occurring between contacting asperities resulting in keep the asperities separated. Besides the thickness of micro-EHL film depend on the viscosity enhancement by the surrounding EHL film. Desorption model by Lee and Cheng [5] in Figure 10 based on the rate of removal of adsorbed molecules is related to the temperature of the asperity, the higher temperature the more likely the molecule will detach itself from the surface due to thermal excitation. The heat of adsorption and the transition temperature to the concentration of the molecules adsorbed onto the surface (θ). Moreover, a range of EHL conditions that the critical scuffing temperature in the contact increases due to higher contact pressures generated in the EHL region. Asperity interaction model in Figure 11 by Ludema [6] based on the initial plastic flow of an asperity caused by normal and frictional stresses transmitted through both viscous and adsorbed film. Repeated cyclic plastic deformation of asperities causes them to break away by plastic fatigue. The particles formed an agglomerate, work harden and carry much of contact load resulting in larger contact stresses causes an increase in temperature, resulting in localized film failure and eventual scuffing. A new scuffing model [7] in Figure 12

based on the failure of the EHL and micro-EHL films by chemical degradation of the entrained lubricant which has been catalyzed by the surrounding surfaces [7].

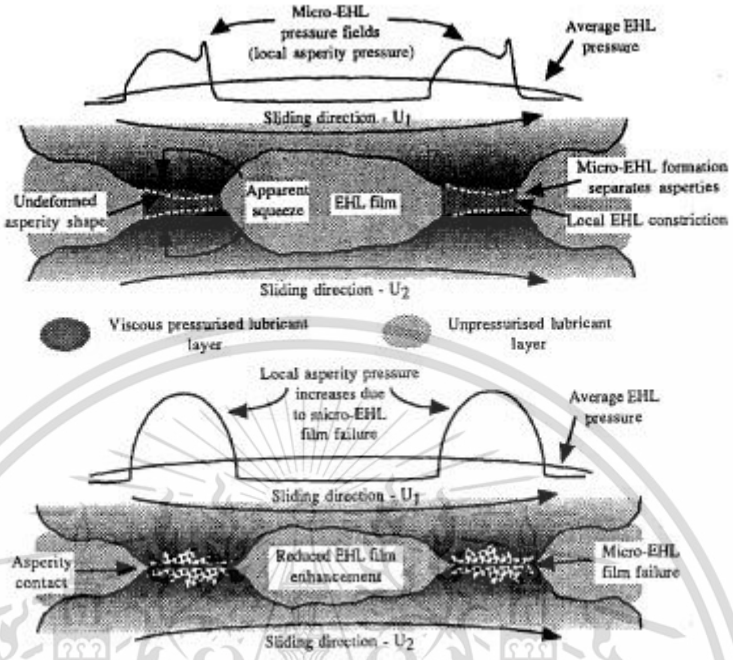


**Figure 9.** Scuffing model by Lee and Cheng. Lubricant viscosity enhancement by EHL films is requiring for micro-EHL films to provide protection film [4].

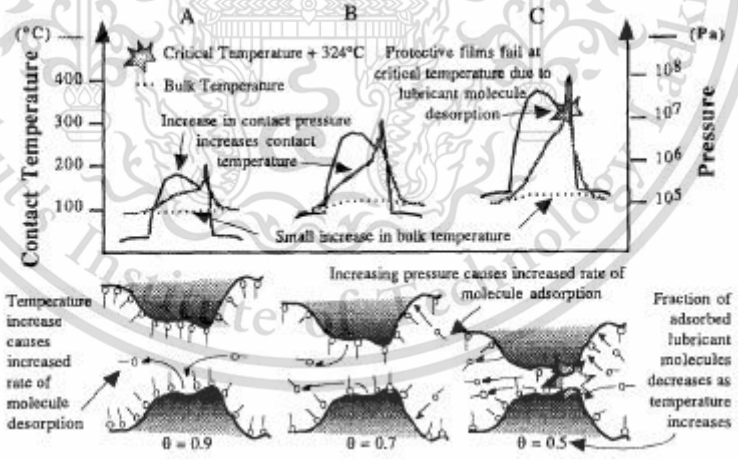


**Figure 10.** Critical lubricant temperature criterion (A) Low temperature and pressures (B) temperature and pressures increases (C) at the critical temperature [5].

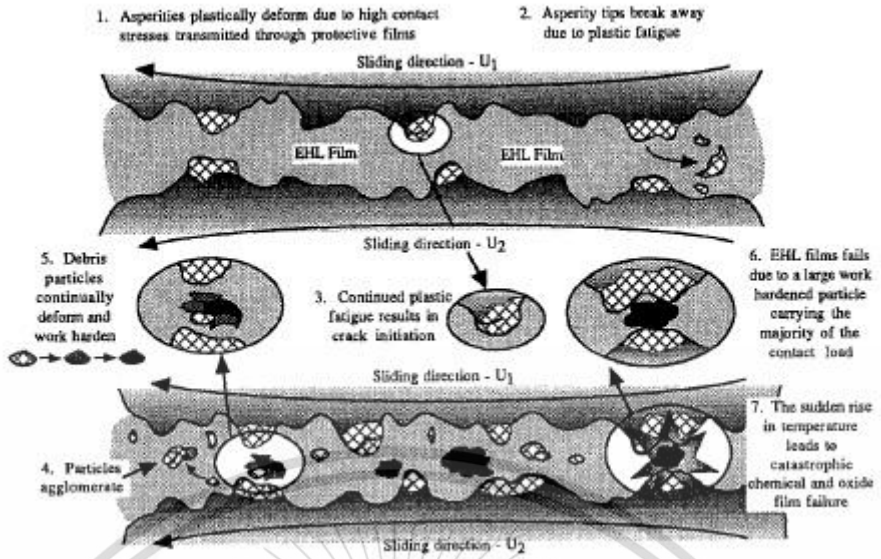


**Figure 11.** Asperity interaction model proposed by Ludema [6].

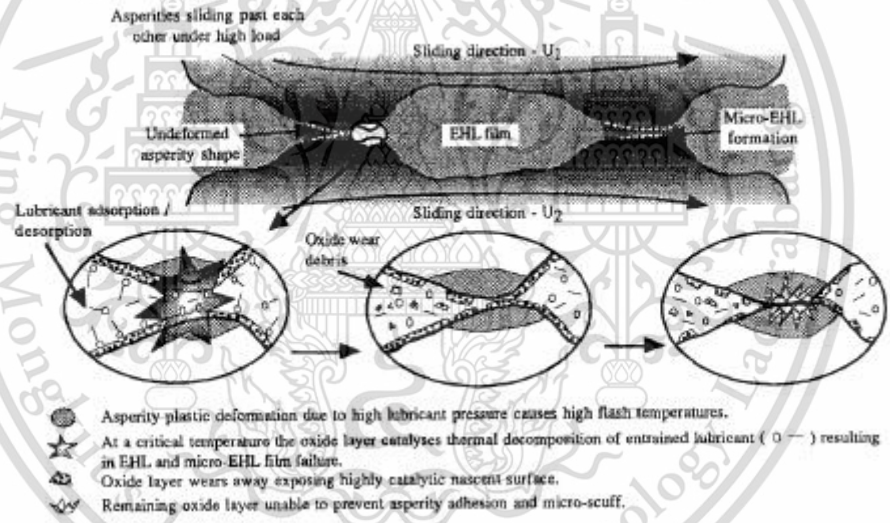


**Figure 12.** Scuffing model based on EHL and micro-EHL film by chemical degradation of the entrained lubricant [7].

2.1.2.2 Mixed lubrication

In this lubrication regime, the surface is transitioning away from boundary lubrication into hydrodynamic lubrication there may be frequent asperity contacts, but at least a portion of the bearing surface remains supported partially by a hydrodynamic film. Model of mixed lubrication mechanism is shown in Figure 13 [1].

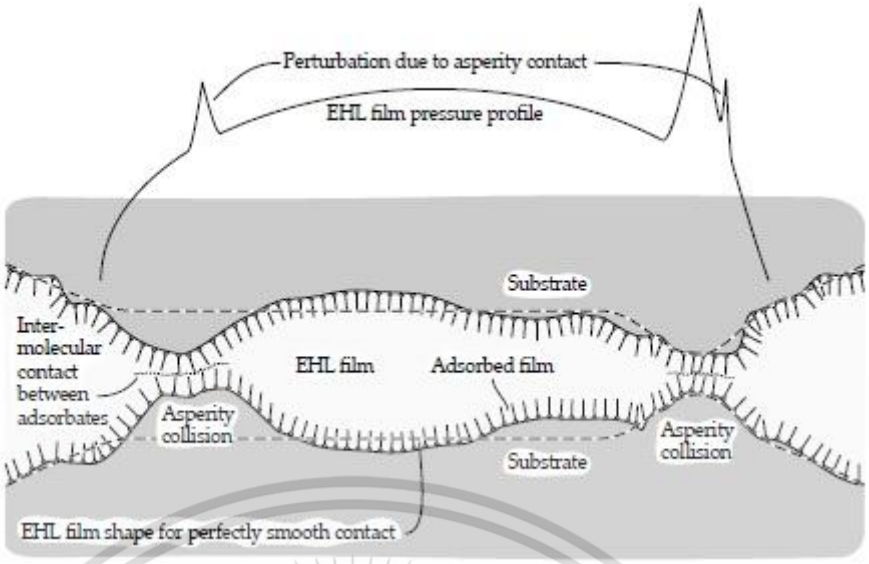


**Figure 13.** Model of mixed lubrication [1].

2.1.2.3 Elastohydrodynamic lubrication

Elastohydrodynamic lubrication can be defined as a form of hydrodynamic lubrication in which the elastic deformations, elastic deformation is shown in Figure 14, of the contacting solids and the change of viscosity with pressure plays a significant role in hydrodynamic lubrication process. In addition, an elastohydrodynamic lubricating film which separates the opposing surfaces of a concentrated contact, resulting in a significant reduction of wear and friction. In this study the contact between two surfaces can be represented by two spheres is enveloped by a circle as shown in Figure 15. The contact parameter for this configuration can calculate according to the formulae as (2.1) [1].

$$\frac{1}{R'} = \frac{1}{R_x} = \frac{1}{R_y} = \frac{1}{R_{ax}} + \frac{1}{R_{bx}} + \frac{1}{R_{ay}} + \frac{1}{R_{by}} \quad (2.1)$$

Where:

$$\frac{1}{R_x} = \frac{1}{R_{ax}} + \frac{1}{R_{bx}}$$

$$\frac{1}{R_y} = \frac{1}{R_{ay}} + \frac{1}{R_{by}}$$

$R_x$ is the reduced radius of curvature in the x direction [m].

$R_y$ is the reduced radius of curvature in the y direction [m].

$R_{ax}$ is the reduced radius of curvature of body A in the x direction [m].

$R_{ay}$ is the reduced radius of curvature of body A in the y direction [m].

$R_{bx}$ is the reduced radius of curvature of body B in the x direction [m].

$R_{by}$ is the reduced radius of curvature of body B in the y direction [m].

The radii of curvature of the sphere are symmetry applies so that $R_{ax} = R_{ay} = R_A$ and $R_{bx} = R_{by} = R_B$. The reduced radius of curvature according to (2.1) is therefore given by

$$\frac{1}{R_x} = \frac{1}{R_y} = \frac{1}{R_A} + \frac{1}{R_B} \quad (2.2)$$

The reduced Young's modulus is defined as:

$$\frac{1}{E'} = \frac{1}{2}\left(\frac{1-\nu_A{}^2}{E_A} + \frac{1-\nu_B{}^2}{E_B}\right) \quad (2.3)$$

Where:

$\nu_A$ and $\nu_B$ are the Poisson's ratios of the contacting bodies A and B respectively.

$E_A$ and $E_B$ are the Young's modulus of the contacting bodies A and B respectively [Pa].

The exact analysis of elastohydrodynamic lubrication by Hamrock and Dowson [9] provided the most important information about EHL. The results of this analysis are the formulae for the calculation of the central and minimum film thickness in EHL contacts, as shown in Figure 16, are in the following form (2.4) and

(2.5). Furthermore, these formulae derived by Hamrock and Dowson apply to any contact and can be used with many materials.

$$\frac{h_c}{R'} = 2.69\left(\frac{U\eta_0}{E'R'}\right)^{0.67}(\alpha E')^{0.53}\left(\frac{W}{E'R'^2}\right)^{-0.067}(1 - 0.61e^{-0.73k}) \quad (2.4)$$

$$\frac{h_0}{R'} = 3.63\left(\frac{U\eta_0}{E'R'}\right)^{0.68}(\alpha E')^{0.49}\left(\frac{W}{E'R'^2}\right)^{-0.073}(1 - e^{-0.68k}) \quad (2.5)$$

Where:

$h_c$ is the central film thickness [m].

$h_0$ is the minimum film thickness [m].

U is the entraining surface velocity [m/s], i.e. $U = \frac{U_A + U_B}{2}$, where the subscripts A and B refer to the velocities of bodies A and B respectively.

$\eta_0$ is the viscosity at atmospheric pressure of the lubricant [Pas].

$E'$ is the reduced Young's modulus [Pa].

$R'$ is the reduced radius of curvature [m].

$\alpha$ is the pressure-viscosity coefficient [$m^2/N$].

W is the contact load [N].

k is the ellipticity parameter defined as; $k = \frac{a}{b}$ where a is the semi-axis of the contact ellipse in the transverse direction [m] and b is semi-axis in the direction of motion [m].

The approximate value of the ellipticity parameter can be calculated with sufficient accuracy formulae:

$$k^{-} = 1.0339\left(\frac{R_y}{R_x}\right)^{0.636}$$

Where:

$R_x$ and $R_y$ are the reduced radii of curvature in the x and y directions respectively.

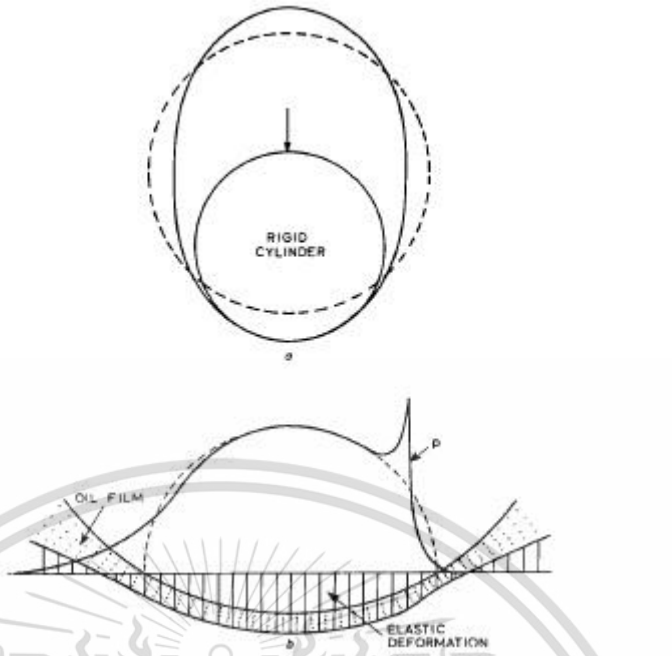


**Figure 14.** Elastic deformations [8].

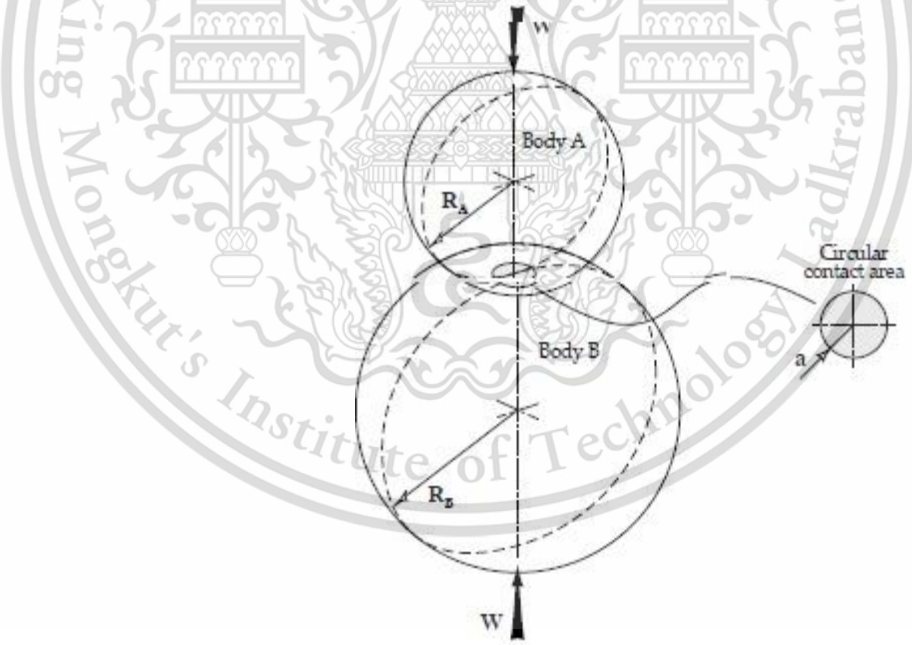


**Figure 15.** Contact between two spheres [1].

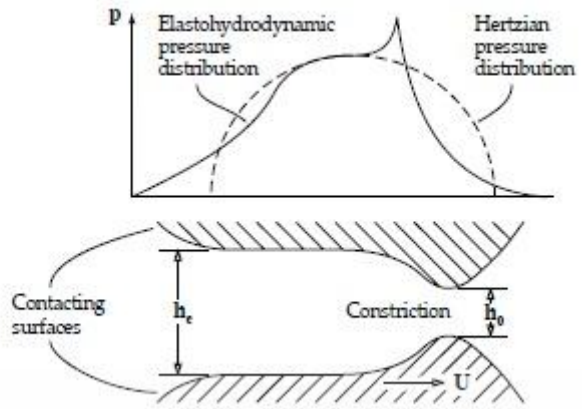


**Figure 16.** Hydrodynamic pressure distributions in an EHL contact; $h_c$ is the central film thickness, $h_o$ is the minimum film thickness [1].

## 2.2 Wear

### 2.2.1 Abrasive wear

Abrasive wear is the loss of material by the passage of hard particles over a surface, which occurs whenever some solid objects, is loaded against particles of a material that have equal or greater hardness. Hard particles may remove material by micro-cutting, micro-fracture, pull-out of individual grain or fatigue by repeated deformations as Figure 17. Abrasive wear comprises two modes: two-body and three-body abrasive wear. Two-body abrasive wear illustrated as the action of sandpaper on the surface, hard asperities pass over the surface like cutting tool [1]. When abrasive grain moves across the metallic surface: the formation plastically deformed grooves and the removal of material in the form of microchips [10]. Besides, angular abrasive particles have been found to produce more wear than spherical particles and the sharp angular particles produce more chips; nevertheless, the spherical particles lead to more plastic deformation [11]. Furthermore, the critical abrasive particles size is a function of the adhesive wear particles size of the material being worn away, if the abrasive particles are smaller than adhesive wear particles then the formation of

adhesive particles prevents the abrasive particles to abrade the surface of material resulting in very little abrasive action [12, 13]. In three-body abrasive wear, the asperities are free to roll as well as a slide over the surface. Three-body abrasive wear can divide into two categories: open and close three-body abrasive wear. Open three-body abrasive wear occurs when two surfaces are far apart or when only one surface is involved in the wear process. Moreover, open three-body abrasive wear can classify into three situations: gouging abrasion, high-stress or grinding abrasion and low-stress or scratching abrasion. Gouging occurs when rocks or other course abrasive particles cut into a surface to remove a relatively large amount of material. High-stress, the objective is to crush abrasive particles, the abrasive particles fracture during the wear process. Low-stress, the abrasive particles do not fracture during the wear process [15]. Close three-body abrasive wear occurs when the abrading particles are trapped between two surfaces which close to each other, the particles may have embedded in one of the surfaces and cause wear on the opposing surface [14]. The mechanism of two-body and three-body abrasive wear is shown in figure 18. The exact analysis of elastohydrodynamic lubrication by Hamrock and Dowson [9] provided the most important information about EHL. The results of this analysis are the formulae for the calculation of the central and minimum film thickness in EHL contacts, as shown in Figure 16, are in the following form (2.4) and (2.5). Furthermore, these formulae derived by Hamrock and Dowson apply to any contact and can be used with many materials.


a) Cutting b) Fracture


c) Fatigue d) Grain pull-out

**Figure 17.** Mechanism of abrasive wear: a) Cutting b) Fracture c) Fatigue and d) Grain pull-out [1].

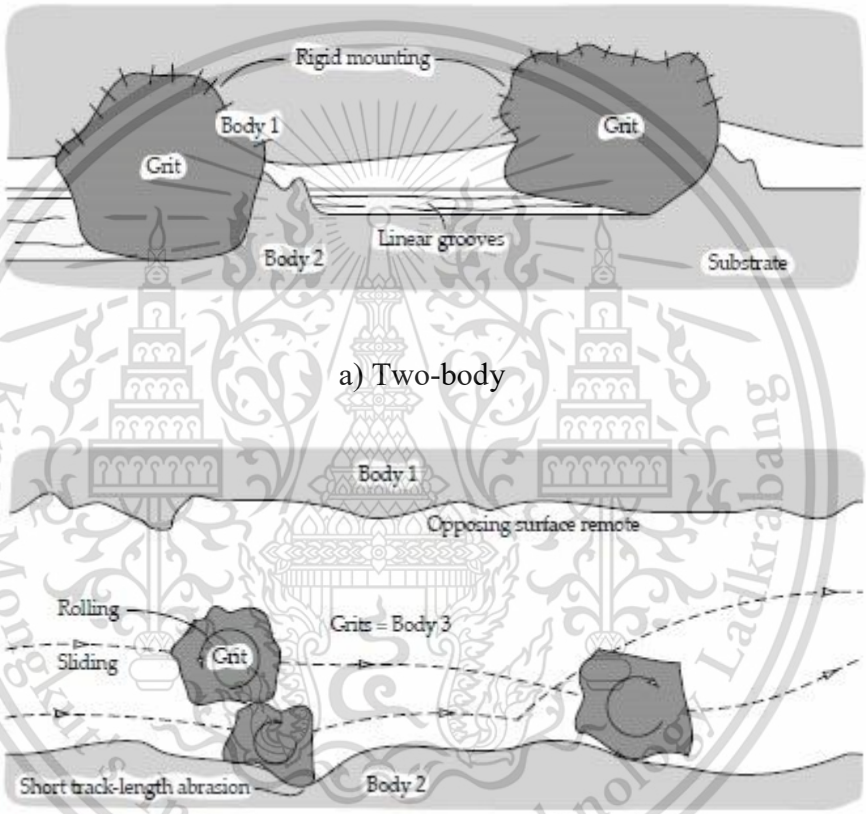


a) Two-body

b) Three-body

**Figure 18.** Mechanism of abrasive wear: a) Two-body and b) Three-body [1].

### 2.2.2 Adhesive wear

Adhesive wear is a very serious form of wear characterized by high wear rates and a large unstable friction coefficient. Adhesive wear causes lubricant breakdown, sliding surfaces are not separated, resulting in wear occurs. When strong material adheres on contact with another material, weak material, weak material will transfer

to strong material by strong adhesion force as shown in Figure 19. Strong adhesion can describe by electron transfer between contacting surfaces, a free electron in material and on contact may be exchanged between two materials to form bonding, the material with a higher electron density donates an electron to the other material as shown in Figure 20 [1]. Sharper asperity, large slope angle, tends to lose material to asperity more than small slope angles [16]. Brittle materials trend to break away with little deformation and produce fewer wear particles when compared to ductile materials [17]. A ductile material which does not produce wear particles, there may still be extensive plastic deformation as shown in Figure 21 [18].

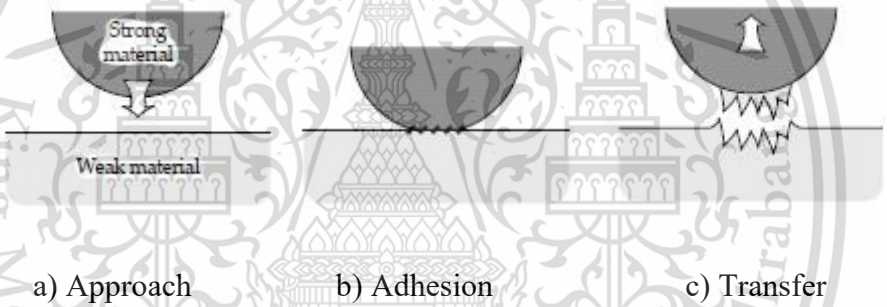


a) Approach b) Adhesion c) Transfer

**Figure 19.** Process of material transfer due to adhesion [1].


**Figure 20.** Electron transfer model in adhesive contact between materials [1].

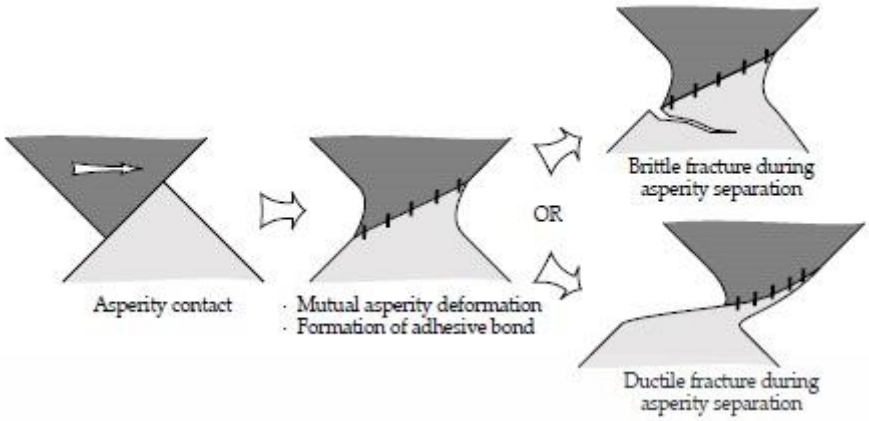


**Figure 21.** Alternative model of deformation in adhesive asperity contact [17].

### 2.2.3 Fatigue wear

Fatigue wear occurs when repeated much time during sliding or rolling of very high local stresses, wear under this condition is determined by the mechanics of crack initiation, crack growth and fracture. The mechanisms of surface crack-initiated fatigue wear as shown in Figure 22. A primary crack originates at the surface at some weak point and propagates downward along a weak plane. A secondary crack can develop from primary crack and connect with an existing subsurface crack when secondary crack reaches the surface a wear particle is released [19]. Most material contains imperfection which acts as nuclei for void formation under plastic deformation, these voids accelerate initiation for crack growth as shown in Figure 23, the rate of voids formation may be increased when hard particles present in metal and crack formation around hard particles is likely to be one of the most important mechanisms of void formation. These voids enlarge with increased deformation since they act as a trap for dislocations; dislocation density builds up at the subsurface layer. Furthermore, these enlarge void will combine to form longer crack parallel to the deformation direction [21]. At some unspecified point the crack finally turns upwards to the surface and wear debris is released, the name of this theory is the

delamination theory of wear [20]. When the material is brittle, delaminate sheets may break into pieces and form many small wear particles. On the contrary, the delaminations of ductile material may

the same or form large particles.

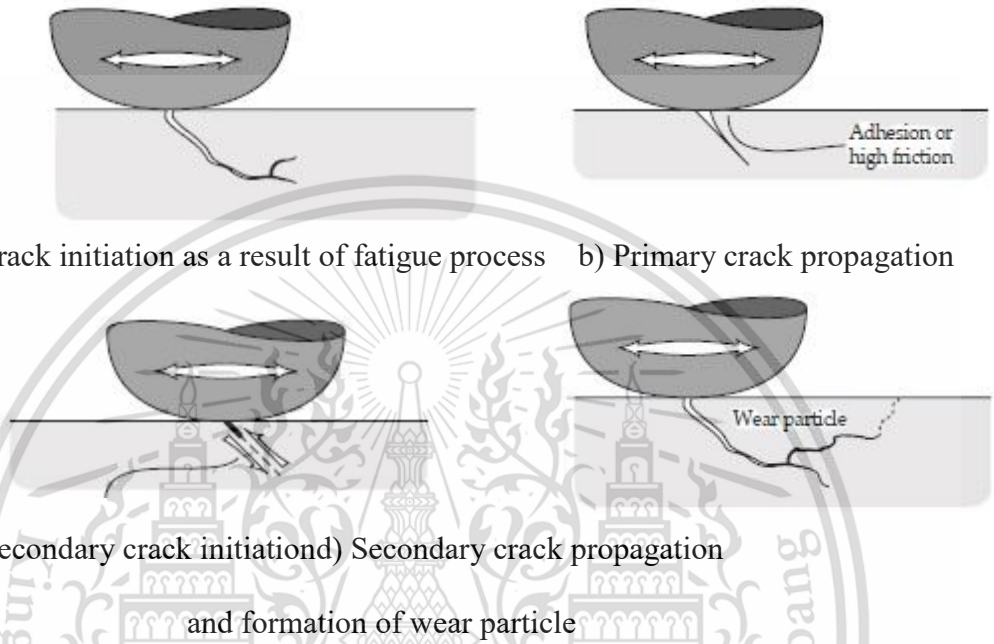


a) Crack initiation as a result of fatigue process b) Primary crack propagation

c) Secondary crack initiationd) Secondary crack propagation

and formation of wear particle

**Figure 22.** Schematic of the process of surface crack initiation and propagation [1].

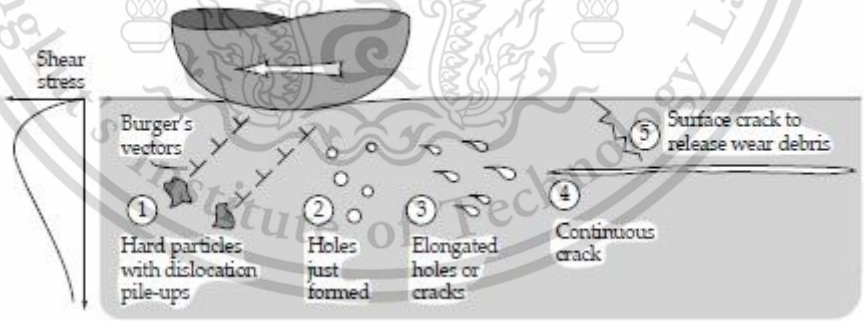


**Figure 23.** Process of subsurface crack formation by growth and link up of voids [1].

### 2.2.4 Fretting wear

Fretting wear occurs when very small amplitude of reciprocating sliding between contacting surfaces is sustained for many cycles; it generates surface micro-cracks by asperity contact. The mechanism of surface micro-cracks initiate in fretting

contacts is shown in Figure 24, the number of surface micro-cracks increases with increased amplitude [22]. Besides, the wear debris produced are often retained within the contact due to small amplitude of sliding, the accumulating wear debris generally separates both surfaces and, in some case, may accelerate the wear process by abrasion [1]. Moreover, Crack initiation in fretting fatigue is controlled by alternating high stress on the contact surface which promote by combining tangential force along the contact surface and bulk alternating stress. The kind of crack path is shown in Figure 25. Stage 0 or the crack initiation stage with slip bands and crystallographic propagation, stage I or shear mode is predominant in the propagation of an oblique crack. The cracks propagate away from the area of initiate stage 0 by the stage II mode or tensile mode. A dominant factor for accelerate crack growth may be stress intensity due to tangential stress, short-crack and mixed-mode, the mixture of stage I and stage II, crack growth behaviors [23].

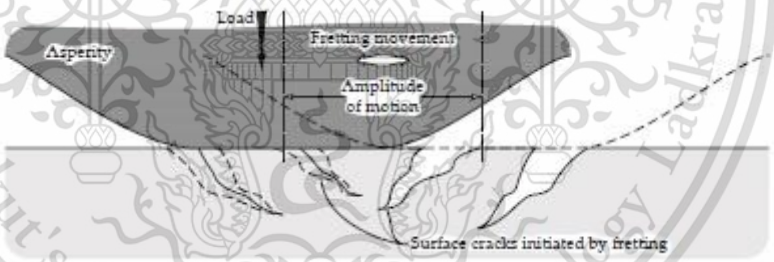


**Figure 24.** Mechanism of surface micro-cracks initiation in fretting contacts [22].

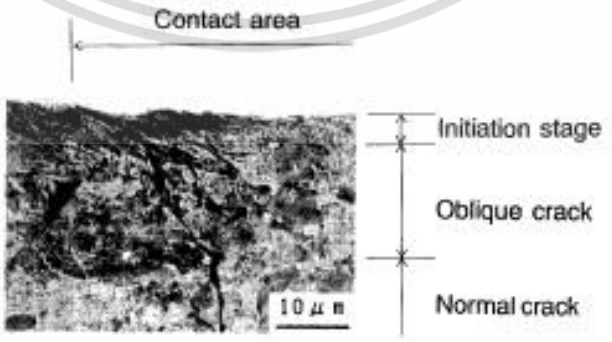


**Figure 25.** an example of typical of fretting fatigue crack path [23].

## 2.3Lubricants

### 2.3.1 Lubricant base stocks

Typical lubricating oil is composed of 95 % base stock and 5 % additives. There is three source of base stock: biological, mineral and synthetic. Besides, base oil can divide into 5 Group: Group I mineral base stock, produced by solvent extraction processes and catalytic hydrogenation, contains less than 90 % saturated hydrocarbon and greater than 0.03 % sulfur and have a viscosity index greater than or equal to 80 and less than 120. Group II mineral base stock, produced by partially hydro-cracking, contains greater than or equal to 90 % hydrogenated saturated hydrocarbons and less than or equal to 0.03 % sulfur and have a viscosity index greater than or equal to 80 and less than 120. Group III mineral base stock, produced by catalytic procedures with a concurrent rearrangement of the carbon backbone during hydrogenation, contains greater than or equal to 90 % saturated hydrocarbon and have a viscosity index greater than or equal to 120. Group IV synthetic base stock, Poly-α-Olefins, produced by catalytic polymerization of low molecular weight end terminated olefins, contains approximately 0 % sulfur and have a viscosity index greater than or equal to 140 and less than 170. Group V synthetic base stock all other oils e.g. ester, poly-glycols and phosphate esters [24-25].

2.3.1.1 Mineral base stock

Mineral oils are the most commonly used lubricants, which manufactured from crude oil. The structure of mineral oil is very complex, the major part of mineral oils comprises of hydrocarbons with approximately 30 carbon atoms in each molecule. The structure of each molecule consists of several aliphatic means straight chains and cyclic carbon chains bonded together. Besides, the mineral oils are also impure, the

impure nature of mineral oils result in a range of useful and harmful properties, e.g. trace compounds provide anti-oxidants and boundary lubrication properties nevertheless, they also cause deposits which can hinder lubrication. The fundamental differences between mineral oils are based on chemical forms, basic chemical forms of mineral oil: paraffinic, naphthenic and aromatic, sulfur content and viscosity [1]. Types of mineral oils are shown in Figure 26 paraffinic means straight chain hydrocarbons containing 15-30 carbon atoms, naphthenic indicates 5- or 6- member cyclic carbon molecules with no unsaturated bond with attached side chains up to 20 carbon atoms long and aromatic oils contain one or more benzene rings with saturated side chains [26]. Moreover, oils are distinguished base on the relative proportion of paraffinic, naphthenic and aromatic component present. A small amount of sulfur in the oil is desirable to give good lubrication and oxidation properties. On contrary, too much sulfur is injurious to the performance of machinery [1].

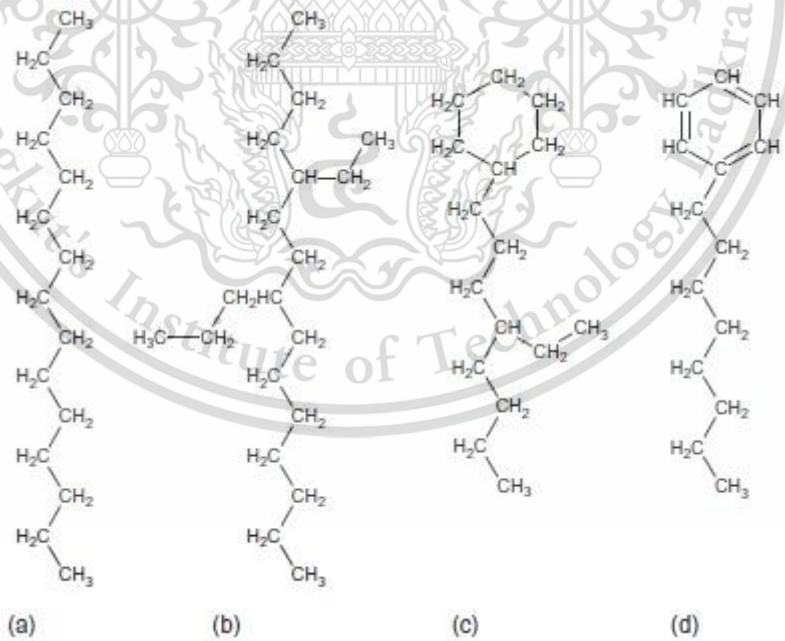


**Figure 26.** Type of mineral oils; a) straight paraffin, b) branched paraffin, c) naphthenic and d) aromatic [26].

2.3.1.2Synthetic base stock

Synthetic lubricants can ordinarily be divided into two groups: fluids intended to provide superior lubrication at ambient or elevated temperature and lubricants for extremes of temperature or chemical attack. In addition, there are three basic types of synthetic lubricant presently in use: synthetic hydrocarbon lubricants, silicon analogues of hydrocarbons and organo-halogens. Chemical structures of the most common synthetic lubricants are shown in Figure 27.

2.3.1.2.1Poly-α –olefins

Poly-α –olefins (PAO) are the most promising general-purpose synthetic lubricants. Olefins or alkenes are unsaturated hydrocarbons with general formula $(-CH2-)_n$ , they consist of a straight chain with unsaturated carbon at one end of the chain, the prefer alkenes is Dec-1-ene [1]. Polymerization and hydrogenation of Dec-1-ene lead to PAO, as a highly branched and fully saturated hydrocarbon as shown in Figure 28 [24].

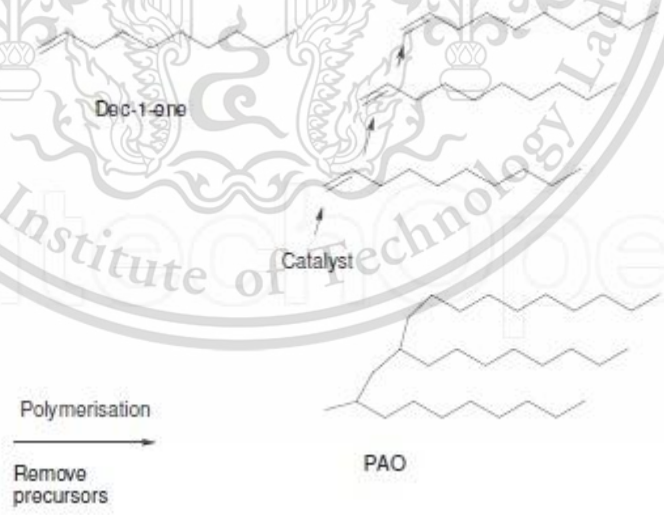


**Figure 27.** Principle of PAO formation [24].

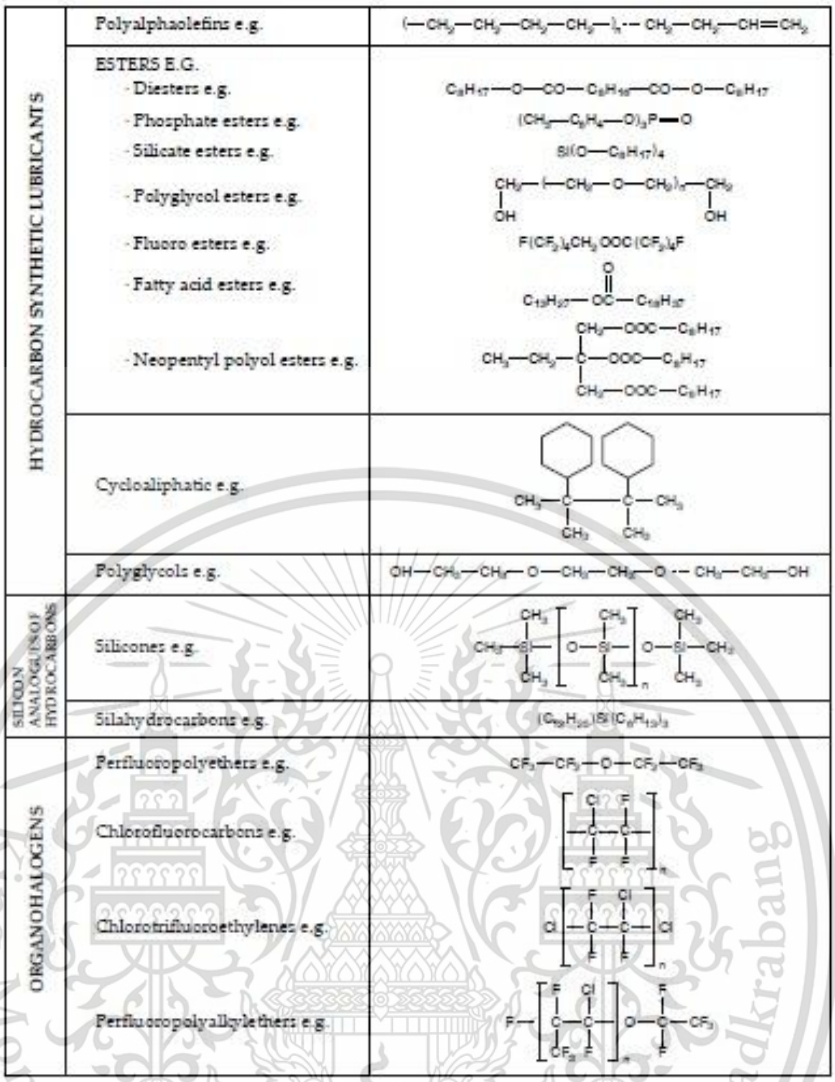


**Figure 28.** Typical structures of the most common synthetic lubricants [1].

2.3.1.2.2Ester

They are produced by reacting an alcohol with organic or inorganic acids. Esters usually have good oxidation stability and excellent viscosity-temperature and volatility characteristics. Dibasic acid ester or Di-ester can operate at high temperature and are used for applications where tolerance to heat is essential. The formation of Di-ester, form by reaction of alcohols with two hydroxyl groups and mono-functional carboxylic acid, is shown in Figure 29. Phosphate esters have better thermal stability than Di-esters nonetheless, which also high surface tension and cause corrosive wear [1].

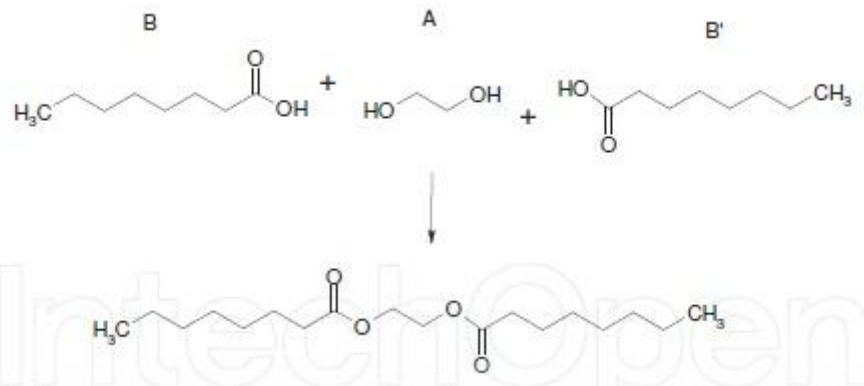


**Figure 29.** Formation of Di-ester by Di-alcohols react with mono-carboxylic acids [24].

2.3.1.2.3Poly-alkylene glycols

Poly-glycols have very good frictional behaviour and excellent lubricants, highly polar nature gives a strong affinity to metals giving low abrasive wear, advantages as lubricants for systems operating at high temperatures, have inverse solubility in water, i.e. water solubility decreases as temperature increases. Furthermore, poly-glycols use as brake fluids [27].

2.3.1.2.4Silioxanes

The most ordinary used silicones are Di-methyl, methyl, phenyl and poly-methyl silicones. Most of the silicones are chemically inert; they have good thermal and oxidation stability, good viscosity-temperature characteristics, low-volatility, toxicity and surface tension. They have poor boundary characteristics, especially with steel; on contrary, they are effective as hydrodynamic lubricants. The formation of silicone is shown in Figure 30 [1].

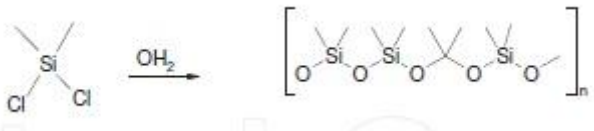


**Figure 30.** Formation of silicone oil [24].

2.3.1.2.5Poly-fluorinated Polyether

These are among the most promising lubricants for high-temperature applications; they have very high oxidation stability and thermal stability, low surface tension and are chemically inert. Structure of Poly-fluorinated Polyether is shown in Figure 31 [1]. PFPE has low adhesion causes creeping along the surface and mal-function if the surfaces are not clean thoroughly; high combustion temperature may cause emission of hydrogen fluoride and fluoro-phosgene which make PFPE formation corrosive, especially on steel alloy composition [24].

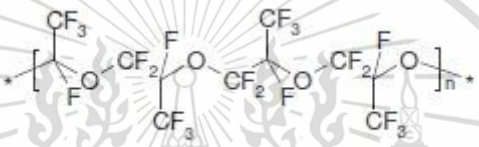

**Figure 31.** Structure of Poly-fluorinated Polyether [24].

**2.3.2 Lubricant additives**

Lubricant additives are chemicals, which are added to oils in quantities of a few weight percent to improve the lubricating capacity and durability of the oil. They have several specific purposes are: improving the wear and friction characteristics by provision for adsorption and extreme pressure lubrication, improving the oxidation resistance, control of corrosion, control of contamination by reaction products, wear particles and other debris, reducing excessive decrease of lubricant viscosity at high temperatures, enhancing lubricant characteristics by reducing the pour point and inhibiting the generation of form [1].

2.3.2.1 Wear and friction improvers

The additive which improves wear and friction properties are probably the most important of all the additives used in oil formulations with the task to separate metal surfaces in the case of heavy loading and to improve their resistance

toward wear in the case of oil film break in the contact [24]. These additives can divide into the following groups: adsorption or boundary additives, anti-wear additives and extreme pressure additives.

2.3.2.1.1 Adsorption or boundary additives

The adsorption or boundary additives are also known as friction modifiers, they used to prevent slip-stick phenomena and noise by reducing frictional forces. The mechanism of their performance is similar to that of the rust and corrosion inhibitors in that they form durable low resistance lubricant film via adsorption on surfaces and via association with the oil, they usually have a polar group (-OH) at one end of the molecule and react with the contacting surfaces. Their mechanism is shown in Figure 32, this mechanism is effective only at relatively low temperatures and loads [1, 28].

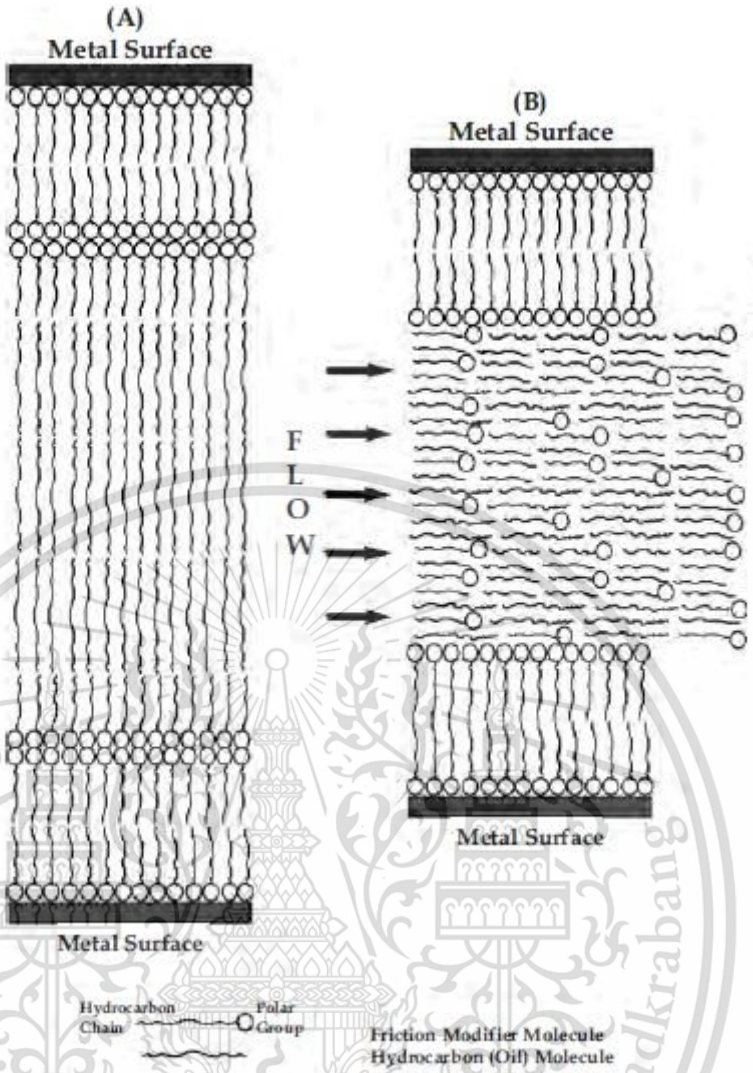


**Figure 32.** Adsorption of friction modifiers on metal [28].

2.3.2.1.2 Anti-wear additives

To protect contacting surfaces at a high temperature above the range of effectiveness of adsorption or boundary agents, anti-wear additives were designed and manufactured. AW additives are mainly designed to reduce wear when the running system is exposed to moderate stress. In engine oils the most ordinary used anti-wear additive is zinc dialkyldithiophosphate (ZDDP), in gas turbine oils tricresylphosphate or other phosphate esters are used, phosphorus anti-wear agents are shown in Figure 33. Furthermore, these additives react with the surfaces through the

mechanism of chemisorption, and the protective surface layer produced is much more durable than that generated by adsorption or boundary agents [1].

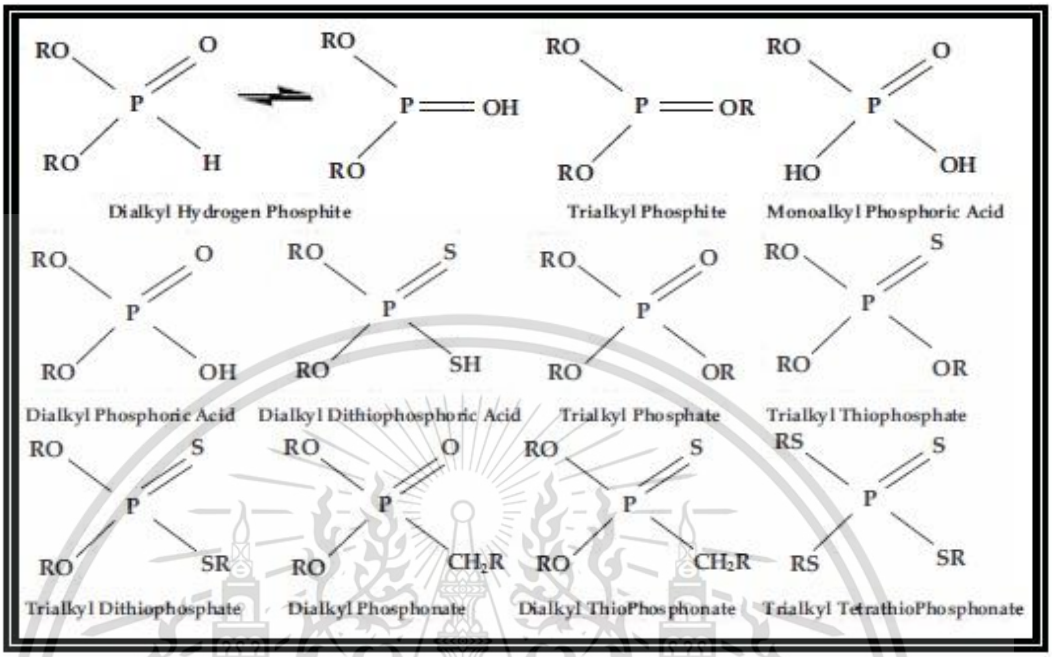


**Figure 33.** Common phosphorus anti-wear agents [28].

2.3.2.1.2.1 Zinc Dialkyldithiophosphate (ZDDP)

ZDDP is a crucial additive commonly used in engine oil formulations; the term anti-wear usually refers to wear reduction at moderate loads and temperatures, for high loads and high temperatures applications of ZDDP may increase wear beyond that of base oil as shown in Figure 34 [29]. The chemical structure of ZDDP is shown in Figure 35, ZDDP are formed by the reaction of one or more alcohol with P2S5 to give appropriate dialklydithiophosphoric acid and then the acid was neutralized by the addition of ZnO to give the product as shown in Figure 36 [31], in addition the different of alcohol mixtures, which can produce a mixture of different ZDDP that can extend the operating temperature range of the anti-wear protection and change physical properties, i.e. oil solubility, viscosity and chemical reactivity of resultant additive. [25, 31]. The surface protective films which are formed as the result of action of ZDDP act as the lubricant, reducing wear and friction

between the two interacting surfaces and the greatest wear reduction occur when a thermal film form first follow by friction between the surface in a ZDDP containing oil to generate the tribofilm, the protective films might be formed by spontaneous decomposition of the additive on worn surface since only small amount of iron is found in the film [1]. The mechanism of ZDDP film formation is shown in Figure 37, adsorption of the anti-wear chemistry to the metal surface and produces a pad-like protective reaction layer; hence a protective reaction layer grows to form a substantial anti-wear film [25]. In addition, the mechanism of reduction of wear involves the formation of pads that cover most of the surface. The formation of a linkage isomer that ultimately binds to the metal surface, followed by a reaction of eliminates the majority of the alkyl substituent and most of the sulfur result in the deposit of zinc polyphosphate at the surface. Iron diffusion to the surface and mixed with zinc polyphosphate/iron phosphate layer with increased iron closer to the surface. The pads appear to be bound to the surface through a thin layer of mixed zinc and iron sulfide, the film is shown in Figure 38 [31].

2.3.2.2 Anti-oxidants

2.3.2.2.1 Oxidation inhibitors

Natural sulfur or nitrogen containing compounds which are present in mineral oils act as oxidation inhibitors by scavenging the radicals produced by the oxidation process. Moreover, sulfur base extreme pressure and anti-wear additives are also entirely effective as anti-oxidants. Widely use as anti-oxidant additives are ZDDP, metal deactivators, a simple hydrocarbon, amines and organic phosphates. Anti-oxidant can be classified into three groups: metal deactivators, radical inhibitors and peroxide decomposers. Metal deactivators inhibit the acceleration of oil oxidation entraining a metal, i.e. iron and copper [1]. Metal

deactivators can classify into two categories; chelating agent and film-forming agents. Chelating agents will form a stable complex with metal ions, reducing the catalytic activity of the metal ions. Film forming agents act two steps. First, they coat the metal surface, preventing metal ions from entering the oil. Second, they minimize corrosive attack of the metal surface by physically restricting access of corrosive species to the metal surface [28]. Radical inhibitors, known as primary anti-oxidants, function by neutralizing the peroxy radicals, radical inhibitors comprise of phenolic anti-oxidants, aromatic amines and compounds containing sulfur and phosphorus [30]. The anti-oxidation mechanism, the first reaction is the production of hydro-peroxide which is generated by the reaction of the additives with peroxide radicals. Next step is the termination of oxidation, the peroxy radicals are completely neutralized and form a relatively inert product and the last step is the deactivation of the additive, the activated additive tends towards mutual neutralization resulting in greater usage of the additives. Peroxide decomposers, known as secondary anti-oxidants, function by neutralizing the hydro-peroxides which would otherwise accelerate the process of oxidation, peroxide decomposers consist of organo-sulfur compounds, organophosphorus compounds and other compounds [30], i.e. ZDDP which functions by decomposing the peroxide radicals and hydro-peroxides radical form during oxidation resulting in prevent acceleration of the oxidation process [1]. Hydro-peroxide decomposer and radical inhibitor are shown in Figure 39 [25].

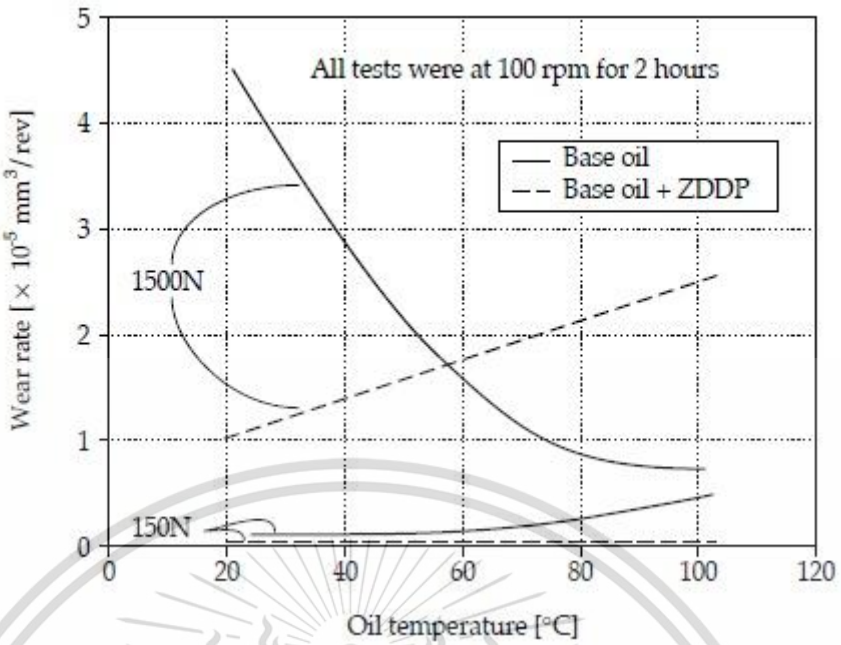


**Figure 34.** Influence of load and temperature on the effectiveness of ZDDP on wear rates [1].

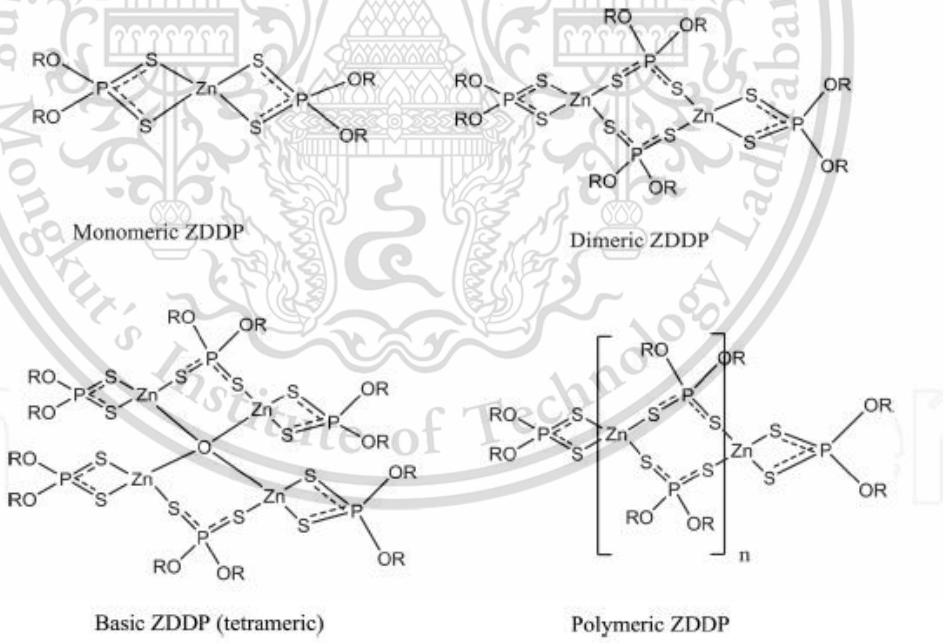


**Figure 35.** Chemical structure of ZDDP [31].

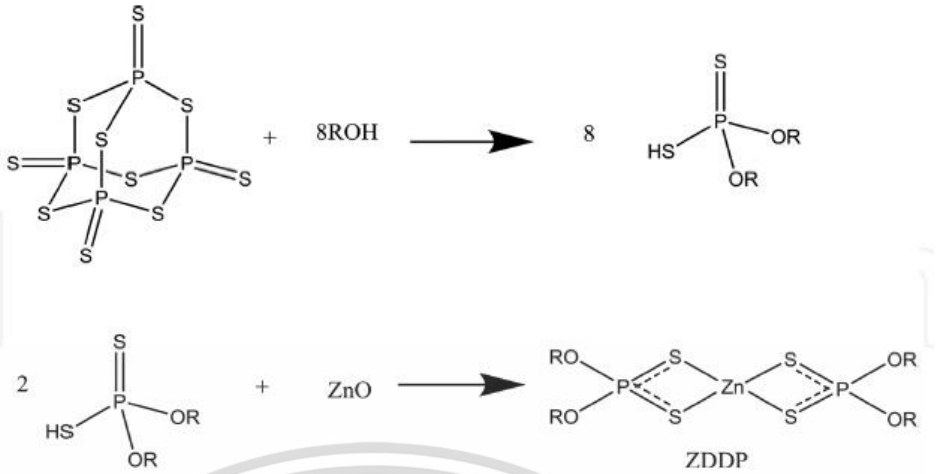


**Figure 36.** Method of preparation of ZDDP [31].

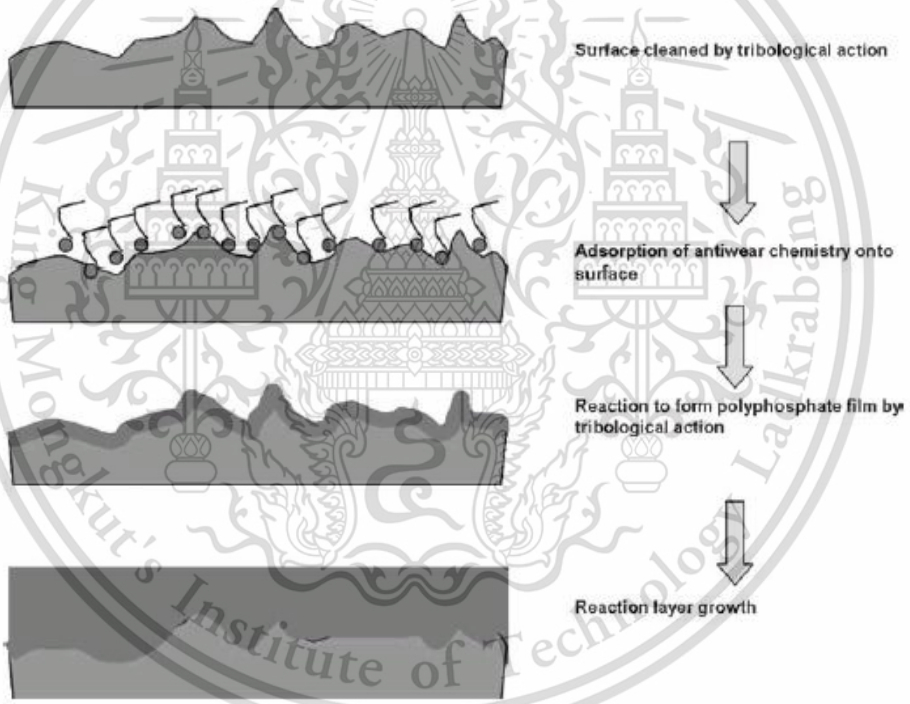


**Figure 37.** Mechanism of ZDDP film formation [25].

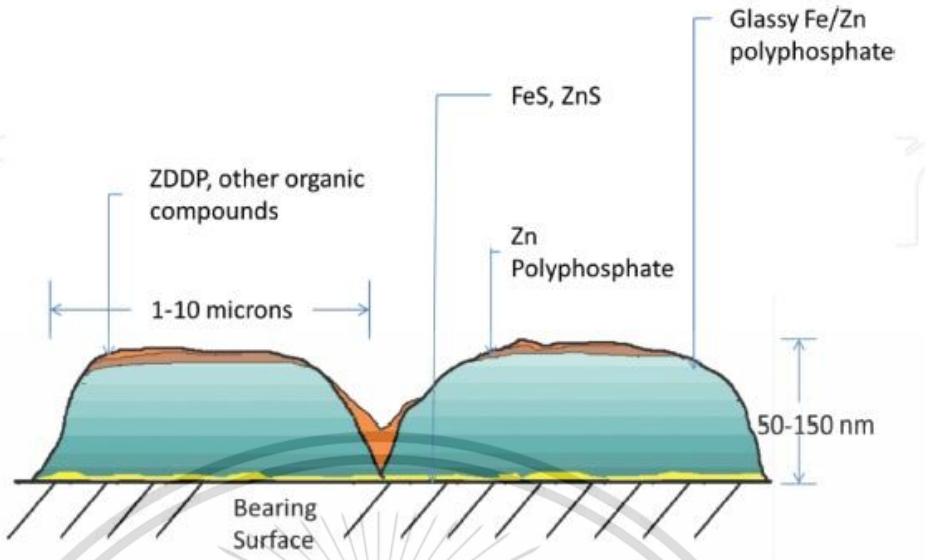


**Figure 38.** Layer structure of surface film formed by ZDDP [31].

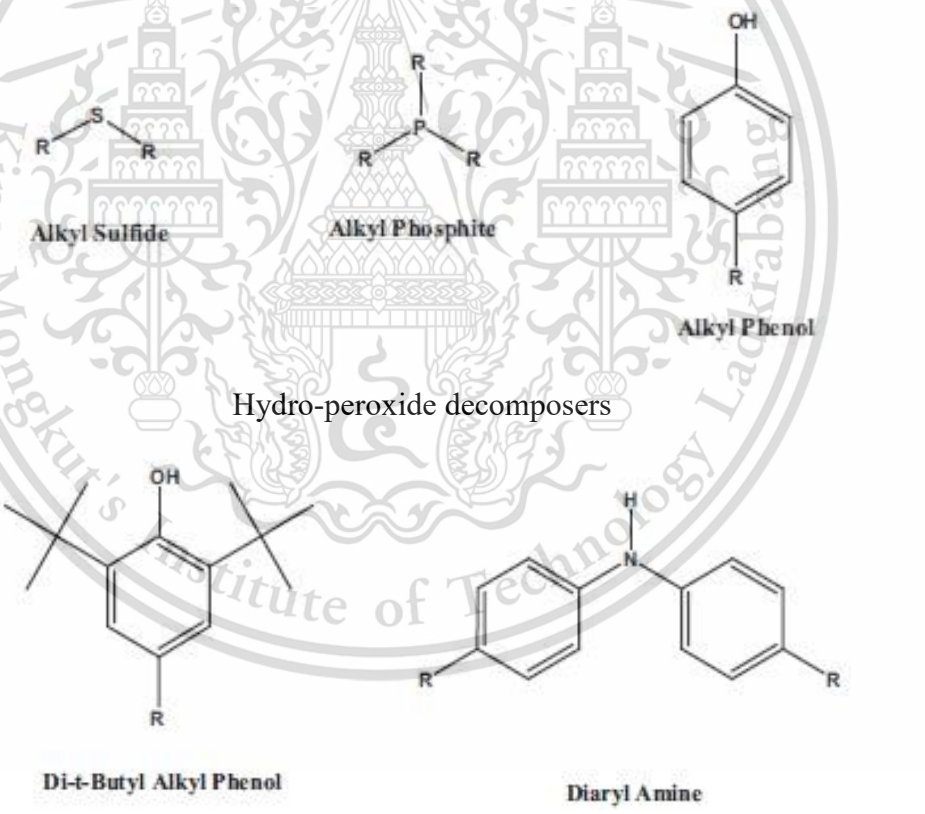


**Figure 39.** Example of hydro-peroxide decomposers and radical inhibitors [25].

2.3.2.3 Contamination control additives

Without proper control of contamination, the oil will lose its lubricity, become corrosive and will be unsuitable for service. Additives which prevent the contamination are known as detergents or dispersants, the primary function of these additives are; to neutralize any acids formed during the burning of fuel, to prevent lacquer and varnish formation on the operating parts of engine, to prevent the flocculation or agglomeration of particles and carbon deposits which may obstruct the oil ways. Dispersants can be classified into two categories; mild dispersant and an over-based or alkaline dispersant. First, a mild dispersant is often comprised of simple hydrocarbons or ash-less compounds, mild dispersants are regularly low molecular weight polymer of methacrylate ester, long chain alcohols or polar vinyl compounds. The function of these additives is to scatter soot and wear particles. Secondary, over-base dispersants are calcium, barium or zinc salts of sulphonic, phenol or salicylic acids, the function of these additives serve to neutralize any acid accumulated in the oil during service. Generally used dispersants are shown in Figure 40. Detergents ordinarily work by stabilizing any colloid particles suspended in the oil as shown in Figure 41 [1]. Moreover, detergents have various functions depending on the specific application i.e., suspend oil-insoluble oxidation or combustion products or both by adsorbing onto the surface in a similar way to dispersants, neutralize inorganic acids and organic acids, reduce corrosion by forming a protective layer on metal surfaces, reduce deposit formation in high temperature zones and provide balanced friction for clutch and synchromesh performance in transmission fluid in conjunction with suitable friction modifier system. Commonly used detergents are sulfonic acids, phenols or salicylic acids, the structure of these detergents are shown in Figure 42

[25].

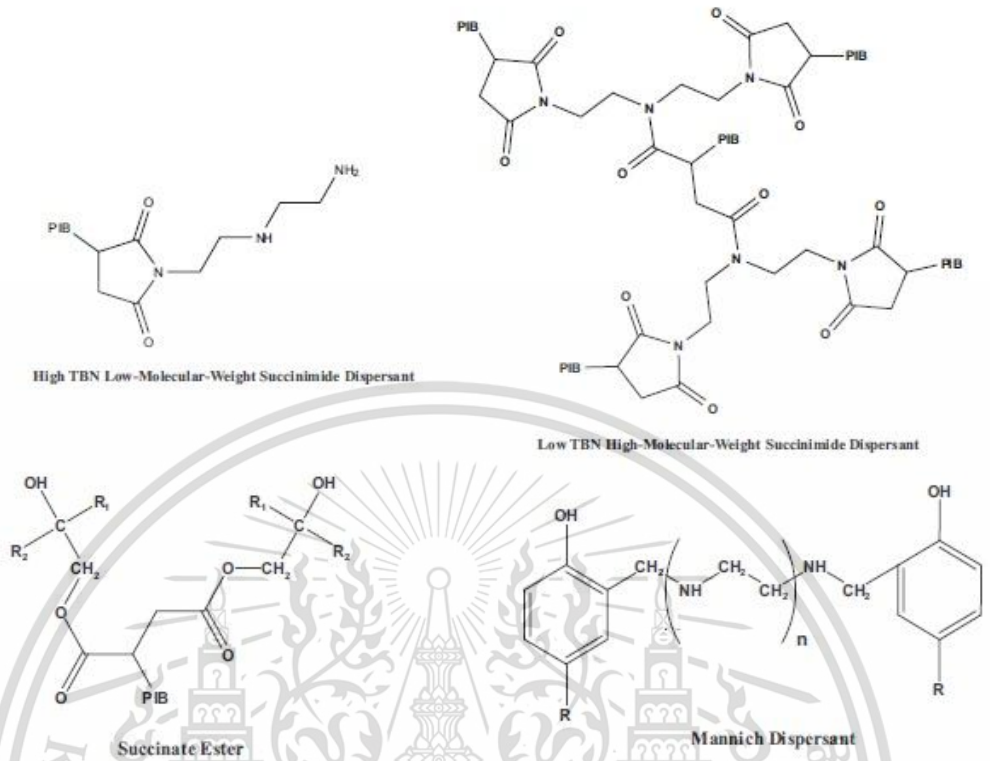


**Figure 40.** generally used dispersants [25].

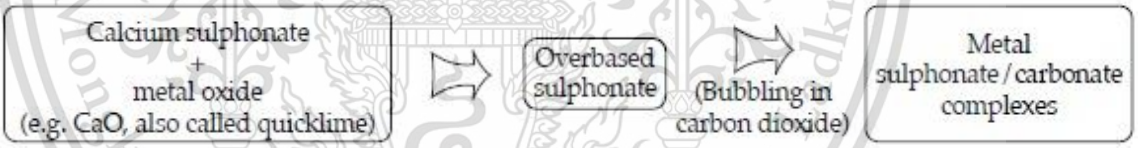


a) Synthesis of sulphonate detergents

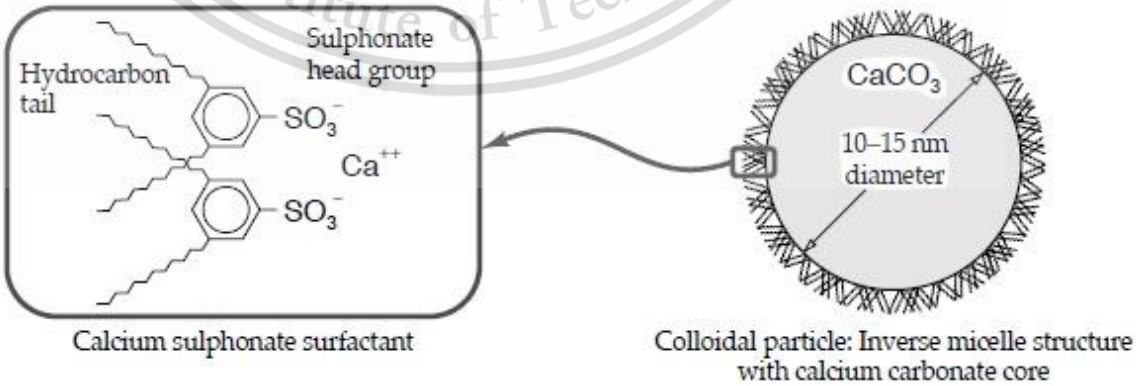


b) Calcium sulphonate/ carbonate complex

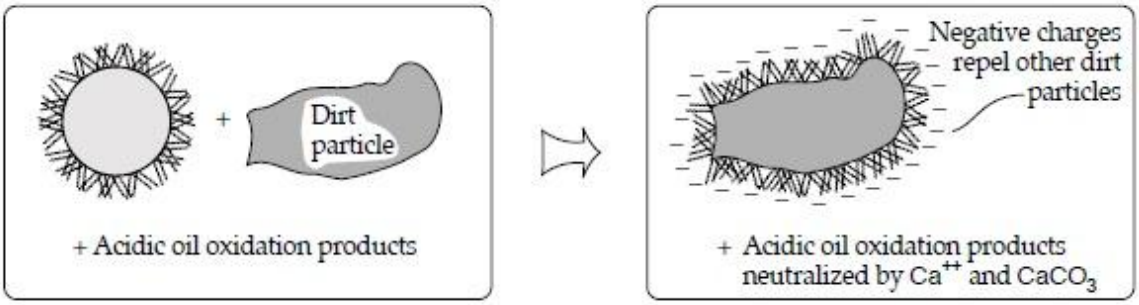


C) Function of sulphonate detergents

**Figure 41.** Synthesis and function of sulphonate detergents [1].

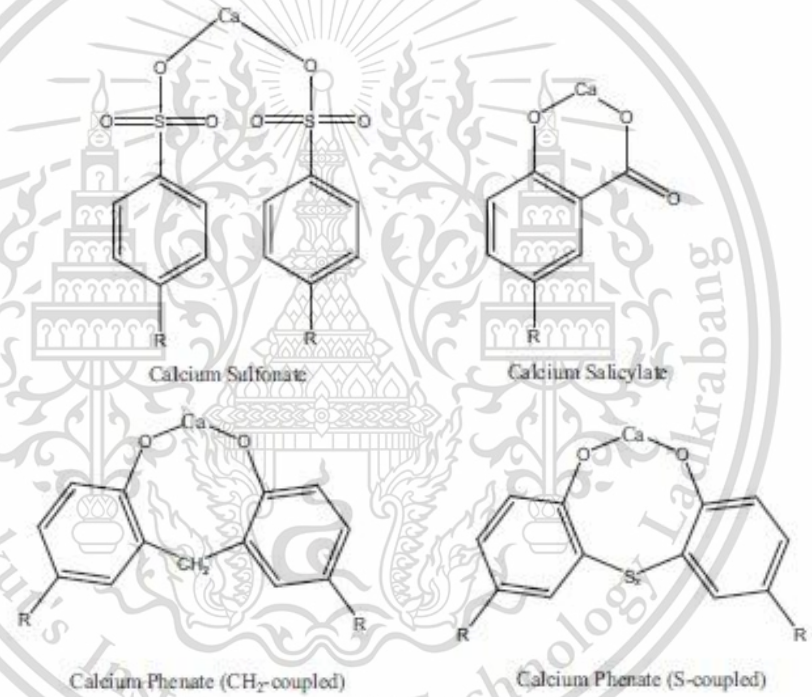


**Figure 42.** commonly used detergents [25].

## 2.4 Oxidation of lubricants

### 2.4.1 Fundamental of oxidations

Mineral oils inescapably oxidize during service and this cause drastically increases in friction and wear which affects the performance of the machinery. The

ageing of lubricants can be classified into two processes:the oxidation process by reaction of the lubricant molecules with oxygen(low temperature, 30-120 °C) is called auto-oxidation and the thermal decomposition (cracking) at high temperature (>120 °C) [30]. The main effect of oxidation is a continuous increase in viscosity and acidity of mineral oil as a function of oxidation time. The normal mechanism of oil oxidation is believed to be a free-radical chain reaction; the precise mechanism is impeded by the complexity and mutability of mineral oil composition. The possible reaction mechanisms can be reduced to four basic steps: initiation, chain-propagation, chain-branching and termination are shown in Figure 43 [25, 30].

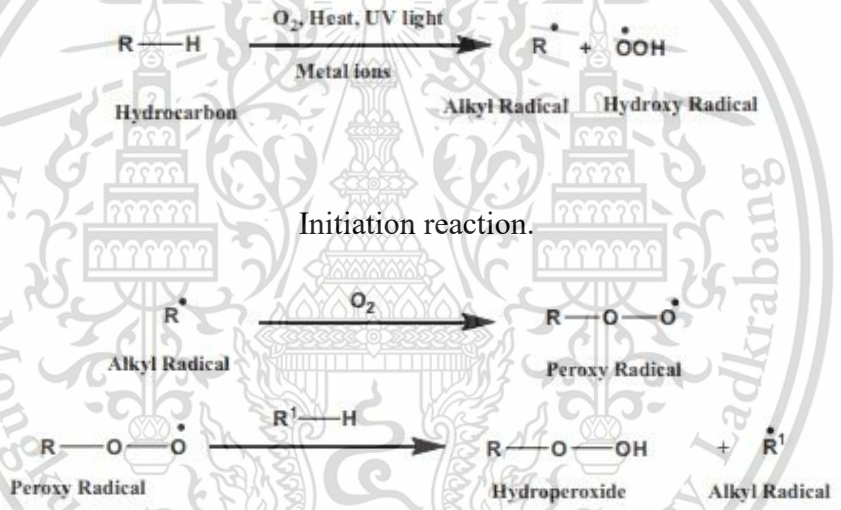


Initiation reaction.

Chain-propagation reactions.

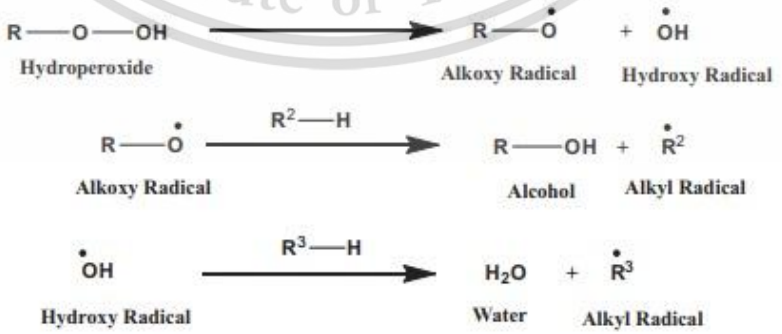


Chain-branching reactions.

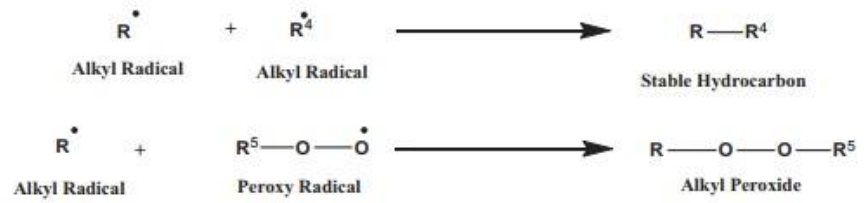


Termination reactions.

**Figure 43.** Oxidation processes [25].

The initial reaction is the C-H bond can be homolytically disengagement under the influence of oxygen, heat, or ultraviolet light (form the combustion process) and can be catalyzed by the presence of metal ions to form free radicals. In the secondary reaction, peroxy radicals are formed, a direct reaction between the alkyl radical and dissolved oxygen, this step is followed by the abstraction of a hydrogen atom from secondary hydrocarbon molecule to form another alkyl radical and hydro-peroxide. In chain-branching reaction, at high temperatures, hydroxy-peroxide separate can result in the formation of alkoxy and hydroxyl radicals, the oxidation product is alkyl-hydro-peroxides (R-O-O-H), di-alkyl peroxides (R-O-O-R°), alcohol (R-O-H), aldehydes (R-C-H-O), ketones (R-R°-C=O), carboxylic acids (R-C-O-O-H), ester (R-C-O-O-R°) can go through several further reactions that can induce to polymeric species that finally become oil-insoluble sludge, lacquer and varnish. At termination reaction, a reaction of a radical with another radical will form a stable hydrocarbon molecule or another hydro-peroxide, which can decompose further by the above mechanism [25]. The presence of metallic wear debris, temperature, the amount of water and oxygen in the oil can accelerate oxidation. Besides, internal combustion engines blow-by gases and nitrous oxide can expedite the oxidation process while nuclear radiation can cause a large accrue in oil viscosity by including

cross-links between hydrocarbon molecules, radiation produces free radicals hence augmenting the rate of oxidation [1].

### 2.4.2 Artificial ageing (oxidation)

Artificial ageing defined as applying severe conditions to the lubricant sample to accelerate lubricant degradation at very short-term scale. The standardized method of the artificial ageing of lubricating oils in this thesis was conducted based on [32]. The schematic diagram of artificial ageing is shown in Figure 44. The lubricant oil is placed in a round-bottomed three-neck glass flask supplied with a cooling device at neck 1, to ageing with ethanol due to high volatility and low boiling point and kept at defined temperature by a hotplate and stirrer. The oil is brought into contact with air zero via glass tube through neck 2. The air flow is adjusted by a rotameter. Neck 3 of the flask is intended for measure lubricating oil temperature by a thermocouple, periodical sampling and lubricant condition monitoring. The oil samples are not exposing to light to avoid the effect of ultraviolet radiation, i.e. induction of photochemical reactions. The artificial ageing procedure was commonly conducted at certain technical characteristic, the main deterioration of the lubricant takes place in the combustion chamber, the temperature of lubricant sample was held at 160 °C to simulate a current condition in the area of the piston rings. The air flow was adjusted at 10L/h and the test duration was always 144h or 6 days. The amount of oil sample introduced into the flask was 300 ml [32].

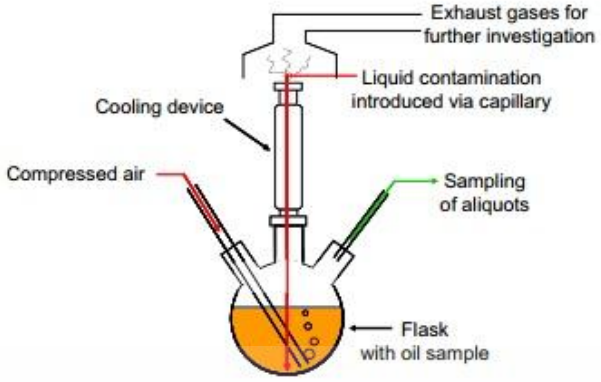


**Figure 44.** Schematic set-up of artificial ageing [32].

# CHAPTER 3

# RESEARCH METHODOLOGY

## 3.1 Experimental apparatus

### 3.1.1 Test rig

3.1.1.1 NSTDA test rig

The first part of this thesis, the tribometer with a ball-on-disc configuration at NSTDA was used to provide a pure sliding contact condition between specimens. A lower specimen holder and lubricant bath were modified to contain the test lubricants. The tribometer with a ball-on-disc configuration and heater system are shown in Figure 45.

**Figure 45.** the tribometer with a ball-on-disc configuration and heater system.

3.1.1.2 TISTR test rig

The second part of this thesis, the tribometer with a ball-on-disc configuration at TISTR was used to provide a pure sliding contact condition between specimens. Because of the original test chamber for ball-on-disc configuration, the original tribometer is shown in Figure 46, could not be tested with lubricant samples at high

temperature hence some modifications are required: a new test specimen holder and an additional external heater system. In addition, lid cover for specimen holder was created to provide prevention of lubricant spillage from a test specimen holder during the test. The modification parts are shown in Figure 47.

**Figure 46.** Original TISTR tribometer (UMT Bruker tribolab).

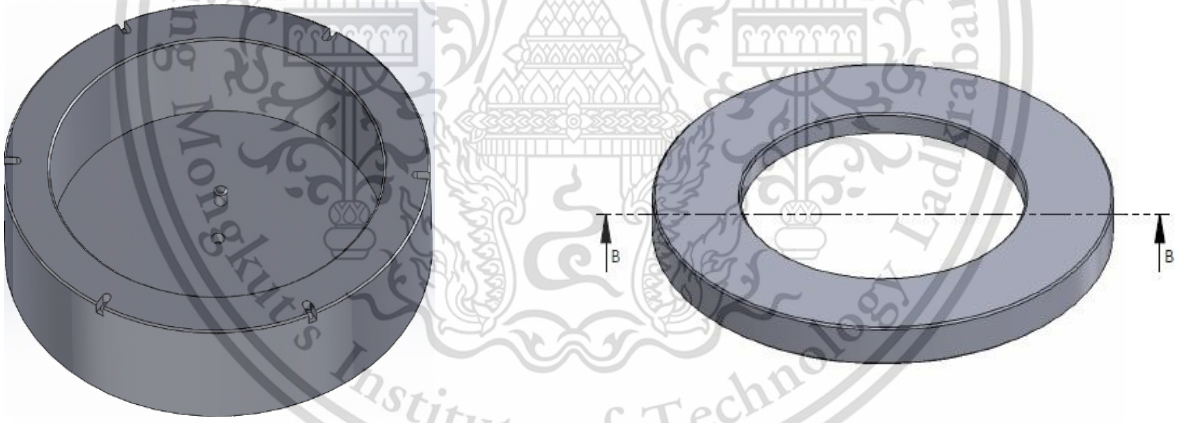


(a) New test specimen holder. (b) Lid cover for specimen holder.

**Figure 47.** Modification part for TISTR tribometer.

### 3.1.2 Material and test conditions

3.1.2.1 NSTDA material and test conditions

The balls used in this thesis were SKF RB 6.35 mm / G20 made of AISI 52100 bearing steel. The discs were AISI 52100 steel and AISI 1050 carbon

steel. The material properties are shown in Table 1 and the test specimens are shown in Figure 48.

**Table 1.** Material properties

| Material properties | AISI 52100 | AISI 1050 |
|---|---|---|
| **Ball hardness (HV)** | 837.06 | 837.06 |
| **Disc hardness (HV)** | 742.5 | 721.5 |
| **Ball elastic modulus (GPa)** | 210 | 210 |
| **Disc elastic modulus (GPa)** | 210 | 205 |
| **Ball surface roughness (nm)** | 100 | 100 |
| **Disc surface roughness (nm)** | 341.60 | 368.10 |

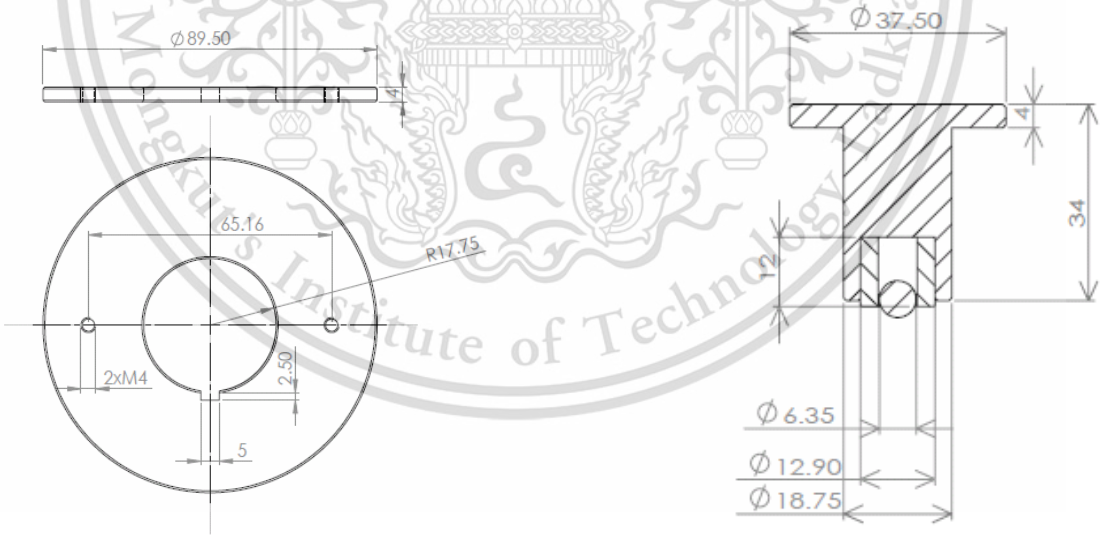


(a) Disc specimens (b) Ball specimens

**Figure 48.** NSTDA test specimens.

Before the test, steel ball and steel disc specimens were cleaned by immersing in isopropanol and petroleum ether in an ultrasonic bath at a temperature of 60 °C for

20 minutes. Tribology test conditions are shown in Table 2. A load of 2.93 N and 3.01 N was applied on AISI 52100 and AISI 1050 disc specimens respectively in order to obtain maximum Hertzian contact pressure of 0.95 GPa. Spindle speed of 60 rpm was applied to archive an entrainment speed of 0.1m/s.

**Table 2.**NSTDA test conditions on tribometer with ball-on-disc configuration.

| Parameters | Value |
|---|---|
| **Maximum contact pressure (GPa)** | 0.95 |
| **Temperature (°C)** | 25, 80, 100 |
| **Test duration (min)** | 120 |
| **Entrainment speed (m/s)** | 0.1 |
| **Test lubricants** | Base oil group II, PAO6, Base oil group II+ZDDP and PAO6+ZDDP |
| **Dimensions (mm)** | Ball=3.18/ Disc=44.75 |

3.1.2.2 TISTR material and test conditions

The balls used in this thesis were SKF RB 6.35 mm / G20 made of AISI 52100 bearing steel. The discs were AISI 52100 steel, the material properties are shown in Table 3 and test specimens are shown in Figure 49.

**Table 3.**Material properties

| Material properties | AISI 52100 |
|---|---|
| **Ball hardness (HV)** | 837.06 |
| **Disc hardness (HV)** | 668.25 |
| **Ball elastic modulus (GPa)** | 210 |
| **Disc elastic modulus (GPa)** | 210 |
| **Ball surface roughness (nm)** | 100 |
| **Disc surface roughness (nm)** | 53 |

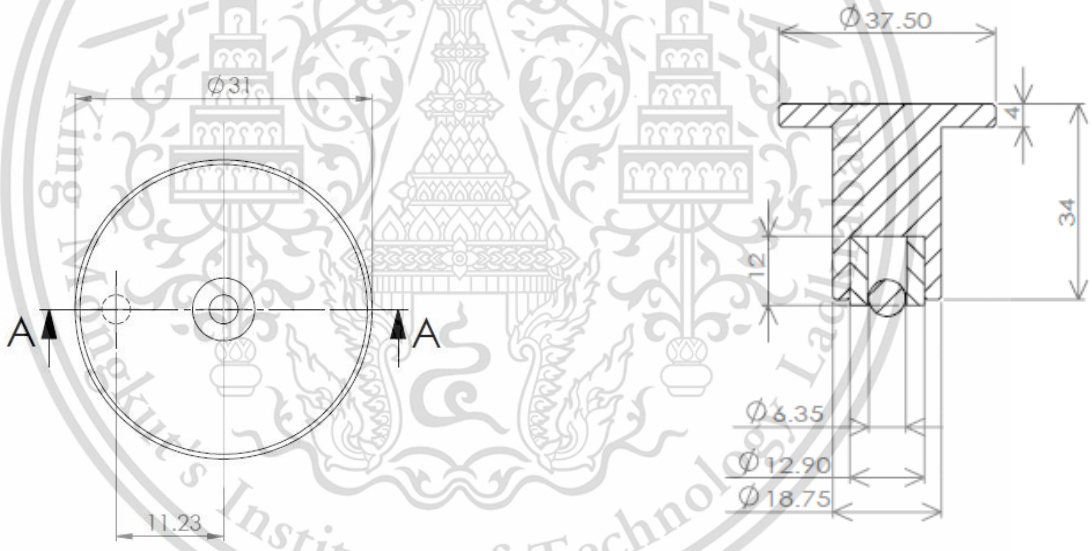


(a) Disc specimens (b) Ball specimens

**Figure 49.** TISTR test specimens.

Before the test, steel ball and steel disc specimens were cleaned by immersed in isopropanol and petroleum ether in an ultrasonic bath at a temperature of 60 °C for 20 minutes. Tribology test conditions are shown in Table 4. A load of 3 N was applied on AISI 52100 to obtain a maximum Hertzian pressure of 0.95 GPa. Spindle speed of 60 rpm was applied to achieve an entrainment speed of 0.1 m/s.

**Table 4.**TISTR test conditions on tribometer with ball-on-disc configuration.

| Parameters | Value |
|---|---|
| **Maximum contact pressure (GPa)** | 0.95 |
| **Temperature (°C)** | 25, 100 |
| **Test duration (min)** | 120 |
| **Entrainment speed (m/s)** | 0.1 |
| **Test lubricants** | Base oil group II, PAO6, Base oil group II+ZDDP and PAO6+ZDDP |
| **Dimensions (mm)** | Ball=3.18/ Disc=15.50 |

ThemaximumHertzian contact pressure was calculated from the Hertzian point contact equation using equation (3.1) by R.S. Dwyer-Joyce [37].

$$P_{max} = \frac{3P}{2\pi a^2} \quad (3.1)$$

$$a = \sqrt[3]{\frac{3PR'}{E'}}$$

$$\frac{1}{E'} = \frac{1-{v_1}^2}{E_1} + \frac{1-{v_2}^2}{E_2}$$

$$\frac{1}{R'} = \frac{1}{R_1} + \frac{1}{R_2}$$

Where $P_{max}$is maximum Hertzian contact pressure [GPa], P is applied load [N], a is contact radius [m], $R'$ is relative radius of curvature [m], $E'$ is reduced modulus [GPa] and $v$ is Poisson's ratio.

Spindle speed was calculated using equation (3.2).

$$U = \omega r \quad (3.2)$$

Where U is an entrainment speed [m/s], ω is spindle speed [rpm] and r is the distance between a centre of lower specimen holder and centre of ball holder [m].

### 3.1.3 Lubricating oils

Group II base stock, Poly-α-olefin 6 (PAO 6), Group II base stock+1.2%wt ZDDP, PAO 6+1.2%wt ZDDP was used as a lubricant. The physical properties are shown in Table 5. Due to the viscosity of Group II base stock+ZDDP and PAO 6+ZDDP, it was not possible to measure kinematic viscosity at 40 ° C with an available test machine. Four efficient bulk properties of test lubricant i.e. density, viscosity, Total Acid Number (TAN) and Oxidation (FTIR) were investigated according to standard ASTM D4052 [33], ASTM D445 [34], ASTM D664 [35] and standard ASTM D7214 [36] respectively. Additionally, the test method or apparatus for each value was viscometer, digital density-meter, potentiometric titration, and FT-IR spectrometry using peak area increase calculation, respectively.

**Table 5.**Physical properties of lubricants

| LUBRICANTS | GROUP II BASE OIL | PAO 6 | GROUP II BASE OIL+ZDDP | PAO 6+ZDDP |
|---|---|---|---|---|
| DENSITY AT 15°C ($G/CM^3$) | 0.838 | 0.817 | 0.840 | 0.819 |
| KINEMATIC VISCOSITY AT 40°C ($MM^2/S$) | 28.450 | 29.730 | N/A | N/A |
| KINEMATIC VISCOSITY AT 100°C ($MM^2/S$) | 5.098 | 5.809 | 5.124 | 5.801 |
| TOTAL ACID NUMBER (MG.KOH/G) | 1.770 | 2.010 | 2.376 | 2.021 |
| OXIDATION (FTIR) (PAI) | 0.000 | 0.000 | 0.000 | 0.000 |

### 3.1.4 Viscometer

Viscometer (Canon mini AV) was used to measure the viscosity of lubricating oils before and after tribological test with tribometer with a ball-on-disc configuration to investigate the effect of bulk properties on tribological performance of the lubricant. Moreover, aged lubricants were measured viscosity to investigate the effect of bulk properties on an ageing characteristic, kinematic viscometer is shown in Figure 50.


**Figure 50.** Kinematic viscometer (Canon mini AV).

### 3.1.5 Digital density-meter

Digital density-meter (Anton Paar DMA 4500) was used to measure the density of lubricating oils as fundamental information of physical properties of lubricating oils. Digital density-meter is shown in Figure 51.


**Figure 51.** Digital density-meter (Anton Paar DMA 4500).

### 3.1.6 Potentiometric titration

Potentiometric titration (Metrohm 809 titrando) was used to measure Total Acid Number (TAN) of lubricating oils before and after tribological test on tribometer with a ball-on-disc configuration to investigate the effect of bulk properties on tribological performance of the lubricant. Furthermore, aged lubricants were measured Total Acid Number (TAN) to investigate the effect of bulk properties on an ageing characteristic, potentiometric titration is shown in Figure 52.

**Figure 52.** Potentiometric titration (Metrohm 809 titrando).

### 3.1.7 FT-IR spectrometry

FT-IR spectrometry (Thermo scientific FT-IR is50 ATR) was used to measure oxidation value, peak area of carbonyl band in FT-IR spectrum was used to calculate peak area increase value (PAI) which represents oxidation of lubricant, before and aftertribological test on tribometer with ball-on-disc configuration to investigate the effect of bulk properties on tribological performance of lubricant.Besides, aged lubricants were measured oxidation value to investigate the effect of bulk properties on an ageing characteristic, FT-IR spectrometry is shown in Figure 53.


**Figure 53.** FT-IR spectrometry (Thermo scientific FT-IR is50 ATR).

### 3.1.8 Surface roughness tester

Surface roughness (Mitutoyo surftest SV-3000) tester was used to measure the roughness profiles of disc specimens before and aftertribological test on tribometer with ball-on-disc configuration to investigate the wear performance of lubricating oils, which can evaluate by volume loss of the disc specimens. In addition, average wear scar depth form roughness profiles of disc specimens were used to calculate volume loss of the disc specimens. Surface roughness tester is shown in Figure 54.

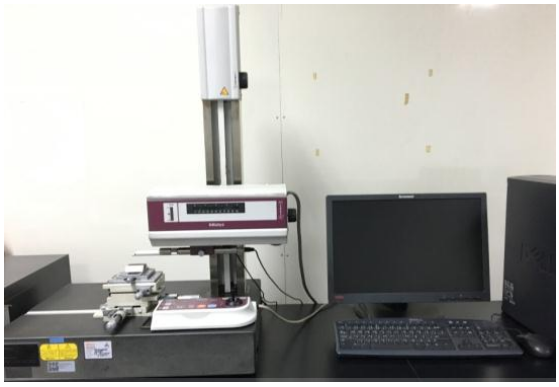

**Figure 54.** Surface roughness tester (Mitutoyo roughness tester).

### 3.1.9 Scanning Electron Microscope (SEM)

Scanning Electron Microscope (FE-SEM SU5000) was used to investigate the worn surface and wear track topography of disc specimens. In addition, SEM micrograph can use to study wear characteristic of a worn surface to classify wear type i.e. abrasive wear, adhesive wear, and fatigue wear. Energy Dispersive X-Ray Spectrometer (EDS) used to analyze an elemental composition or contaminant which presence in a worn surface. SEM-EDS machine is shown in Figure 55.

**Figure 55.** SEM-EDS (FE-SEM SU 5000)

### 3.1.10 Optical Microscope (OM)

Optical Micro Scope Eclipse (LV-N, LV100DA-U)was used to investigate the worn surface and wear track topography of disc specimens. Besides, OM micrograph

can be used to compare and evaluate worn surface of disc specimens with different lubricating oils. OM machine is shown in Figure 56.

**Figure 56.** Optical Microscope Eclipse (LV-N, LV100DA-U)

### 3.1.11 Polishing machine

Owing to difficulty of wear characterize after tribology experiment or after ball-on-disc wear test because of the rough and grinding surface of disc specimens. Pre-treatment phase is necessary to prepare the disc specimens surface like mirror and have surface roughness approximately 0.053um. The methods for pre-treatment are describe as below. Polishing machine is shown in figure 57.

1. Use 120 grit sand papers with polishing machine to polish surface of disc specimens.
2. Use 240 grit sand papers with polishing machine to polish surface of disc specimens.
3. Use 400 grit sand papers with polishing machine to polish surface of disc specimens.
4. Use 600 grit sand papers with polishing machine to polish surface of disc specimens.

5. Use 800 grit sand papers with polishing machine to polish surface of disc specimens.
6. Use 1,200 grit sand papers with polishing machine to polish surface of disc specimens.
7. Use 2,400 grit sand papers with polishing machine to polish surface of disc specimens.
8. Use 4,000 grit sand papers with polishing machine to polish surface of disc specimens.
9. Use polishing cloth with poly-diamond suspension 6 micron and polishing machine to polish surface of disc specimens.
10. Use polishing cloth with poly-diamond suspension 1 micron and polishing machine to polish surface of disc specimens.


**Figure 57.** Polishing machine (Struers Labopol-5).

### 3.1.12 Nano-search Microscope

Nano-search Microscope (Olympus LEXT OLS-4500) consists of two modes: laser and roughness mode roughness mode of this machine was used to measure 2D and 3D roughness profiles of disc specimens. Furthermore, wear depth profile and wear scar diameter were evaluated by laser mode of this machine. Besides, Laser

mode was used to investigate the worn surface and wear track topography of disc specimens. Nano search Microscope was shown in Figure 58.

**Figure 58.** Nano-search Microscope (Olympus LEXT OLS-4500)

## 3.2 Experimental approach

### 3.2.1 Investigate the effect of ZDDP on tribological performance of lubricants

This part of this thesis comprises of three parts. (I) Pre-test phases where four efficient bulk properties of test lubricant i.e. viscosity, density, Total Acid Number (TAN) and Oxidation value (FTIR) were investigated to perceive general information of physical properties of lubricating oils. (II) Test phases, where the effect of the tribological performance of lubricants was investigated in a tribometer with a ball-on-disc configuration. (III) Post-test phases, where bulk properties of lubricant were measure again to study the effect of ZDDP on tribological performance of lubricants. In addition, the effect of ZDDP on wear performance of lubricants was evaluated by wear volume, estimated from the resulting wear scar depth on the disc specimens.

Wear performance of lubricants was evaluated by wear volume. Wear volume of the disc was calculated using equation (3.3). Furthermore, depth of wear scar was calculated wear scar profile in Figure 59.

$$V_L = \frac{M_L}{D} \times 1000 \qquad (3.3)$$

Where VL is wear volume of disc specimen [$mm^3$],$M_L$ismass loss of disc specimen [g] and D is density of disc specimen [$g/cm^3$]

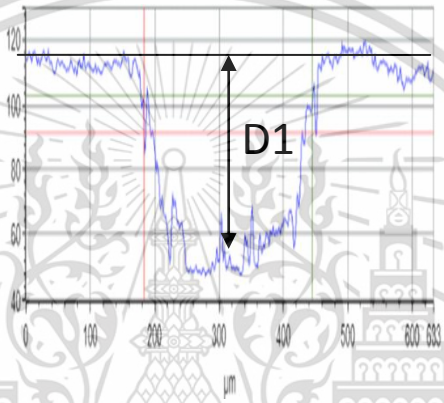


**Figure 59.** Example of wear scar profile from tested disc specimens.

### 3.2.2 Artificial ageing with oxidation and the addition of ethanol

Artificial ageing experiment with air was conducted based on [32]. Schematic set-up of an artificial ageing method is shown in Figure 60 and set-upof an artificial ageing method with addition of ethanol is shown in Figure 61. The lubricant oil is placed in a round-bottomed three-neck glass flask equipped with a cooling device (laboratory condenser) at the center neck of the flask in order that ageing with the addition of ethanol because of a high volatility due to a low boiling point of 78 °C. For this reason, the dosing device had to be cooled down to ensure that the intended amount of ethanol is added to the oil. Besides, addition of ethanol1% of ethanol in

relation to the engine oil volume per days.In addition, kept lubricating oil at a defined temperature by a hot plate and stirrer. The lubricating oil is brought into contact with air zero via glass tube at the right neck of the flask; the air flow is adjusted by a rotameter. At the left neck of the flask is intend for temperature measurement of lubricating oil via thermocouple and for periodic sampling, for all ageing procedure applied sampling of about 50 ml was done after artificial ageing was finished for lubricating oil condition monitoring, i.e. viscosity, Total Acid Number (TAN) and oxidation value (FTIR). Besides, the lubricant oil sample is not exposed to light to keep away from the effect of ultraviolet radiation.

The artificial ageing conditions are based on [32], the temperature of the lubricant sample was steadily held at 160 °C to simulate general conditions in the area of the piston rings. The air flow was adjusted at 10 L/h, the test duration was usually 144h or 6 days and the amount of lubricant sample introduced into the flask was 300 ml.

**Figure 60.** Schematic set-up of artificial ageing method.

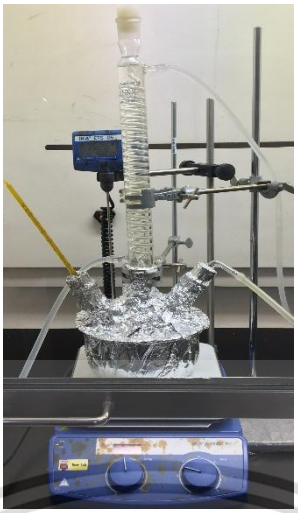

**Figure 61.** Schematic set-up of artificial ageing method with addition of ethanol.

### 3.2.3 Investigate the effect of aged lubricant on tribological performance of lubricants

This part of this thesis aged lubricants with oxidation (pure air zero) and the addition ethanol (air zero and ethanol) was brought into lubricating the contact between ball and disc specimens on the tribometer with ball-on-disc configuration. Furthermore, after a tribological test, the effect of aged lubricant on wear performance of lubricants was evaluated by wear volume, estimated from the resulting wear scar depth on the disc specimens. Besides, bulk properties of lubricant i.e. viscosity, TAN and oxidation value (FTIR) was evaluated to study the effect of chemical properties on wear performance of the lubricant.

# CHAPTER 4

## RESULTS AND DISCUSSIONSPART I

Test lubricant which was used in this research comprises of Group II base stock, Group II base stock mixed with ZDDP, PAO 6 base stock and PAO6 base stock mixed with ZDDP. Three efficient bulk properties of test lubricant, i.e. kinematic viscosity, Total Acid Number (TAN) and oxidation value (FTIR) were investigated according to standard ASTM D445 [34], ASTM D664 [35] and standard ASTM D7214 [36] consecutively. The physical properties of lubricant after the tribological experiment at a different temperature, i.e. 25 °C, 80 °C and 100 ° C and different material of disc specimens: AISI 52100 and AISI 1050 are shown in Figure 62 and 63. According to the results, it could be seen that the change in kinematic viscosity and Total Acid Number values were slightly decreased when the operating temperature was increased. These results agree with the previous research by Morina et al. [40]. It was proposed that when operating temperature increase leads to a decrease in viscosity. The trend of lubricants without ZDDP and ZDDP-containing lubricants are similar. One reason for this behavior could be that at high operating temperature, the performance of bulk properties of model lubricants will ameliorate.

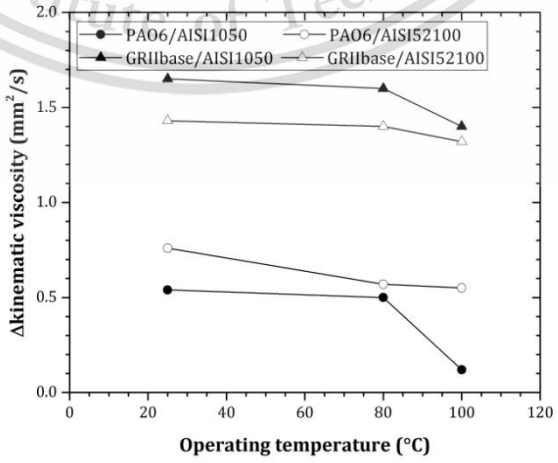

**Figure 62.** Kinematic viscosities of lubricants after tribological experiment.

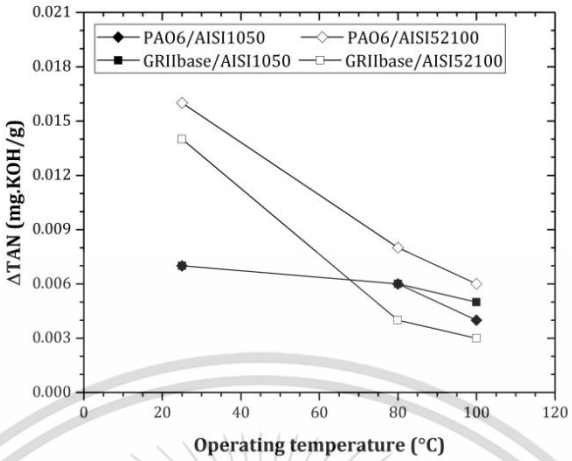


**Figure 63.** Total Acid Number (TAN) of lubricants after tribological experiment.

### 4.1 Effect of material on wear performance of model lubricants

The disc specimens which test at NSTDA tribometer with ball-on-disc configuration composed of two different types of material: AISI 52100 bearing steel and AISI 1050 carbon steel which is commercially available for a roller bearing and needle bearing washer successively. Furthermore, the elemental composition of AISI 52100 and AISI 1050 are shown in Table 6 [41-42]. In accordance with the result in Figure 64, resemblances of disc volume loss were noticed between AISI 52100 and AISI 1050 material. Due to the similarity of disc volume loss of two different materials, disc specimens that test at TISTR tribometer with ball-on-disc configuration were diminished to AISI 52100 bearing steel only.

**Table 6.** Elemental compositions of materials [41-42].

| Material | AISI 52100 | AISI 1050 |
|---|---|---|
| **C (%)** | 0.98-1.1 | 0.47-0.55 |
| **Cr (%)** | 1.3-1.6 | - |
| **Fe (%)** | 96.5-97.32 | 98.46-98.92 |
| **Mn (%)** | 0.25-0.45 | 0.60-0.90 |
| **P (%)** | ≤ 0.025 | ≤ 0.040 |
| **Si (%)** | 0.15-0.30 | - |
| **S (%)** | ≤ 0.025 | ≤ 0.050 |

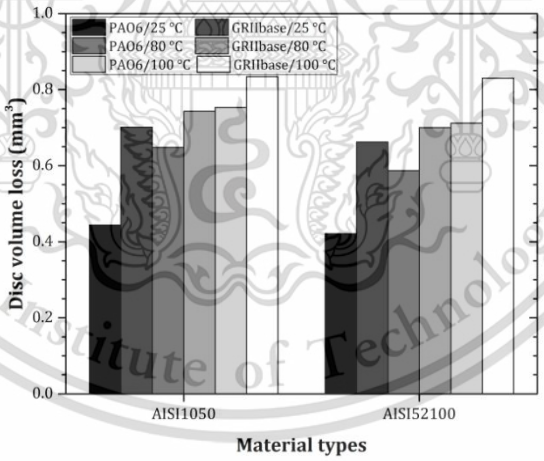


.

**Figure 64.** Effect of specimen material on wear performance.

### 4.2 Effect of lubricant types on wear performance of model lubricants

In this thesis two group of base stock: Group II base stock and PAO 6 base stock, which are hydro-treated base oil or mineral base oil and Group IV base oil or synthetic lubricant consecutively, which out an introduction of ZDDP anti-wear additive, were used to investigate the effect of different lubricant base stock on wear performance of lubricants. In compliance with the result in Figure 65, Group II base stock resulted in higher disc volume loss than PAO 6 base stock. It could be because Group II base stock had less kinematic viscosity than PAO 6 base stock or in the other word, PAO 6 base stock has better wear performance than Group II base stock. The influence of operating temperature on wear performance of model lubricants will be further discussed in section 4.3.

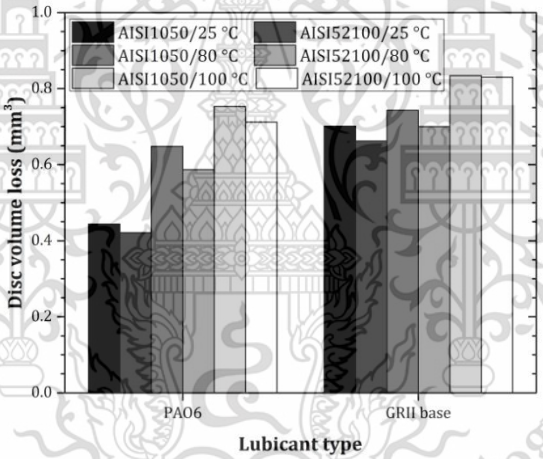


**Figure 65.** Effect of lubricants types on wear performance

### 4.3 Effect of operating temperature on wear performance of model lubricants

The effect of an operating temperature at NSTDA tribometer with ball-on-disc configuration was investigated by variation of oil bath temperature to 25 °C, 80 °C and 100 °C. From Figure 66, the disc volume loss of test lubricating oils without

ZDDP anti-wear additive exceedingly increased when the operating temperature was increased. The results were in accordance with the previous work published by Morina et al. [40]. It could be linked to a reduction of viscosity which would result in more severe lubrication conditions with more asperities contact. From Figure 67, the disc volume loss of ZDDP-containing lubricants considerably decreased when the operating temperature was increased. The results were in good agreement with the recent studies by [43-45]. It could be attributed to a thicker ZDDP tribofilm being formed at a higher temperature as reported by [43-45]. From figure 68, it could be seen that wear was reduced when ZDDP anti-wear additive was added into both base stocks used in this thesis. The example of roughness profiles of tested disc specimens at 25 °C, 80 °C and 100 °C are shown in Figure 69. It could be seen that the depth of wear scar increased when the operating temperature was increased. Owing to operating temperature at 80 °C and 100 °C wear performance of lubricant are not significantly different, the operating temperature of oil bath of TISTR tribometer with ball-on-disc configuration was lessened to 25 °C and 100 °C only.

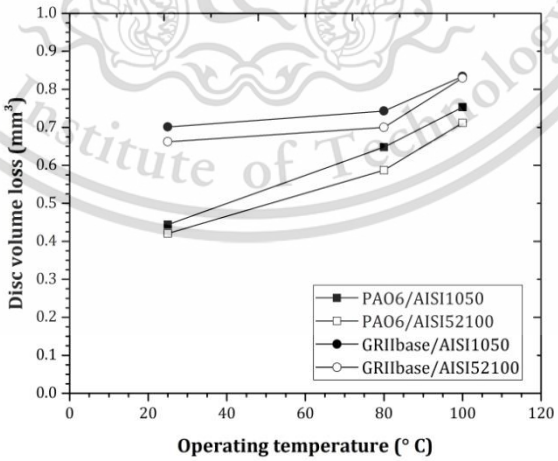

**Figure 66.** Effect of operating temperature on wear performance of lubricant without ZDDP.

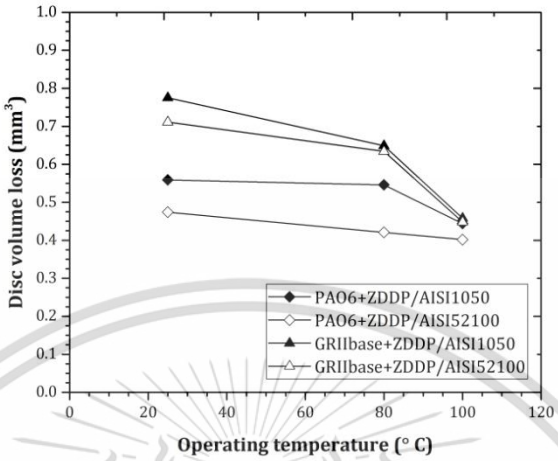


**Figure 67.** Effect of operating temperature on wear performance of ZDDP-containing lubricants.

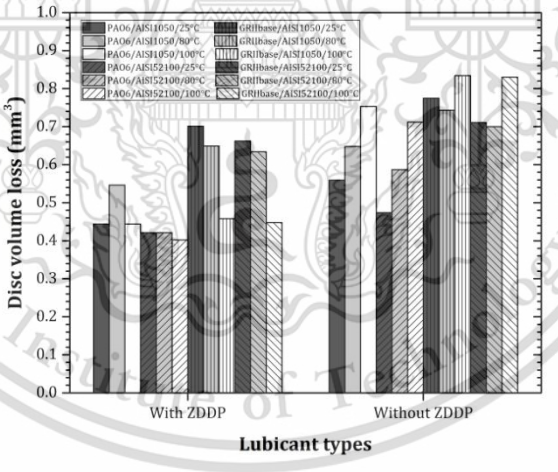

**Figure 68.** Effect of ZDDP anti-wear additive on wear performance.

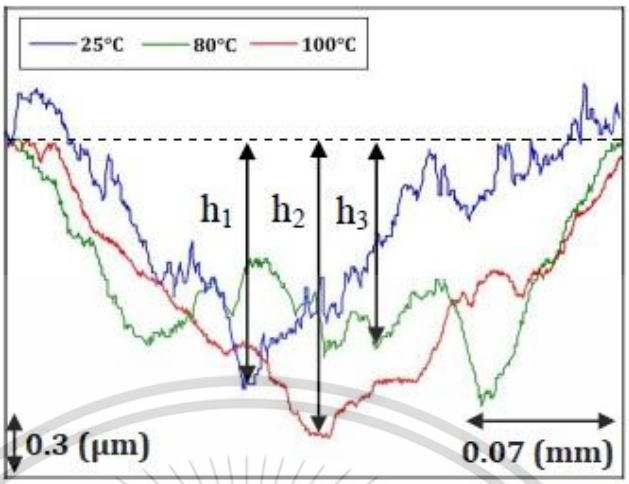


**Figure 69.** Comparison of wear scar profile from disc specimens at different operating temperature.

### 4.4 Lubricant film thickness calculation using elasto-hydrodynamic lubrication theory

In this thesis, lubricant film thickness comprises of central film thickness and minimum film thickness. The formulae for calculation of the central and minimum film thickness in elastro-hydrodynamic lubrication (EHL) contacts are in following form (2.4) and (2.5), these formulae derived by Hamrock and Dowson [9] which can apply to any contact and can be used with any material.

$$\frac{h_c}{R'} = 2.69\left(\frac{U\eta_0}{E'R'}\right)^{0.67}(\alpha E')^{0.53}\left(\frac{W}{E'R'^2}\right)^{-0.067}(1 - 0.61e^{-0.73k}) \quad (2.4)$$

$$\frac{h_0}{R'} = 3.63\left(\frac{U\eta_0}{E'R'}\right)^{0.68}(\alpha E')^{0.49}\left(\frac{W}{E'R'^2}\right)^{-0.073}(1 - e^{-0.68k}) \quad (2.5)$$

Where:

$h_c$ is the central film thickness [m].

$h_0$ is the minimum film thickness [m].

U is entrainment surface velocity [m/s].

$\eta_0$ is the viscosity at atmospheric pressure of the lubricant [Pas].

$E'$ is the reduced Young's modulus [Pa].

$R'$ is the reduced radius of curvature [m].

$\alpha$ is the pressure-viscosity coefficient [$m^2$/N].

W is the contact load [N].

k is the ellipticity parameter.

The contact between ball-on-disc configuration which used in this thesis can be represented by two spheres is enveloped by a circle, the contact parameter can calculate in accordance with the formulae as (2.1) [1].

$$\frac{1}{R'} = \frac{1}{R_x} = \frac{1}{R_y} = \frac{1}{R_{ax}} + \frac{1}{R_{bx}} + \frac{1}{R_{ay}} + \frac{1}{R_{by}} \quad (2.1)$$

Where:

$$\frac{1}{R_x} = \frac{1}{R_{ax}} + \frac{1}{R_{bx}}$$

$$\frac{1}{R_y} = \frac{1}{R_{ay}} + \frac{1}{R_{by}}$$

$R_x$ is the reduced radius of curvature in the x direction [m].

$R_y$ is the reduced radius of curvature in the y direction [m].

$R_{ax}$ is the reduced radius of curvature of body A in the x direction [m].

$R_{ay}$ is the reduced radius of curvature of body A in the y direction [m].

$R_{bx}$ is the reduced radius of curvature of body B in the x direction [m].

$R_{by}$ is the reduced radius of curvature of body B in the y direction [m].

The radii of curvature of the sphere are symmetry applies so that $R_{ax} = R_{ay} = R_A$ and $R_{bx} = R_{by} = R_B$. The reduced radius of curvature according to (2.1) is therefore given by

$$\frac{1}{R'} = \frac{1}{R_x} + \frac{1}{R_y} = 2\left(\frac{1}{R_A} + \frac{1}{R_B}\right) \quad (2.2)$$

Where:

$$\frac{1}{R_x} = \frac{1}{R_y} = \frac{1}{R_A} + \frac{1}{R_B}$$

According to ball-on-disc configuration $R_x = R_A = 6.35 \times 10^{-3}$ [m] and $R_y = R_B = 44.75 \times 10^{-3}$ respectively [m].

$$\frac{1}{R'} = 2\left(\frac{1}{3.18 \times 10^{-3}} + \frac{1}{44.75 \times 10^{-3}}\right)$$

$$R' = 1.48 \times 10^{-3}\text{[m]}$$

The reduced Young's modulus is defined as: (2.3).

$$\frac{1}{E'} = \frac{1}{2}\left(\frac{1-\nu_A{}^2}{E_A} + \frac{1-\nu_B{}^2}{E_B}\right) \quad (2.3)$$

Where:

$\nu_A$ and $\nu_B$ are the Poisson's ratios of the contacting bodies A and B respectively.

$E_A$ and $E_B$ are the Young's modulus of the contacting bodies A and B respectively [Pa].

The Poisson ratio of ball and disc are 0.3, Young's modulus of a ball and AISI 52100 disc specimens are $2.1 \times 10^{11}$ [Pa] and Young's modulus of AISI 1050 disc specimens is $2.05 \times 10^{11}$ [Pa].

$$E_1' = 2.31 \times 10^{11}\text{[Pa]}$$

$$E_2' = 2.28 \times 10^{11}\text{[Pa]}$$

Where:

$E_1'$ is reduce Young's modulus of AISI 52100 disc specimens.

$E_2'$ is reduce Young's modulus of AISI 1050 disc specimens.

The lubricant central film thickness and minimum film thickness are shown in Table7, Table 8 and Figure 70. Both lubricant film thicknesses are depended on disc specimen's materials, lubricant base stocks and operating temperature. In accordance with the result, lubricant film thicknesses of AISI 52100 disc specimens have slightly higher than AISI 1050 disc specimens, it could be attributed to AISI 52100 disc specimens have higher mechanical properties and tribological performance than AISI 1050 disc specimens. Besides, lubricant film thicknesses substantially decreased when operating temperature was increased, the results corroborate with the previous results in section 4.3 effect of operating temperature on wear performance of model lubricants it can be illustrated which operating temperature was increased, film thickness will be decreased resulting in a cause more wear, it could be linked to more severe lubrication conditions with more asperities contact. Furthermore, PAO6 base stocks have lubricant film thicknesses trivially higher than Group II base stocks, the results support with the recent results in section 4.2 effect of lubricant types on wear performance of model lubricants, it could be because PAO 6 base stocks have better wear performance than Group II base stocks. Nevertheless, the lubricant film thicknesses of Group II base stocks at an operating temperature of 25 °C have considerably higher than PAO 6 base stocks at an operating temperature of 25 °C.

**Table 7.** Central lubricants film thicknesses.

| Material | Lubricant | temperature(°C) | $h_c$(nm) |
|---|---|---|---|
| AISI 52100 | PAO6 base stock | 25 | 123.36 |
| | | 80 | 34.25 |
| | | 100 | 22.79 |
| | Group II base stock | 25 | 162.66 |
| | | 80 | 33.90 |
| | | 100 | 20.97 |
| AISI1050 | PAO6 base stock | 25 | 123.25 |
| | | 80 | 34.22 |
| | | 100 | 22.77 |
| | Group II base stock | 25 | 162.52 |
| | | 80 | 33.87 |
| | | 100 | 20.95 |

**Table 8.**Minimum lubricants film thicknesses.

| Material | Lubricant | temperature(°C) | $h_{min}$(nm) |
|---|---|---|---|
| AISI 52100 | PAO6 base stock | 25 | 101.507 |
| | | 80 | 27.796 |
| | | 100 | 18.409 |
| | Group II base stock | 25 | 130.984 |
| | | 80 | 27.103 |
| | | 100 | 16.720 |
| AISI1050 | PAO6 base stock | 25 | 101.463 |
| | | 80 | 27.784 |
| | | 100 | 18.401 |
| | Group II base stock | 25 | 130.926 |
| | | 80 | 27.091 |
| | | 100 | 16.712 |

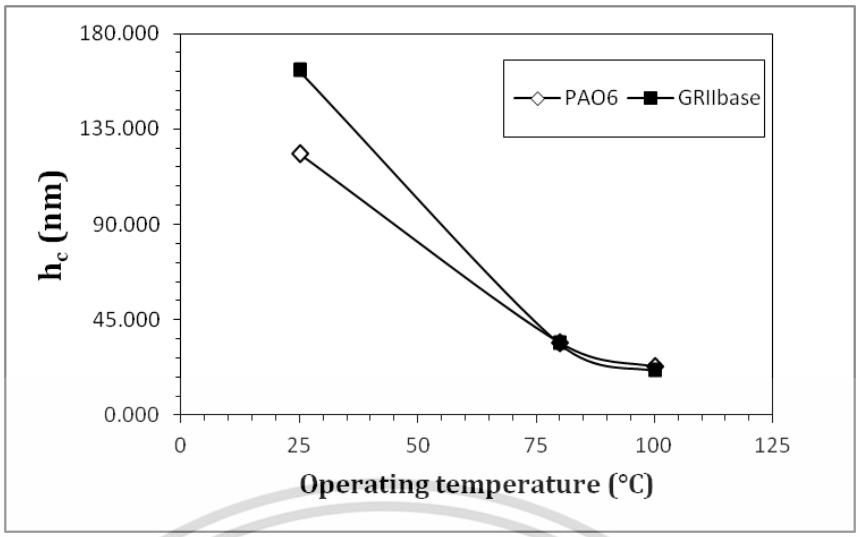


(a) Central film thicknesses.

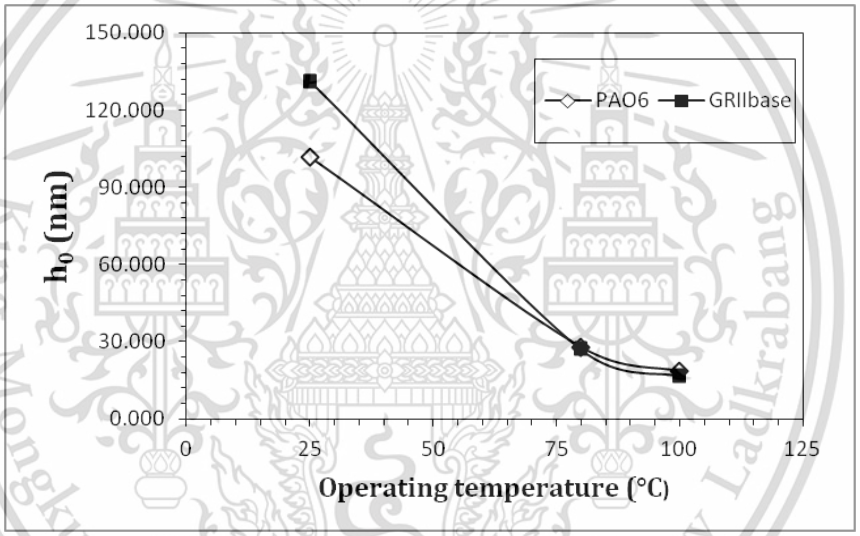


(b) Minimum film thicknesses.

**Figure 70.** Lubricant film thicknesses.

### 4.5 Optical Microscope and Scanning Electron Microscope wear mechanism qualitative analysis

Figure 71 and 73 have shown Optical Microscope micrographs at 5 magnifications of the wear track observed on disc specimens at different operating

temperatures: 25 °C, 80 °C and 100 °C. Furthermore, Figure 72 and 74 have shown Optical Microscope micrographs with higher resolution at 20 magnifications, in accordance with the results, wear track is in parallel along with the sliding direction in the case of low operating temperature, the wear track is narrow than higher operating temperature which can imply that while operating temperature was increased wear will probably increase. The results are in line with the precedent result in section 4.3 effect of operating temperature on wear performance of model lubricants. Besides, wear characteristic in low and moderate operating temperatures which have grooves parallel along with the sliding direction, that were mechanisms of abrasive wear [1]. Wear characteristic in a high operating temperature range which has grooves parallel along with the sliding direction nonetheless, which has some form of some crack and delamination in the wear track zone, which are the mechanism of abrasive wear and fatigue wear consecutively [1]. In order that investigates qualitative wear mechanism analysis, table size 7 x 53 grids, 5 x 53 grids and 16 x 53 grids were created related to operating temperature at 25 °C, 80 °C and 100 °C respectively as shown in Figure 75. In Figure 76, qualitative wear mechanism show that influential wear mechanism is abrasive wear nevertheless, fatigue wear mechanism present in a high operating temperature range.

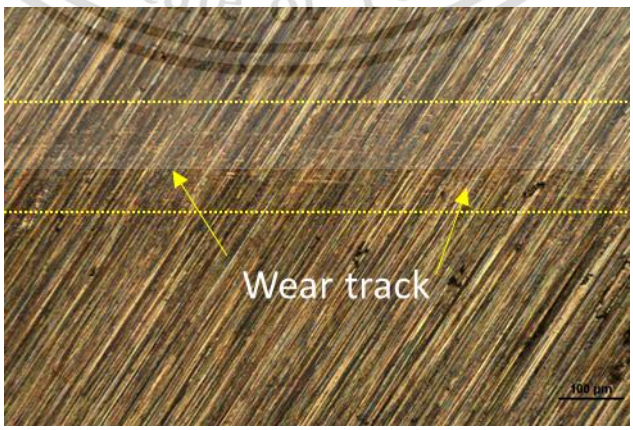


(a) 25 °C

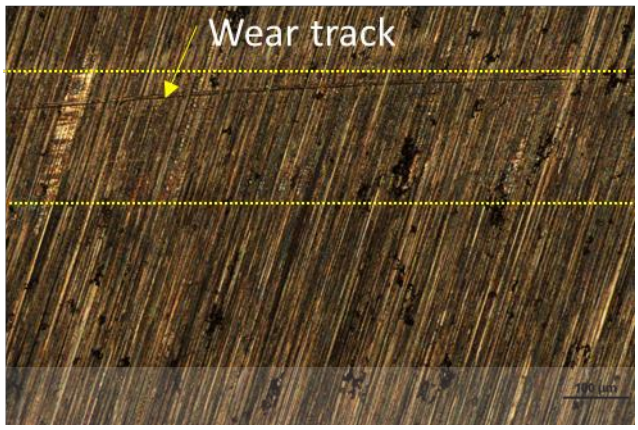


(b) 80 °C

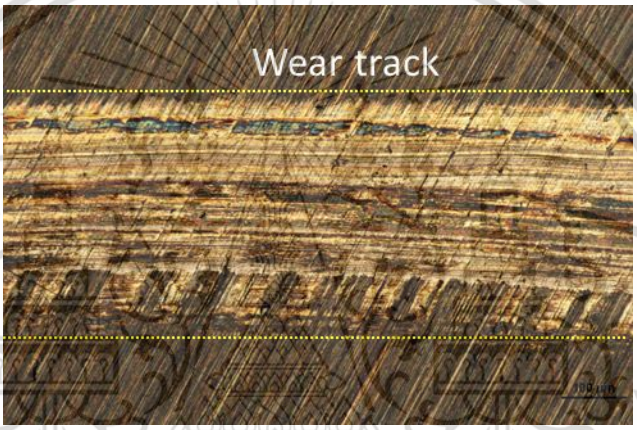


(c) 100 °C

**Figure 71.** OM micrographs of disc specimens at 5 magnifications with wear track identify.

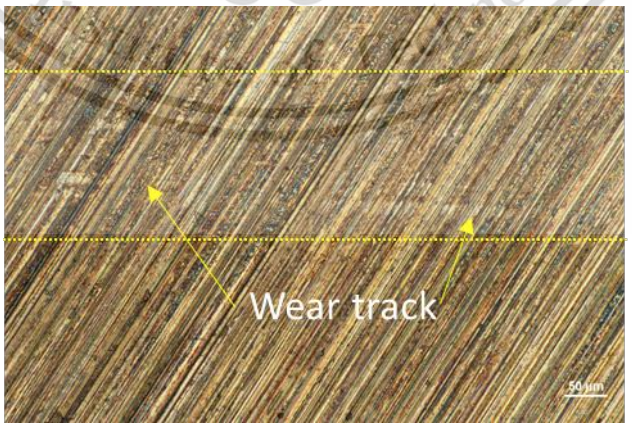


(a) 25 °C

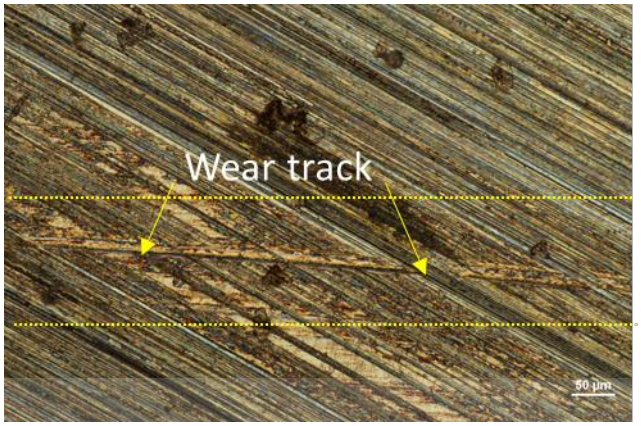


(b) 80 °C


(c) 100 °C

**Figure 72.** OM micrographs of disc specimens at 20 magnifications with wear track identify.

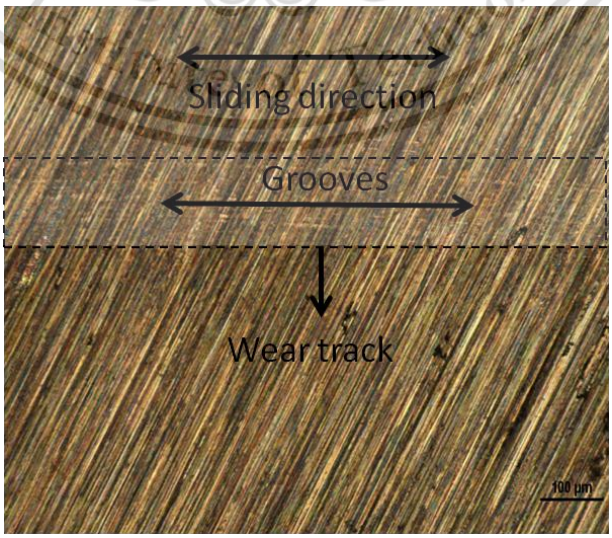

(a) 25 °C

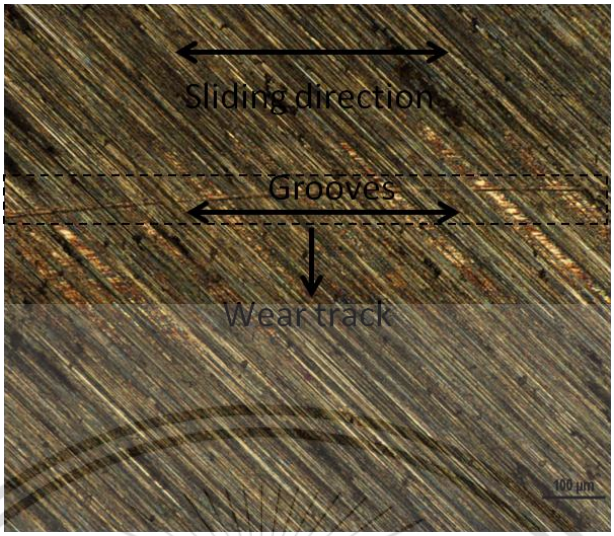


(b) 80 °C

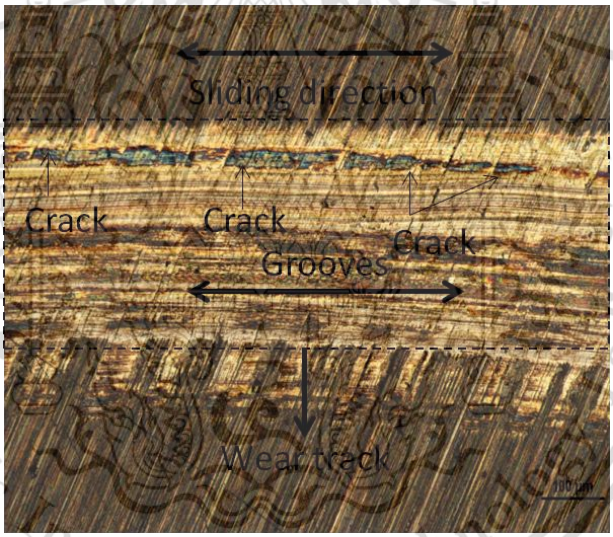


(c) 100 °C

**Figure 73.** OM micrographs of disc specimens at 5 magnifications with wear classify.

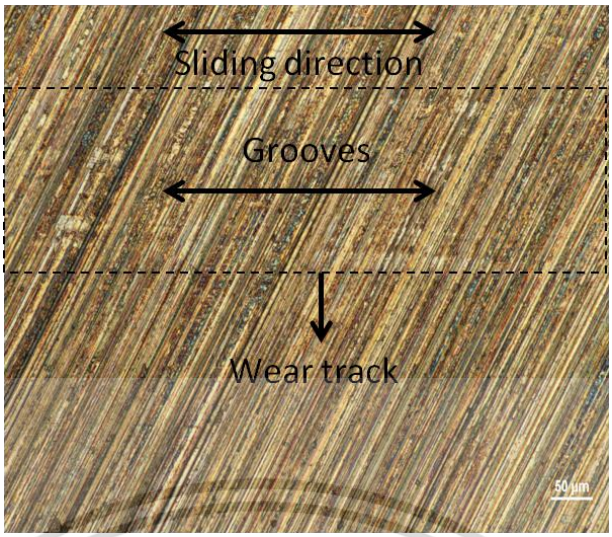


(a) 25 °C

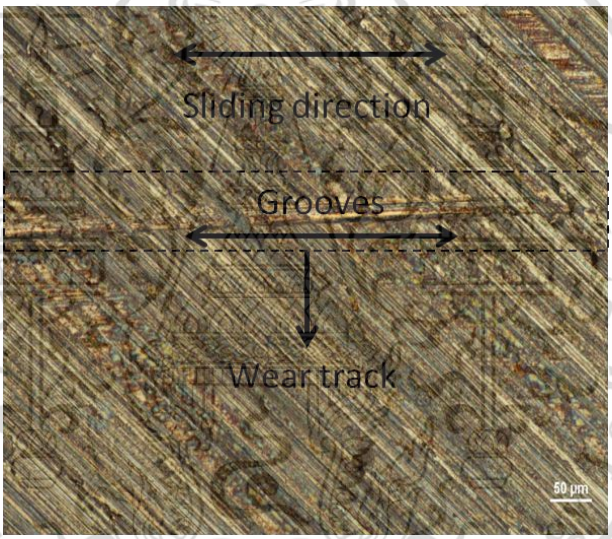


(b) 80 °C

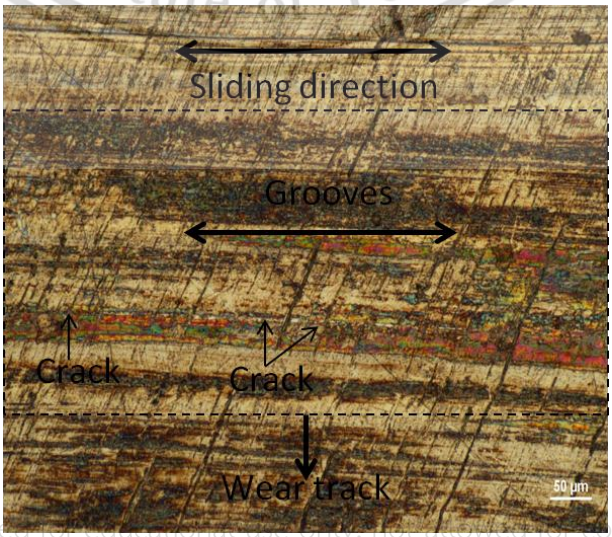

(c) 100 °C

**Figure 74.** OM micrographs of disc specimens at 20 magnifications with wear classify.

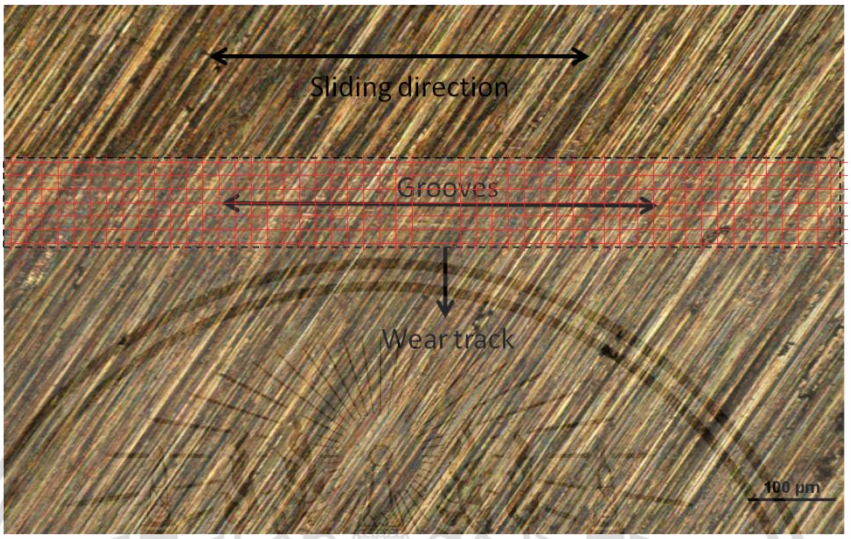


(a) 25 °C

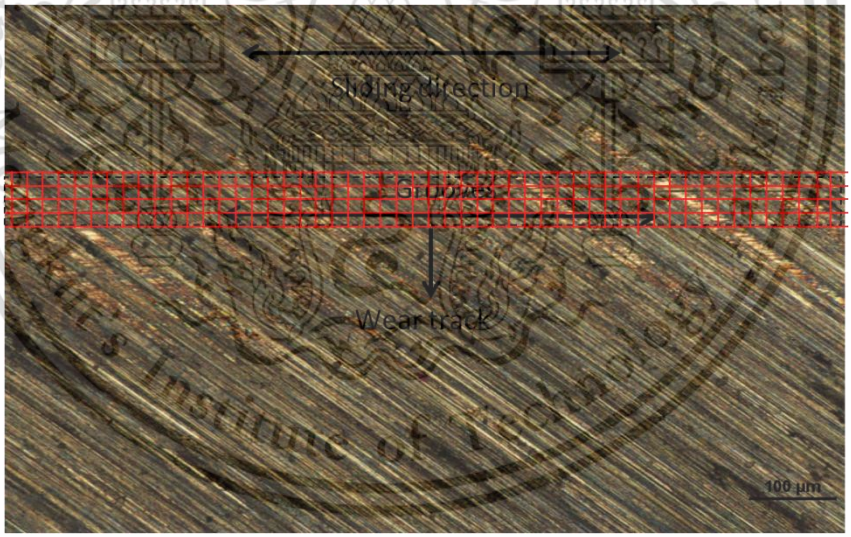


(b) 80 °C

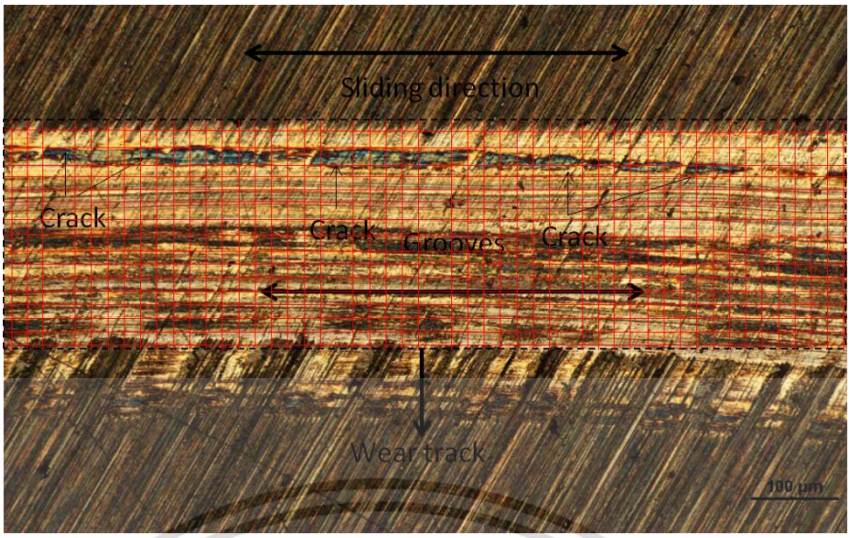


(c) 100 °C

**Figure 75.** OM micrographs of disc specimens at 5 magnifications with grid analysis.

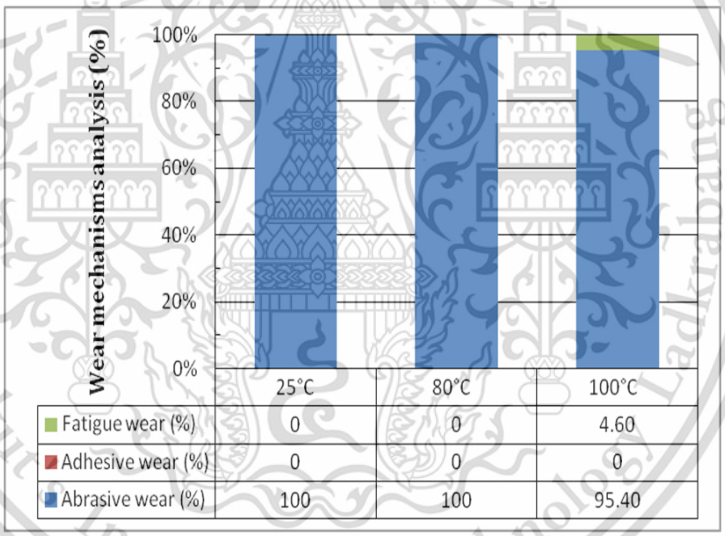


**Figure 76.** OM wear mechanisms qualitative analysis of disc specimens.

Figure 77 and 79 have shown Scanning Electron Microscope micrographs at 500 magnifications of the wear track observed on disc specimens at different lubricant base stock: PAO6 base stock and Group II base stock. Furthermore, Figure 78 and 80 have shown Scanning Electron Microscope micrographs with higher resolution at 3,000 magnifications, according to the results; wear tracks are parallel along with sliding direction, plastic deformation and some crack and delamination are observed

in both PAO 6 base stock and Group II base stock respectively, which are abrasive wear, adhesive wear and fatigue wear mechanism consecutively [1]. To study qualitative wear mechanism analysis, table of 38 x 53 grids were created for both PAO6 and Group II base stock as shown in Figure 81. In Figure 82, qualitative wear mechanism analysis showed that Group II base stock have more abrasive and fatigue wear mechanism than PAO 6 base stock notwithstanding; Group II base stock has less adhesive wear mechanism than PAO 6 base stock. It could be attributed to Group II base stock gave a lower wear performance than PAO 6 base stock the results is in accordance with the previous results in section 4.2 effect of lubricant types on wear performance of model lubricants.

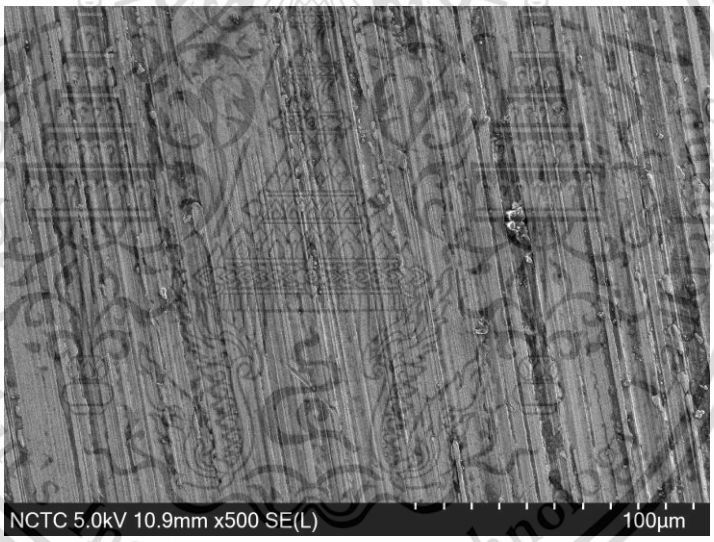


(a) PAO 6 base stock


(b) Group II base stock

**Figure 77.** SEM micrographs of disc specimens at 500 magnifications.

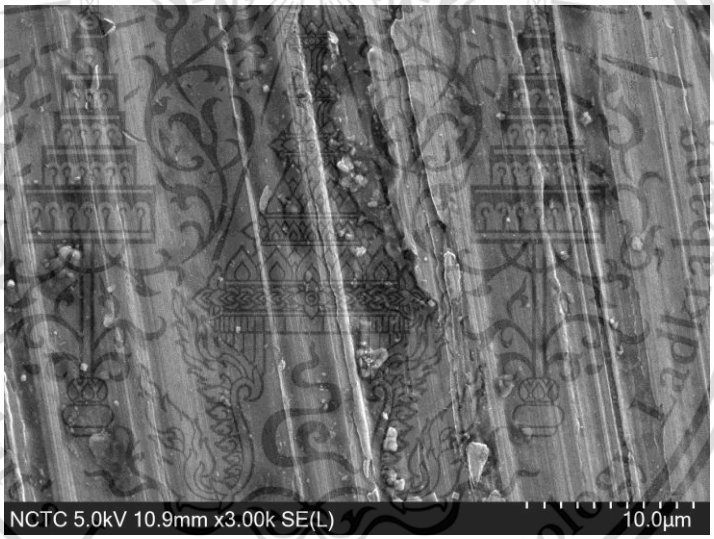


(a) PAO 6 base stock

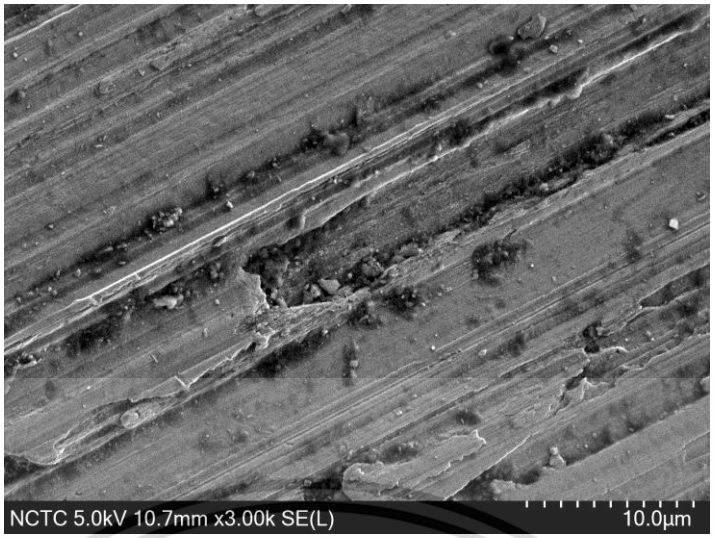


(b) Group II base stock

**Figure 78.** SEM micrographs of disc specimens at 3,000 magnifications.

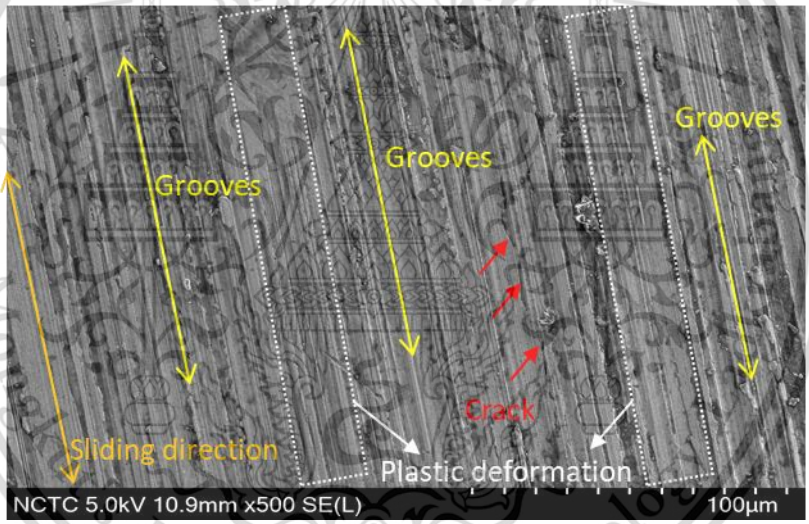


(a) PAO 6 base stock

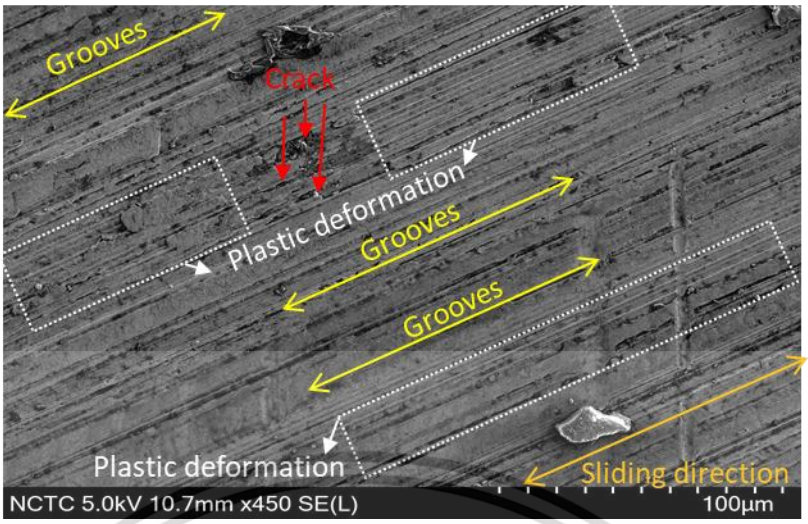


(b) Group II base stock

**Figure 79.** SEM micrographs of disc specimens at 500 magnifications with wear classify.

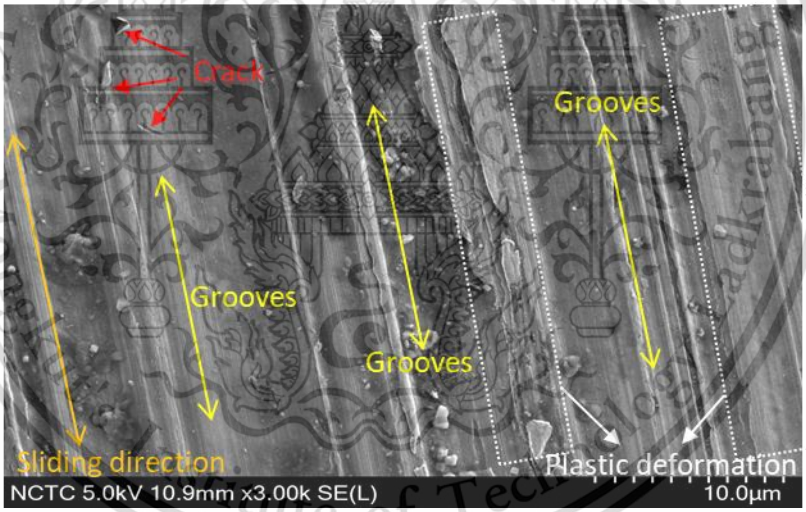


(a) PAO 6 base stock

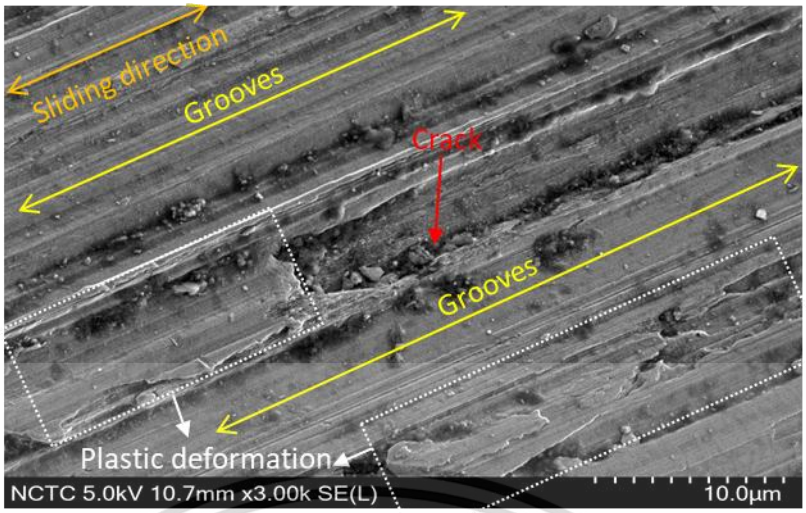


(b) Group II base stock

**Figure 80.** SEM micrographs of disc specimens at 3,000 magnifications with wear classify.

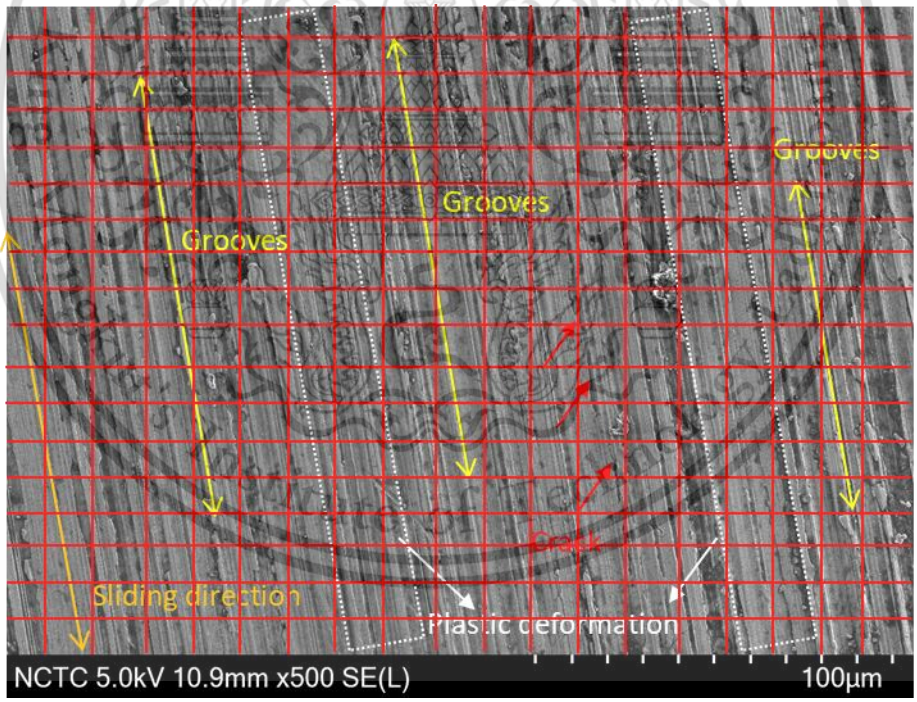


(a) PAO 6 base stock

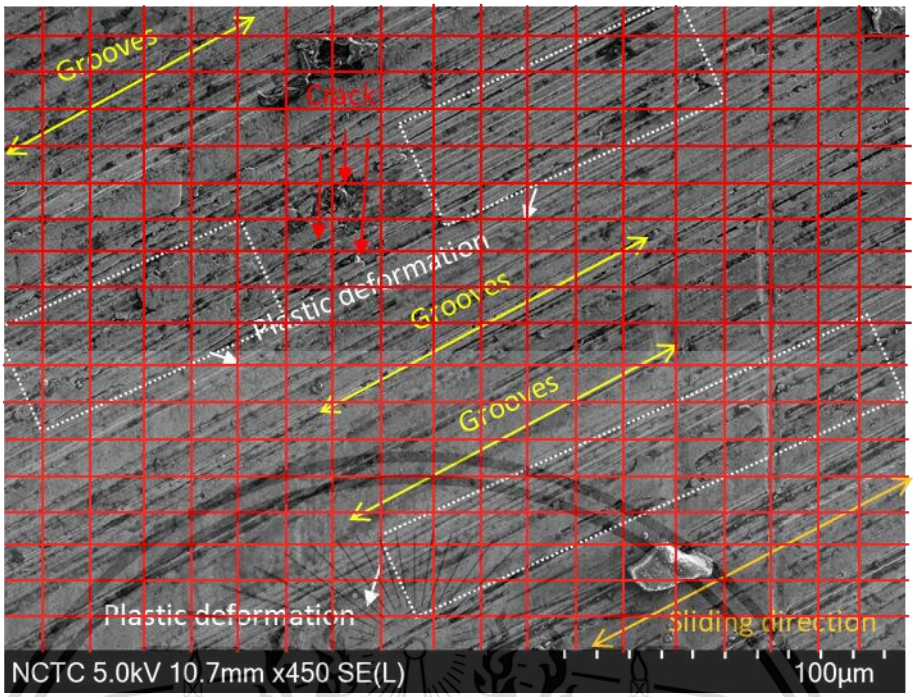


(b) Group II base stock

**Figure 81.** SEM micrographs of disc specimens at 3,000 magnifications with grid analysis.

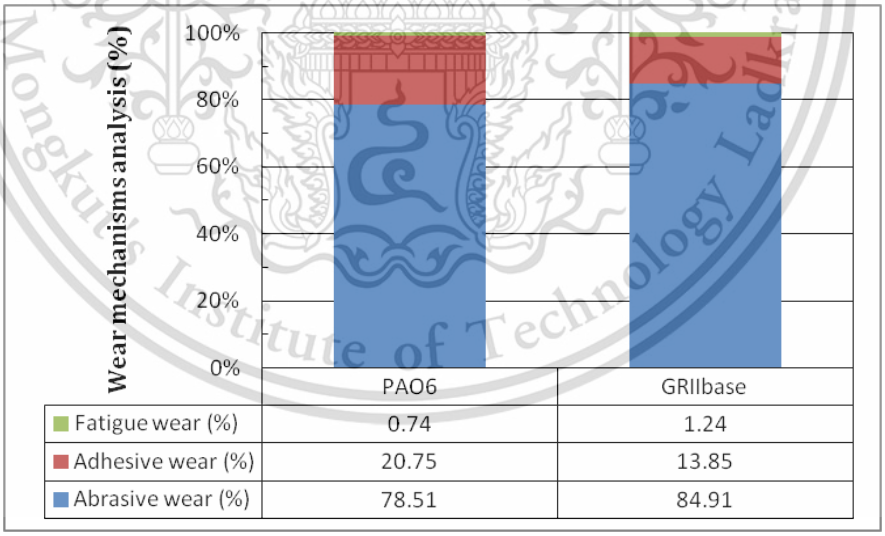


| | PAO6 | GRIIbase |
|---|---|---|
| Fatigue wear (%) | 0.74 | 1.24 |
| Adhesive wear (%) | 20.75 | 13.85 |
| Abrasive wear (%) | 78.51 | 84.91 |

**Figure 82.** SEM wear mechanisms qualitative analysis of disc specimens

# CHAPTER 5

# RESULTS AND DISCUSSIONSPART II

In this part of a thesis, the entire tribological experiments were conducted on TISTR tribometer with ball-on-disc configuration. Apart from original lubricant samples, other groups of lubricant samples were ageing with oxidation and additional ethanol in order that investigates the effect of aged lubricant on tribological performance of model lubricants. Besides, the operating temperatures were diminished from 25 °C, 80 °C and 100 °C to 25 °C and 100 °C only and disc specimens' material were lessened form AISI 52100 and AISI 1050 disc specimens to AISI 52100 disc specimens only because of the wear behavior of lubricants at moderate and high operating temperature meaningless different and wear behavior of both disc specimens material also insignificant different consecutively.

## 5.1 Study the ageing characteristic of lubricants by aged with oxidation and the addition of ethanol

The degradation of lubricating oil by artificial alteration can evaluate by three efficient bulk properties of lubricants, i.e. kinematic viscosity, Total Acid Number (TAN) and Oxidation value were investigated according to standard ASTM D445, ASTM D664 and standard ASTM D7214 respectively. In addition, the test method or apparatus for each value was viscometer, digital density meter, potentiometric titration and FTIR spectrometry using peak area increase (PAI) calculation method, consecutively. Moreover, the changeable color of lubricating oil, the formation of

sludge and vanish presence in lubricating oils were also used as deterioration parameter of aged lubricants.

### 5.1.1 Aged lubricants with oxidation

Lubricant sample which used in ageing experiment comprises of Group II base stock and PAO 6 base stock. After lubricant samples aged with oxidation, the three efficient bulk properties of lubricants, i.e. kinematic viscosity, Total Acid Number (TAN) and oxidation value were changed. In accordance with the results from Figure 83-85 and Figure 88-90 results of Group II base stocks and PAO 6 base stocks consecutively, the kinematic viscosity value, Total Acid Number (TAN) value and Oxidation value (FTIR) were substantially increased when oxidation time or ageing time was increased. It could be attributed to a mechanism of thermal decomposition or normal oxidation mechanism which compose of four mechanisms; initiation, chain-propagation, chain-branching and finally termination mechanism. The oxidation mechanisms are shown in Figure 93, the oxidation products consist of alkyl-hydro-peroxides (R-O-O-H), di-alkyl peroxide (R-O-O-R°), aldehydes (R-C=O-H), ketones (R-C=O-R°), carboxylic acids (R-C=O-O-H and ester (R-C=O-O-R°). In addition, the oxidation product can go through several further reactions that can induce to polymeric species will form more stable hydrocarbon which has higher molecular weight [25, 30]. Furthermore, FTIR absorbance spectrum of both Group II base stocks and PAO 6 base stocks are shown in Figure 86 and 91. In accordance with the result, the FTIR absorbance peaks at approximately 1700 cm-1 were a carbonyl peak, when the oxidation time was increased carbonyl peak considerably increased hence these carbonyl peaks are brought into calculated the peak area increase (PAI) using standard ASTM D7214. Besides, PAI values are illustrated the oxidation values as shown in

Figure 84. Moreover, the FTIR absorbance spectrum peak at approximately 1200 $cm^{-1}$ It was attributed to ester. In Figure 87, shown that the mutability of color of Group II base stocks with oxidation time, when oxidation time was increased the color of Group II base stock changed from colorless to light yellow, yellow, light orange, orange, brown, dark brown and eventually become black consecutively. In Figure 92, shown that the instability of color of PAO 6 base stocks with oxidation, when oxidation time increased the color of PAO 6 changed from colorless to light yellow, yellow, orange, light brown, brown and finally become black. In addition,artificial ageing with additional of ZDDP anti-wear additive the formation of sludge has occurred at the end of experiment as shown in Figure 94-95. To ensure that the formation of sludge, lacquer and varnish presence in lubricating oil further morphologies investigation are necessary, i.e. SEM, OM and chemical investigation, i.e. GC-MS, ICP-OES, XRF.

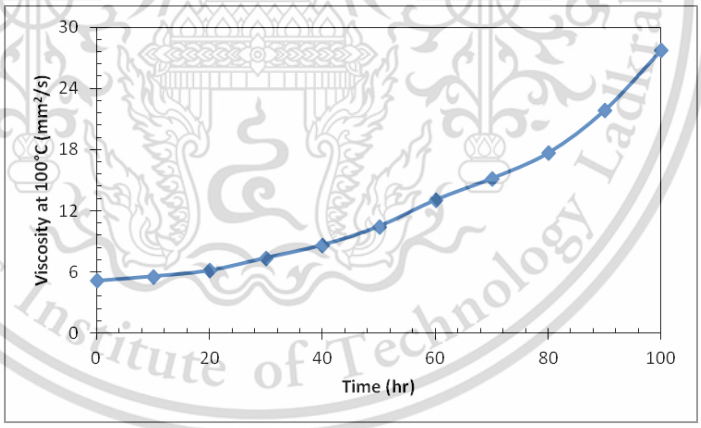


**Figure 83.** Viscosity values of Group II base stocks after ageing with oxidation.

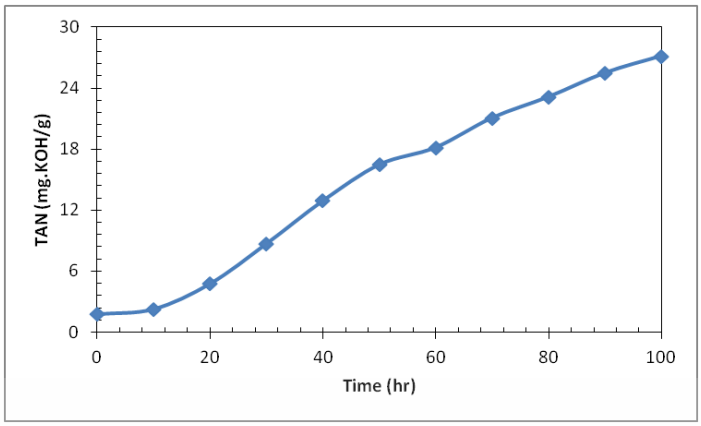


**Figure 84.** Total Acid Number values of Group II base stocks after ageing with oxidation.

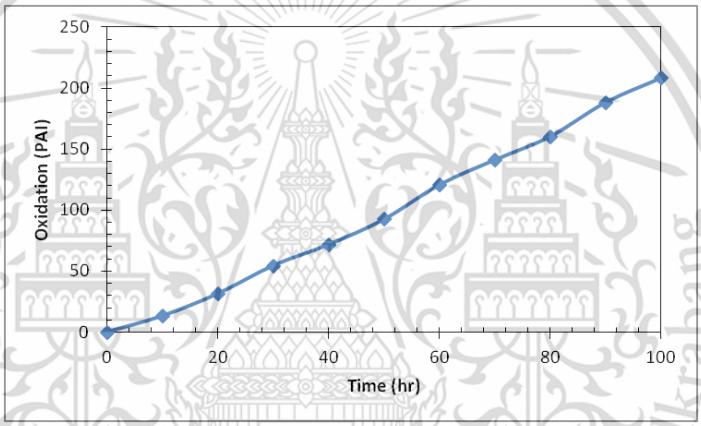


**Figure 85.** Oxidation values of Group II base stocks after ageing with oxidation

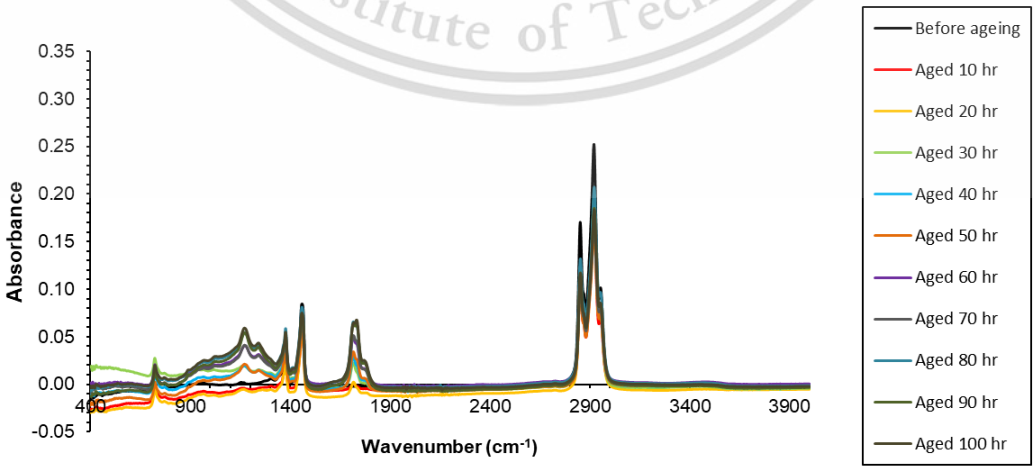

**Figure 86.** Comparison of FTIR absorbance spectrum of Group II base stocks after ageing with oxidation.

**Figure 87.** Changeable color of Group II base stocks after ageing with oxidation.

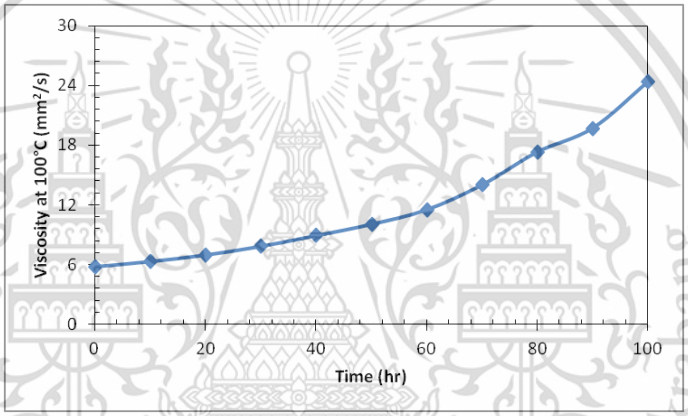


**Figure 88.** Viscosity values of PAO 6 base stocks after ageing with oxidation.

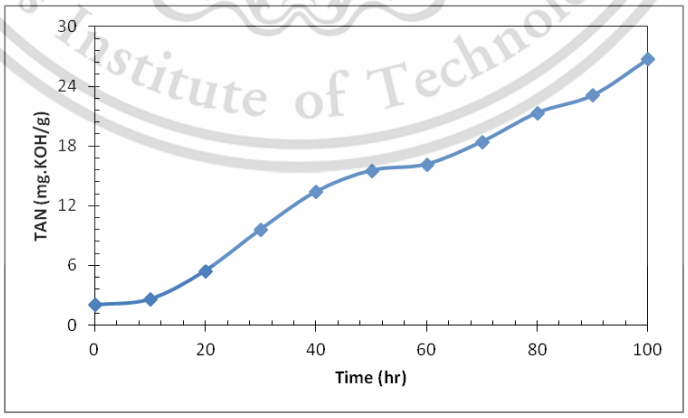

**Figure 89.** Total Acid Number values of PAO 6 base stocks after ageing with oxidation.

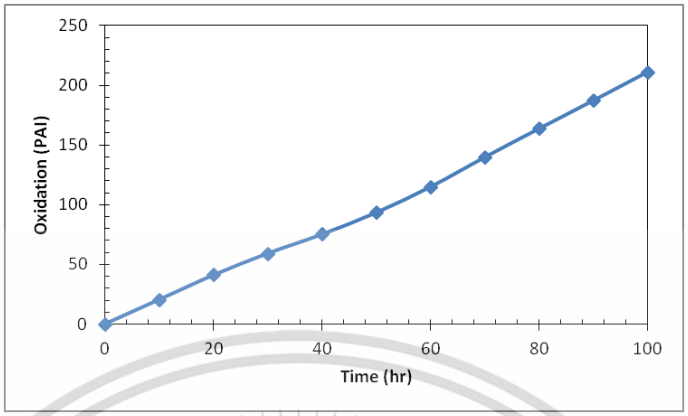


**Figure 90.**Oxidation values of PAO 6 base stocks after ageing with oxidation.

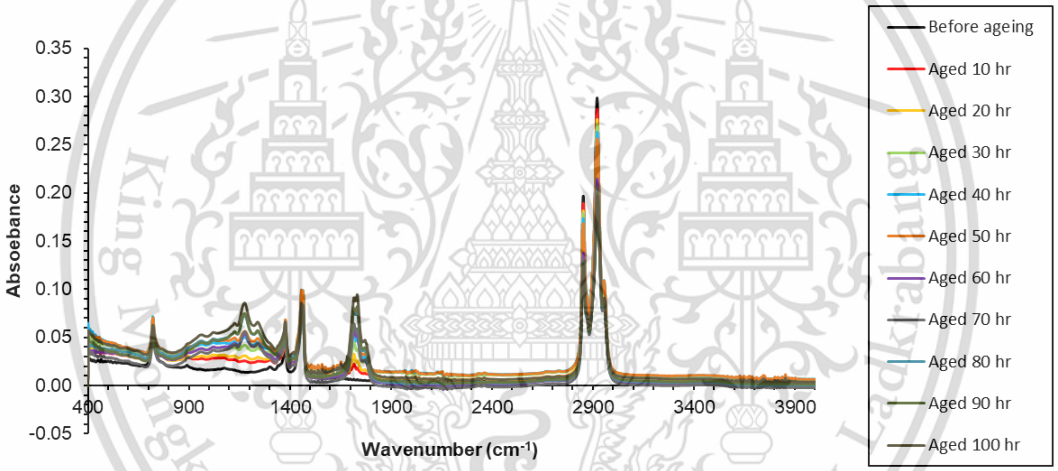


**Figure 91.** Comparison of FTIR absorbance spectrum of PAO 6 stocks after ageing with oxidation.

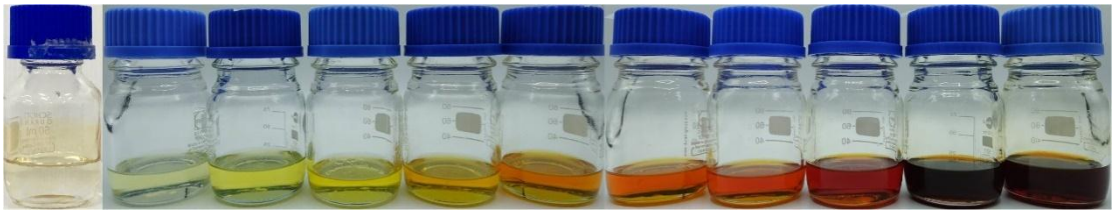

**Figure 92.** Changeable color of PAO 6 base stocks after ageing with oxidation.

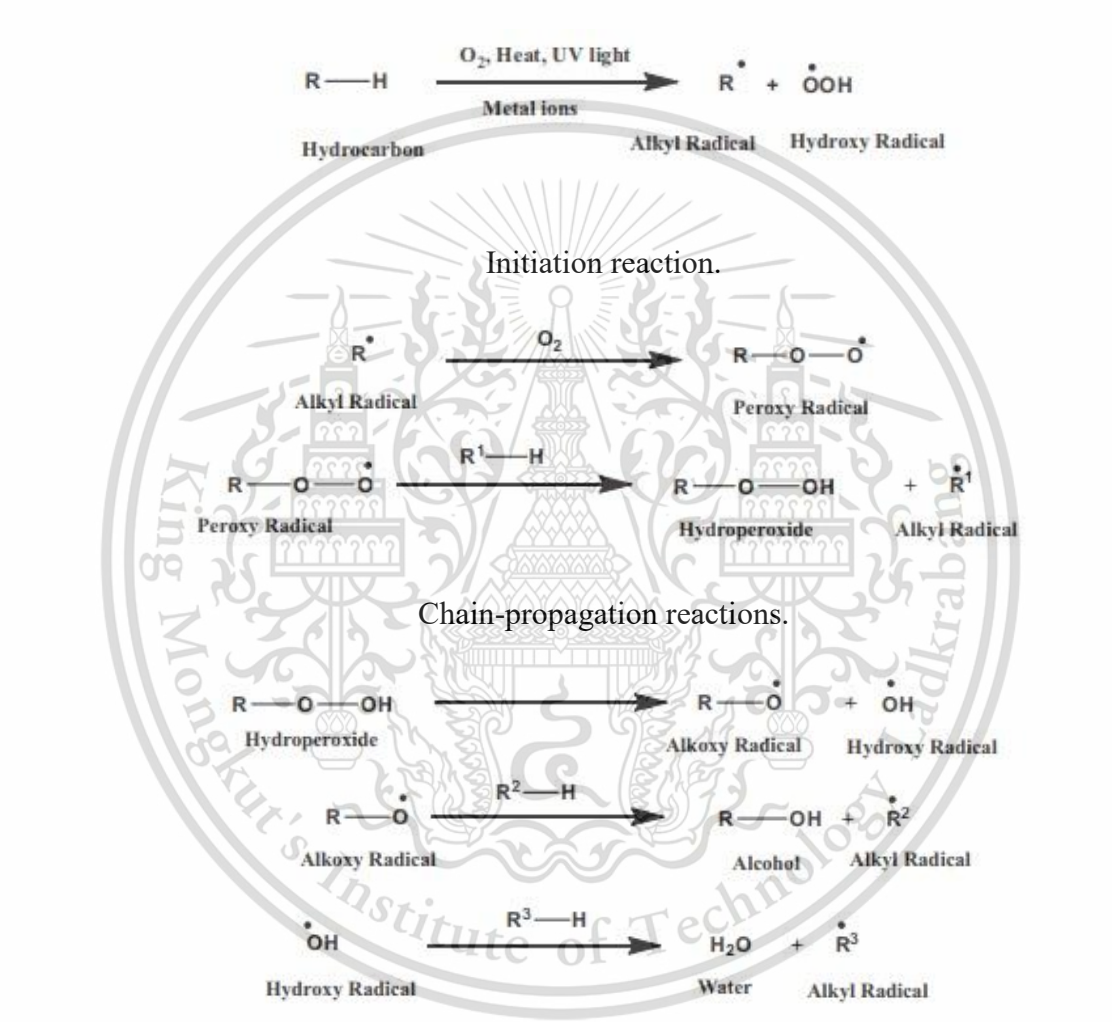

**Figure 93.**Oxidation mechanisms.

**Figure 94.** The formation of sludge of GRIIbase+ZDDP lubricants.

**Figure 95.**The formation of sludge of PAO6+ZDDP lubricants.

### 5.1.2 Aged lubricants with ethanol

Toperform artificial ageing with ethanol the cooling device was added at the center neck of the flask in set-up artificial ageing apparatus as shown in Figure 96. Because of a high volatility since a low boiling point of 78 ° C. For this reason, the dosing device had to be cooled down to ensure that the intended amount of ethanol is added into the lubricating oils.

The results after artificial ageing with addition of ethanol, the three efficient bulk properties of lubricants, i.e. kinematic viscosity, Total Acid Number (TAN) and

Oxidation (PAI) values were drastically increased when oxidation time or ageing time was increased. These results agree with the results of artificial ageing with air. It could be because to a thermal decomposition or normal oxidation mechanisms. Form mechanisms that mention earlier, the oxidation product consist of alkyl-hydro-peroxides (R-O-O-H), di-alkyl peroxides (R-O-O-R°), aldehydes (R-C=O-H), ketones (R-C=O-R°), carboxylic acids (R-C=O-O-H) and esters (R-C=O-O-R°). Furthermore, oxidation product can go through several further reactions that can be induce to polymeric species will form more stable hydrocarbon which has higher molecular weight. Form FTIRspectral data inform about carbonyl band that was occurred in the oxidation product whereas, spectral data was not enough to characterize what carbonyl band refer to, i.e. aldehydes, ketones, carboxylic acids or esters. To receive more information about oxidation product which mention earlier further investigations are necessary, i.e. GC-MS, ICP-OES, XRF, etc.Besides, the objective of these artificial ageing is ethanol has existed in the lubricating oil. Form this objective the FTIR investigation is significant to ensure that alcohol band was occurred in the spectral data of these lubricating oils. If alcohol band does not exist in the spectral data, it could be attribute to alcohol species was transform to another species or ethanol has evaporated out of lubricating oils.

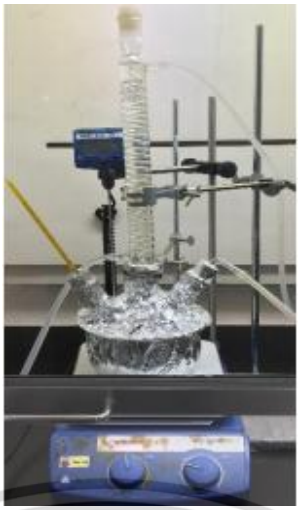

**Figure 96.** Schematic set-up of artificial ageing method with additional of ethanol.

The three efficient bulk properties of lubricant, i.e. kinematic viscosity, Total Acid Number (TAN) and oxidation value (FTIR) were investigated according to standard ASTM D445 [34], ASTM D664 [35], and standard ASTM D7214 [36] respectively. The chemical properties of lubricant after tribological experiment at a different operating temperature, i.e. 25 ° C and 100 ° C are shown in Figure 97-106. In accordance with the results, it could be seen that the change of kinematic viscosity, Total Acid Number (TAN) and Oxidation (PAI) values were substantially decreased when operating temperature was increased. These results are in line with the earlier results in the chapter 4 test lubricants which test on NSTDA tribometer with ball-on-disc configuration. It was proposed that when operating temperature increase lead to a decrease in viscosity. The reason of these behavior could be because at high operating temperature, the performance of bulk properties of model lubricants will enhance.

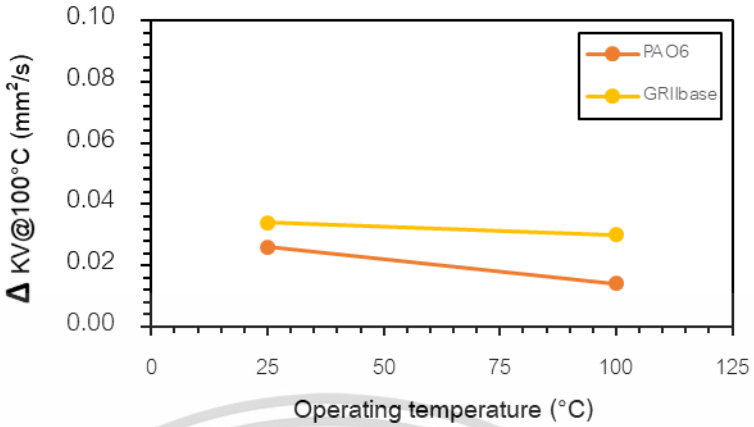


**Figure 97.** Kinematic viscosity of lubricants without ZDDP after tribological experiments.

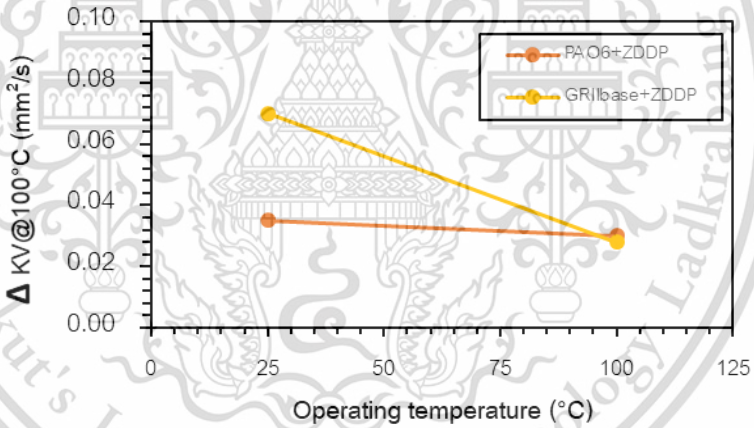


**Figure 98.** Kinematic viscosity of lubricants with ZDDP after tribological experiments.

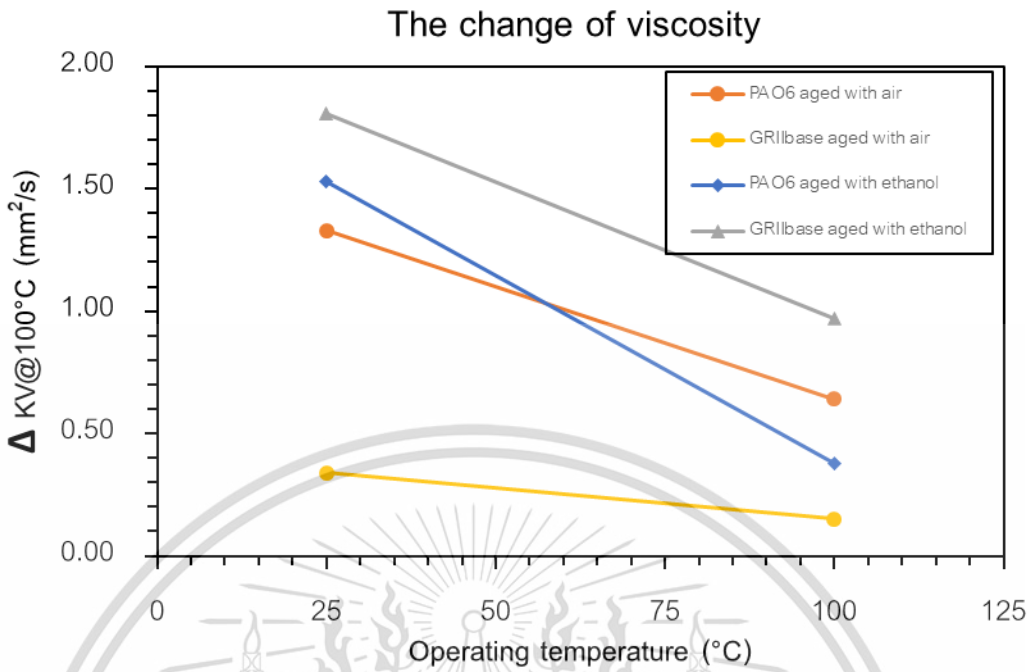


**Figure 99.** Kinematic viscosity of aged lubricants without ZDDP after tribological experiments.

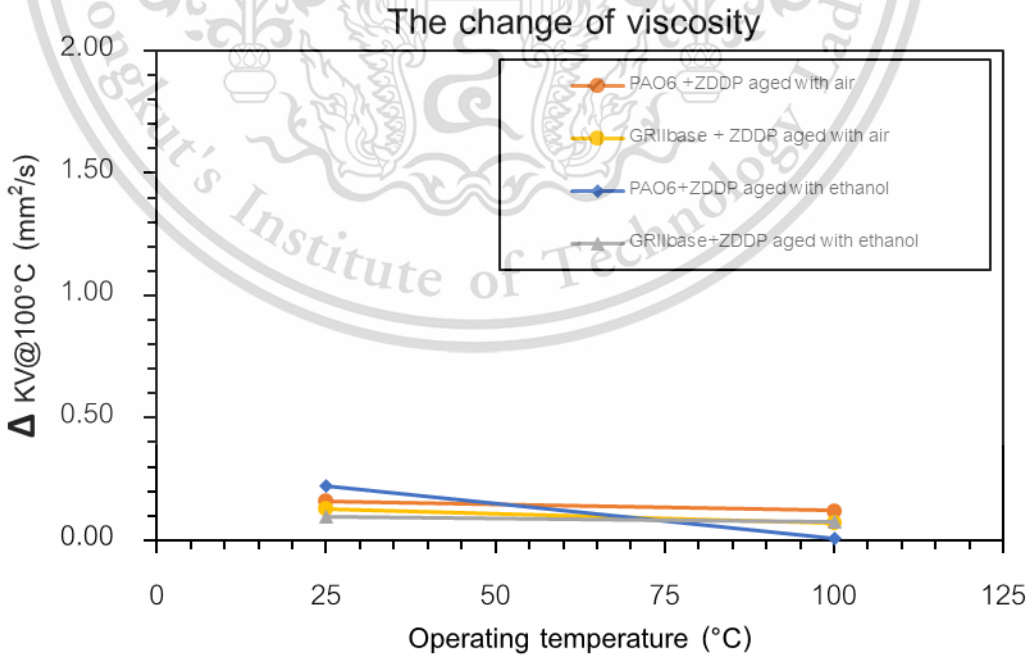

**Figure 100.** Kinematic viscosity of aged lubricants with ZDDP after tribological experiments.

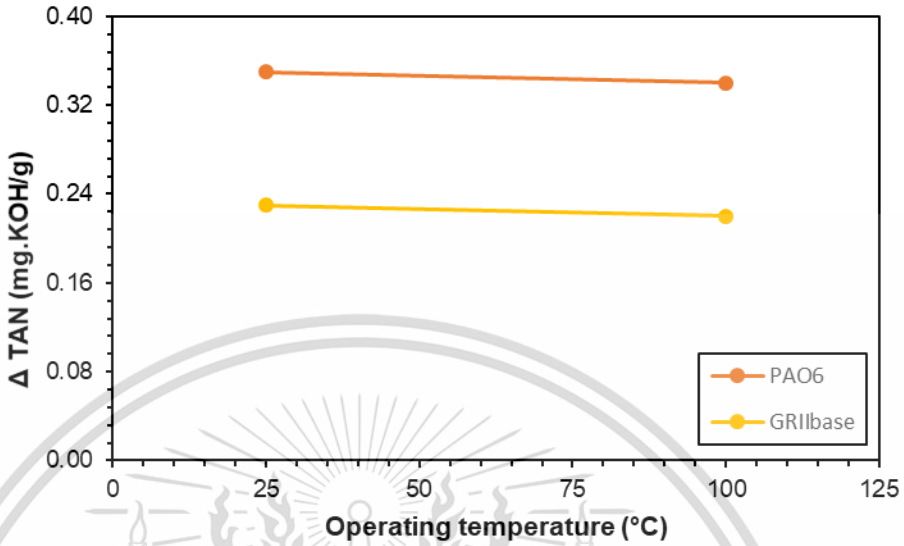


**Figure 101.** Total Acid Number (TAN) of lubricants without ZDDP after tribological experiments.

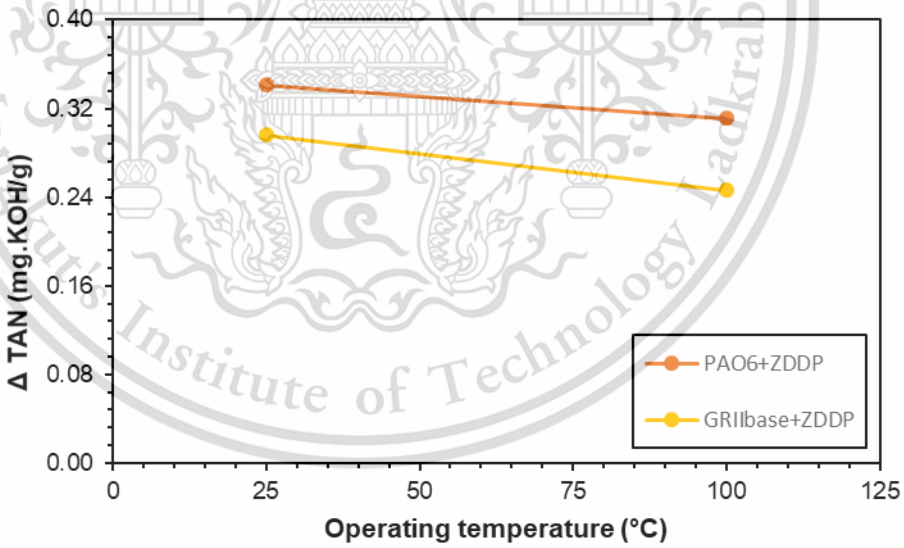

**Figure 102.** Total Acid Number (TAN) of lubricants with ZDDP after tribological experiments.

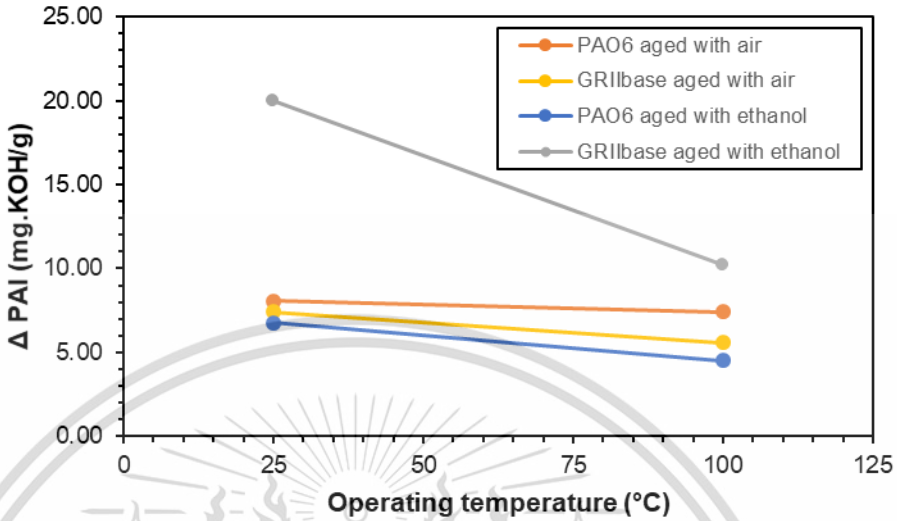


**Figure 103.** Total Acid Number (TAN) of aged lubricants without ZDDP after tribological experiments.

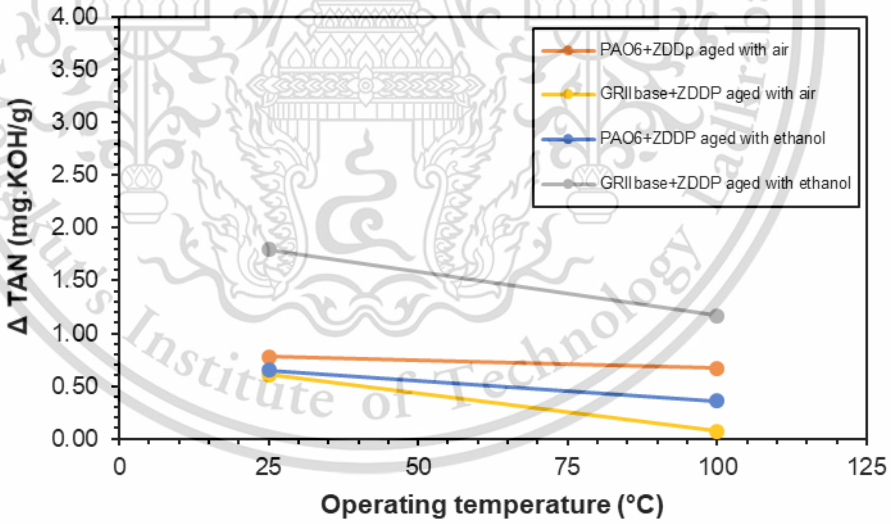

**Figure 104.** Total Acid Number (TAN) of aged lubricants with ZDDP after tribological experiments.

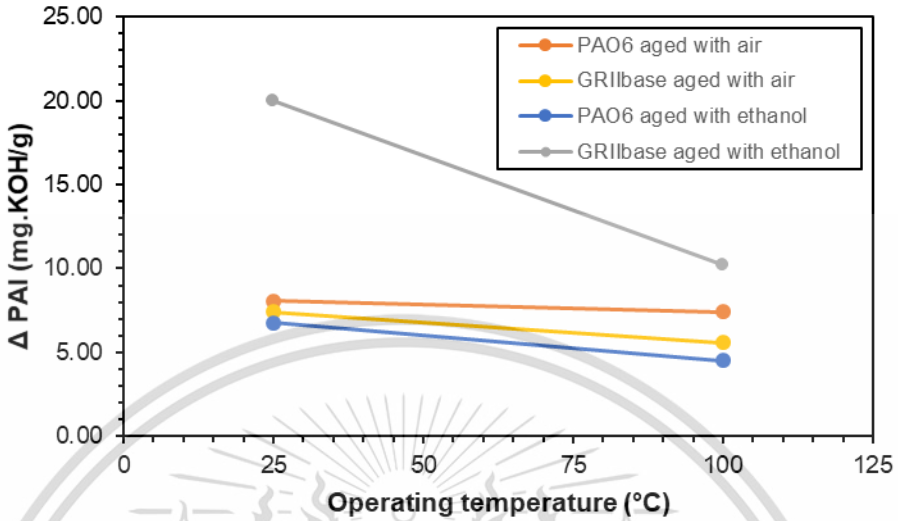


**Figure 105.** Oxidation (PAI) of aged lubricants without ZDDP after tribological experiments.

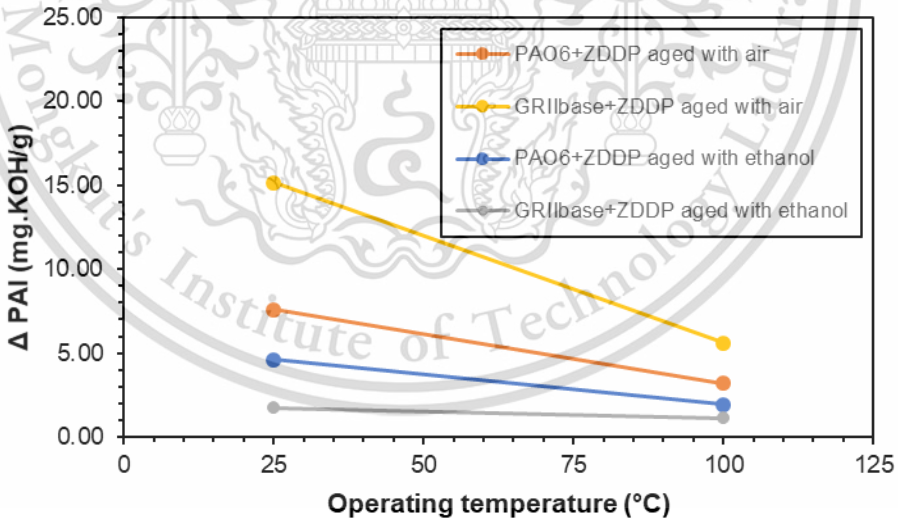


**Figure 106.** Oxidation (PAI) of aged lubricants with ZDDP after tribological experiments.

## 5.2 Study tribological performance of lubricants that was performed on TISTR tribometer with ball-on-disc configuration

### 5.2.1 The effect of lubricant types on wear performance of model lubricants

In this part of thesis model lubricants consist of PAO6 base stocks, Group II base stocks, PAO6 base stocks+ZDDP and Group II base stocks+ZDDP. According to the result in Figure 107, Group II base stocks resulted in higher volume loss than PAO6 base stocks and Group II base stocks + ZDDP resulted in higher volume loss than PAO6 base stocks + ZDDP respectively. More over lubricants with ZDDP anti-wear additive has better wear performance than lubricants without ZDDP anti-wear additive.It could be attribute to ZDDP protective-tribofilm has formed on the rubbed surface, resulting in wear reduction. The comparisondepth of wear scar at different types of model lubricant is shown in Figure 108. It could be seen that Group II base stocks and Group II base stocks with addition of ZDDP anti-wear additive resulted in higher depth of wear scar than PAO6 base stocks and PAO6 base stocks with addition of ZDDP anti-wear consecutively.

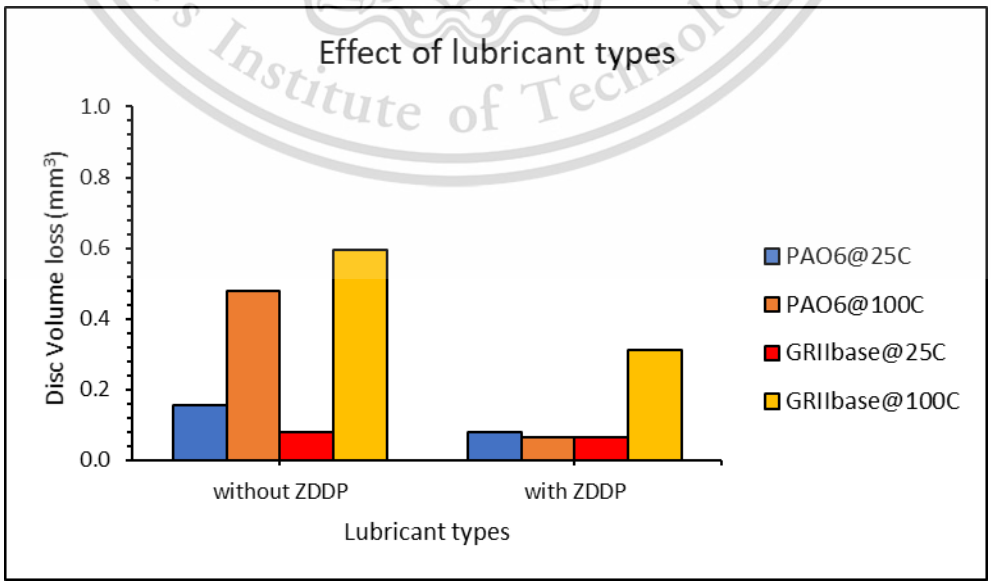

**Figure 107.** Effect of lubricants types on wear performance

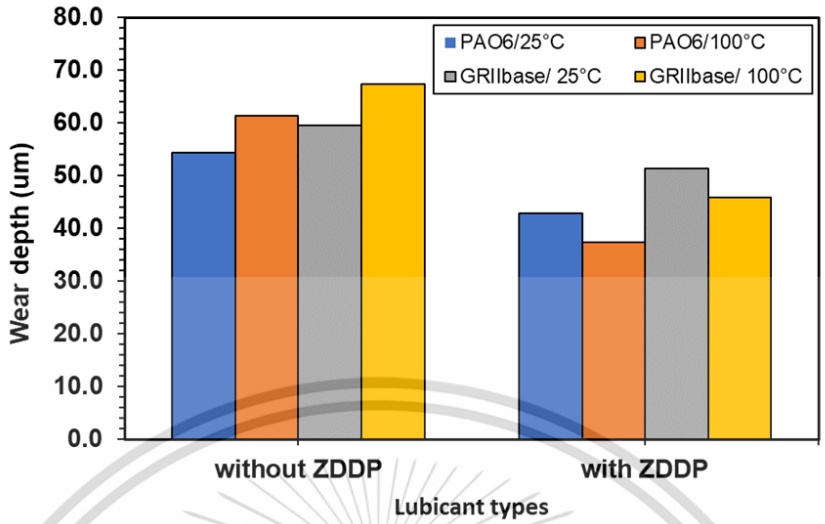


**Figure 108.** Comparison depth of wear scar at different types of lubricant

### 5.2.2 The effect of operating temperature on wear performance of model lubricants

The effect of an operating temperature at TISTR tribometer with ball-on-disc configuration was investigated by variation of lubricant bath operating temperature to 25 °C and 100 °C. In accordance with result from Figure 109, volume loss of lubricant without ZDDP anti-wear additive considerably increased when operating temperature was increased. The results were in line with the previous result in chapter 4. It could be attribute to a reduction of viscosity which would result in more severe lubrication condition with more asperity contact. Form Figure 110, the volume loss of ZDDP-containing lubricants substantially decreased when operating temperature was increased. The results werein good agreement with the previous research by [43-45]. It could be because a thicker ZDDP tribofilm being formed at a higher operating temperature as reported by [43-45].Besides,it could be implied that wear was reduced when ZDDP anti-wear additive was introduced into both base stocks that used in this

thesis.The comparison depth of wear scar at different operating temperature with and without ZDDP anti-wear additive are shown in Figure 111 and 112 respectively. It can be insinuated that depth of wear drastically increased when volume loss was increased, and depth of wear considerably decreased when volume loss was decreased without and with ZDDP anti-wear additive severally.

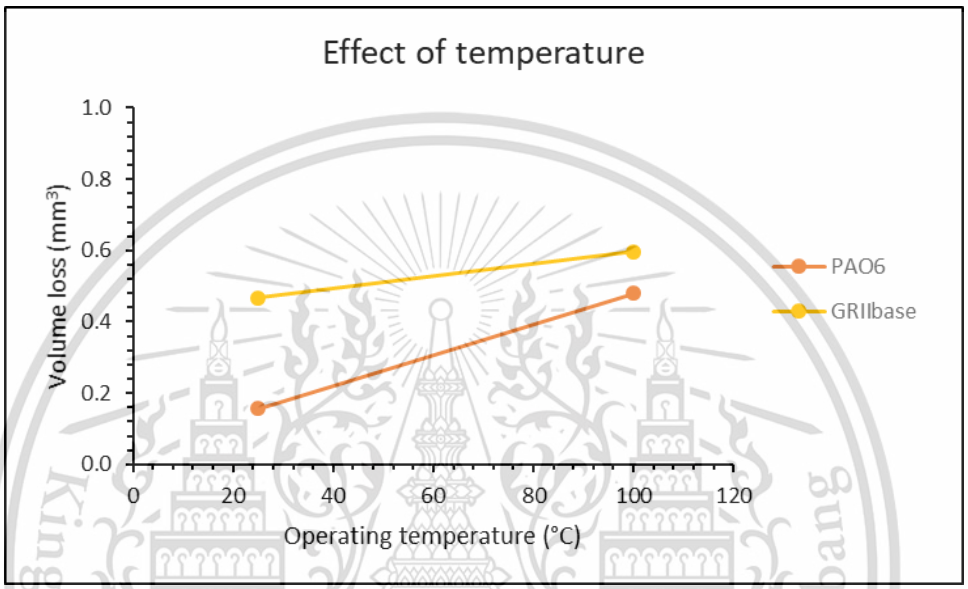


**Figure 109.** Effect of operating temperature on wear performance of lubricant without ZDDP

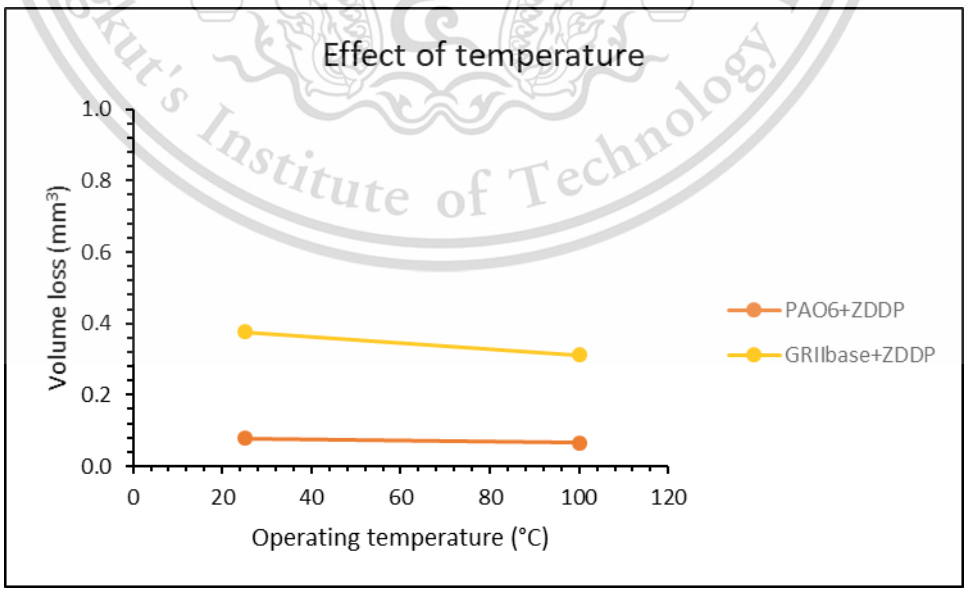

**Figure 110.** Effect of operating temperature on wear performance of lubricant with ZDDP

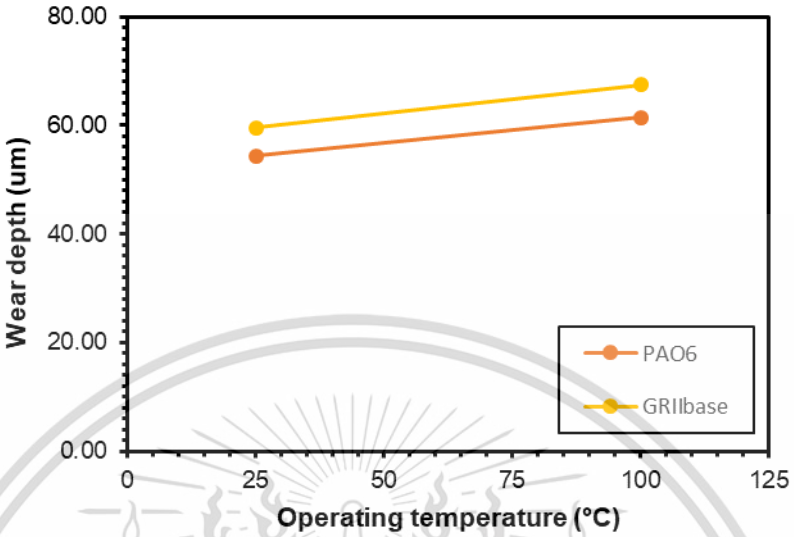


**Figure 111.** Comparison depth of wear scar at different operating temperature of lubricant without ZDDP

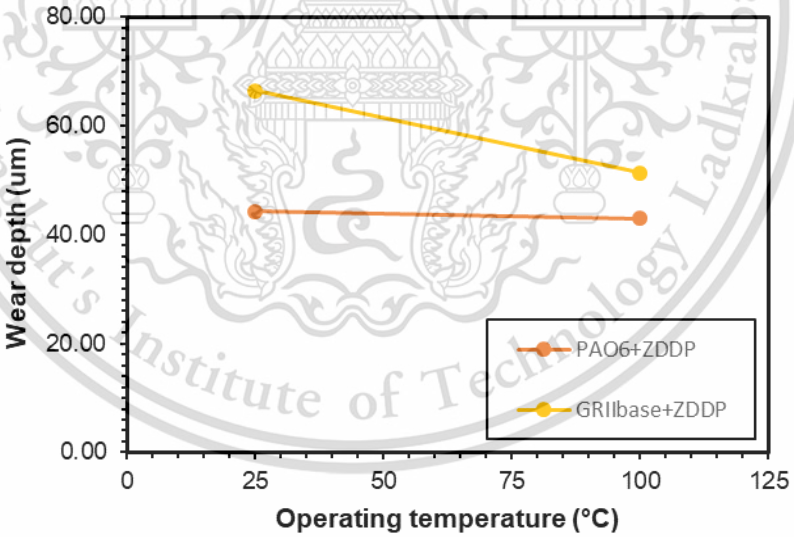


**Figure 112.** Comparison depth of wear scar at different operating temperature of lubricant with ZDDP

### 5.2.3 The effect of aged lubricants on wear performance of model lubricants

The effect of aged lubricants wasinvestigatedon tribometer with ball-on-disc configuration by variation of oil bath temperature to 25°C and 100°C and test with different type of aged lubricants consist of without ZDDP anti-wear additive and with addition of ZDDP anti-wear additive. Besides, can further divided into two sub-categories of ageing procedure: ageing with air and ageing withadditional of ethanol. In accordance with the results form Figure 113 and 114, volume loss of aged lubricant with and without ZDDP anti-wear additivesubstantially increase when operating temperature was increased. Furthermore, aged lubricant with addition of ethanol resulted in lower volume loss than aged lubricant with air. The results are in line with the previous research by [38-39]. It could be because the viscosity value of aged lubricants with additional of ethanol has higher than aged lubricants without additional of ethanol. When viscosity was higher, the friction force and coefficient of friction (COF) between tribological contactsof rubbed surfacedecrease, resulting in wear reduction.Form Figure 115-116, the results show that wear depth of aged lubricants with and without ZDDP anti-wear additive considerably increased when operating temperature was increased. The result of wear depth comparison is in good agreement with wear volume results. Form Figure 117, the results show that the aged lubricants have depth of wear scar drastically lower than non-aged lubricants. It could be attribute to aged lubricants has viscosity lower than non-aged lubricants. Moreover, form Figure 118, the results show that the aged lubricants without ZDDP additive have depth of wear scar drastically lower than aged lubricants with ZDDP additive. It could be attributing to aged lubricantswith ZDDP additive has viscosity lower than aged lubricants without ZDDP additive.Furthermore, at higher operating temperature aged ZDDP-containing lubricants have wear depth increased. It could be

attribute to ZDDP depletion or some ZDDP play an importance role as anti-oxidants from aged ZDDP-containing lubricants as shown in FTIR spectrum in Figure 119. Besides, aged lubricants with ethanol have lower wear depth than aged lubricants with air. It could be because aged lubricants with ethanol has more sludge formation occurred as shown in Figure 120 resulted in higher friction reduced cause higher wear reduction. In addition, more thinner sludge film being form at higher operating temperature resulted in wear augmentation as shown in Figure 121.

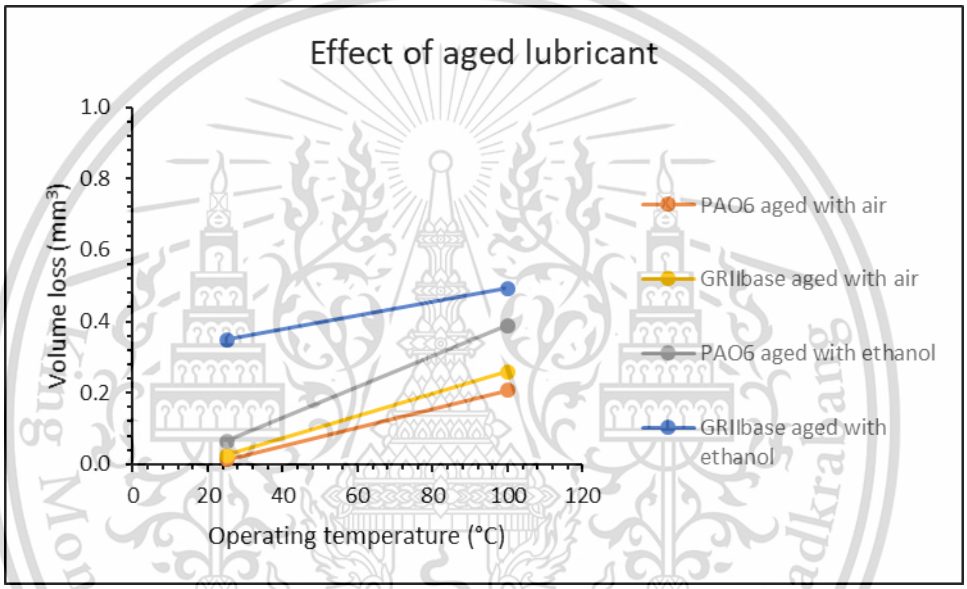


**Figure 113.** Effect of aged lubricant on wear performance of lubricant without ZDDP

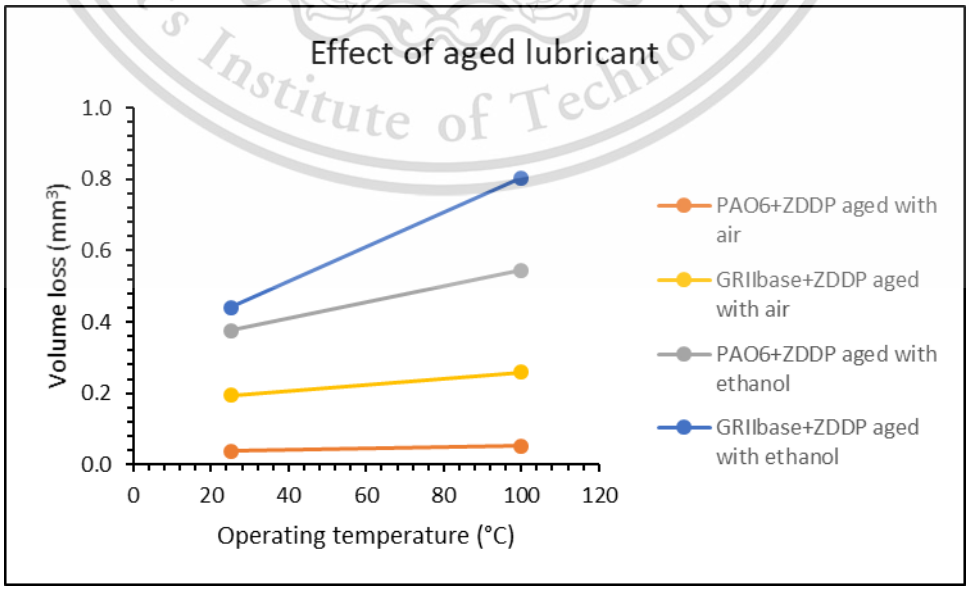

**Figure 114.** Effect of aged lubricant on wear performance of lubricant with ZDDP

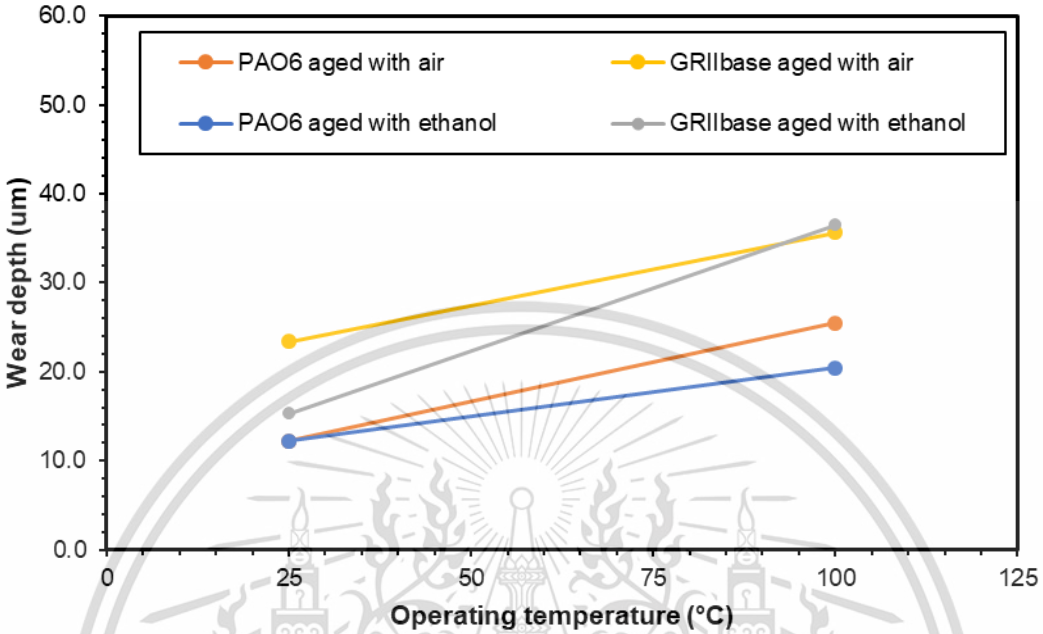


**Figure 115.** Comparison depth of wear scar at different aged lubricant of lubricant withoutZDDP

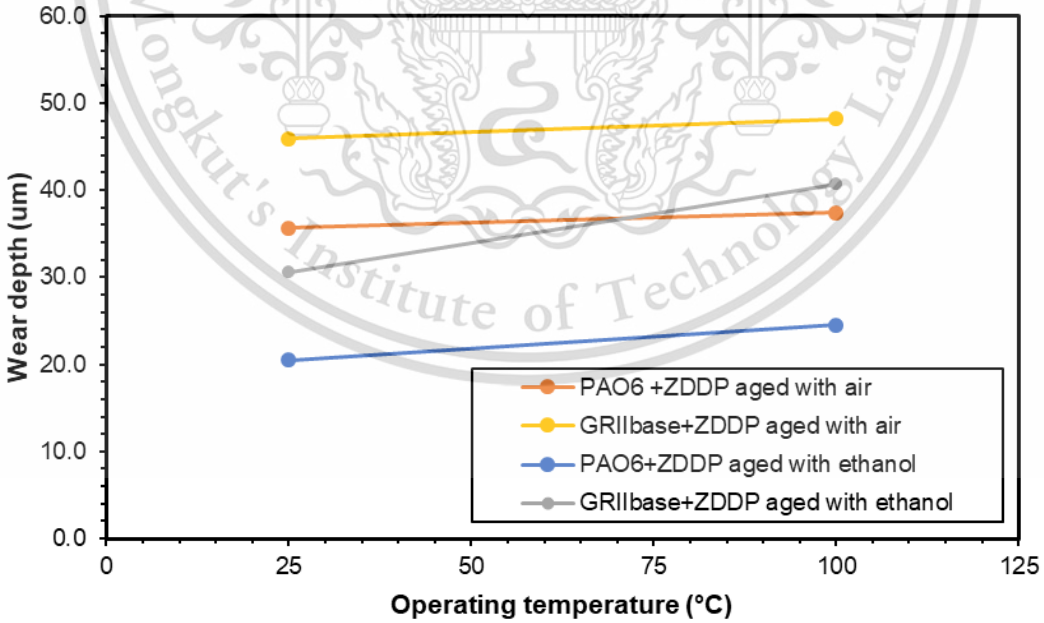

**Figure 116.** Comparison depth of wear scar at different aged lubricant of lubricant with ZDDP

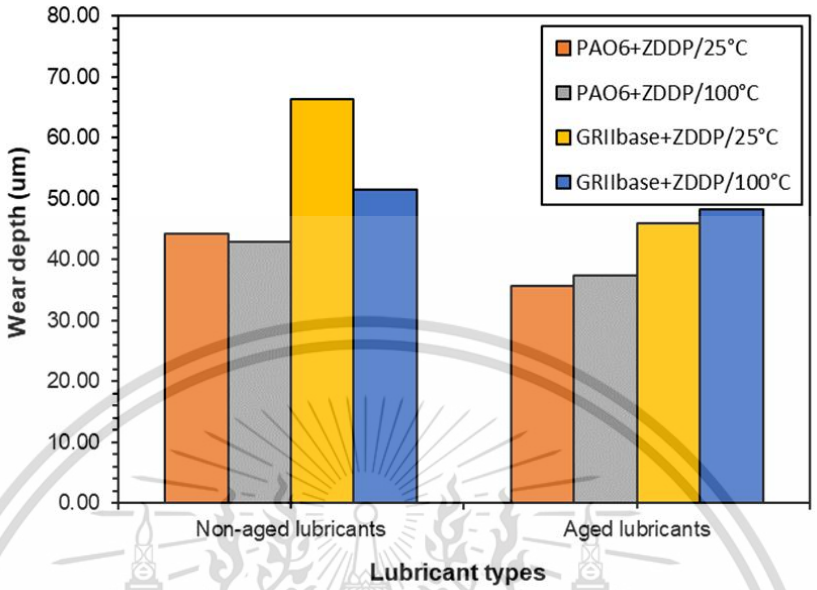


**Figure 117.** Comparison depth of wear scar between aged and non-aged lubricants of model lubricants

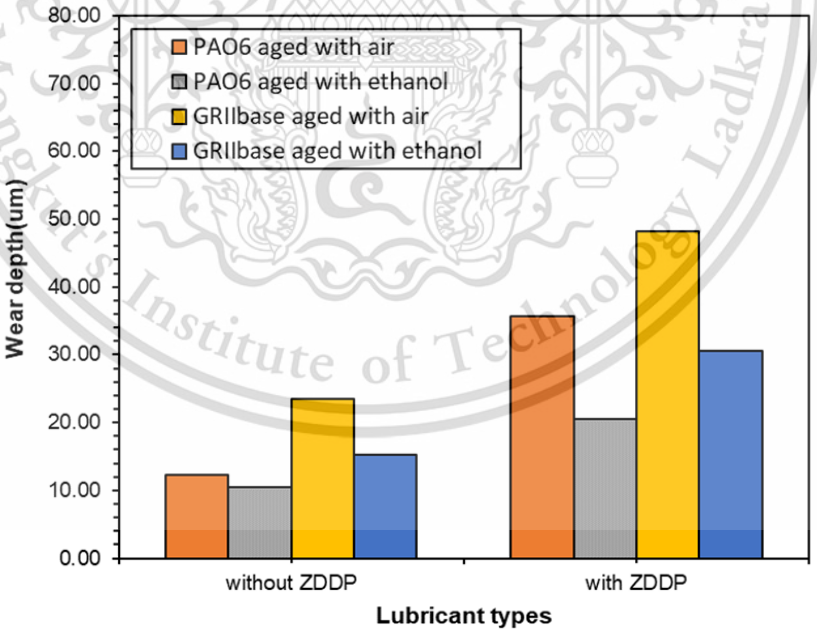


**Figure 118.** Comparison depth of wear scar between aged lubricants with and without ZDDP of model lubricants

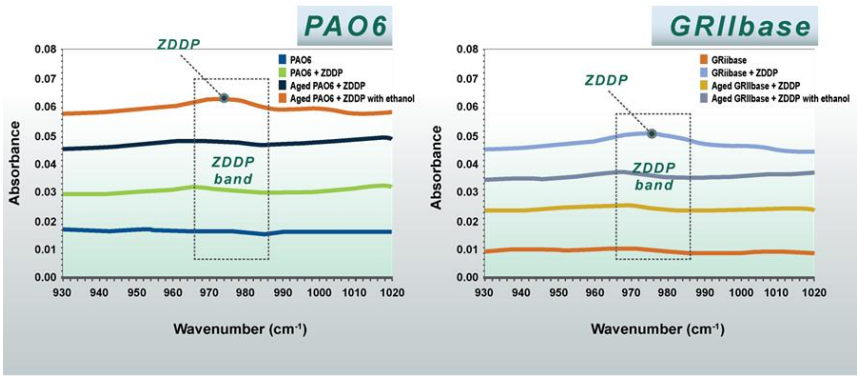


**Figure 119.** Comparison FTIR spectrum of lubricants with different base stocks

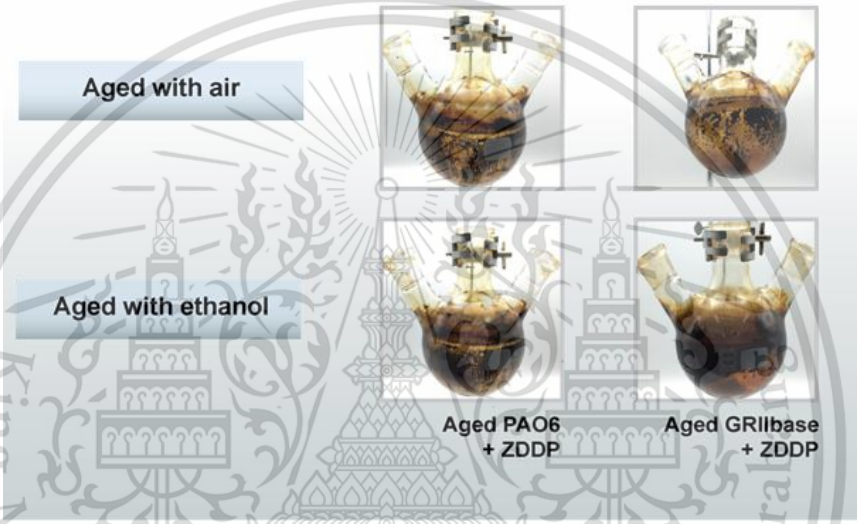


**Figure 120.** Comparison sludge formation of aged ZDDP-containing lubricant with different base stocks and different ageing method.

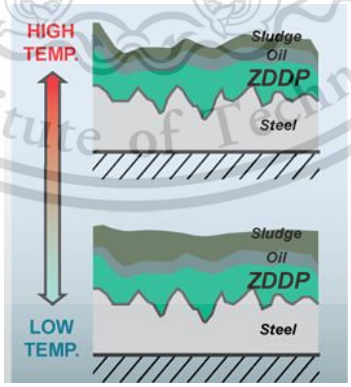


**Figure 121.** Schematic diagram of ZDDP film, oil film and sludge film formations on rubbed surface.

# CHAPTER 6

# CONCLUSIONS

In order to investigate the effect of ZDDP on the tribological performance of lubricants, the Zinc Dialkyldithiophosphate (ZDDP) was mixed with lubricating oils at the constant composition of 1.2% by weight per weight. Moreover,in order to investigate the effect of aged lubricants on the tribological performance of lubricants, both base stocks, i.e. Group II base stock and PAO6 base stock were artificially ageing with air. Furthermore, apart from normal ageing process with air, another group of lubricants were also aged with additional of ethanol. All the tribological tests in this thesis were conducted on tribometer with ball-on-disc configuration by varying operating temperature of 25°C and 100°C at constant load and constant spindle speed. The experimental results could be concluded as follows:

1. It was found that wear depth from testing lubricants without ZDDP increased when operating temperature was increased. It was because when an operating temperature was increased, the viscosity of the test lubricant decreased significantly compared to lower temperature, hence resulting thinner oil film thickness between moving surfaces according to EHL film thickness theory. The higher the temperature, the less oil film thickness presented between contacting surfaces, a higher chance of asperity contacts leading to a higher friction resulted in wear aggravation.
2. On the other hand, resulting wear depth of ZDDP-containing lubricants decreased when operating temperature was increased. It could be attributed to a thicker sacrificial ZDDP tribofilm being formed at a higher operating temperature resulted in wear reduction. In addition, the effect of ZDDP

tribofilm thickness was more prominent than that of oil film thickness at a higher temperature, resulted in wear reduction instead of wear aggravation.

3. Aged lubricants were found to result in a lower wear depth than non-aged lubricants. It could be attributed to all aged lubricants (with air and with air and ethanol) having an overall higher viscosity than those of non-aged lubricants. When viscosity increased, resulting oil film thickness between surface contact was also increased indicating less asperity contacts and therefore a wear reduction.
4. Aged lubricants with ZDDP gave a higher wear depth than lubricants without ZDDP. It could be attribute to both of aged lubricants without ZDDP at operating temperature 25°C and 100°C have higher viscosity than aged lubricants with ZDDP at operating temperature 25°C and 100°C respectively when viscosity increased cause oil film thickness also increased. In addition, when oil film thickness increased cause distance between rubbed surface increased resulted in wear reduction.
5. Aged lubricants with air and ethanol had a lower wear depth than lubricants aged with only air. It could be attributed to both of aged lubricants with ethanol with and without ZDDP having a higher viscosity than aged lubricants with aged lubricants with air with and without ZDDP respectively. Additionally, a higher amount of sludge formation was observed in the aged lubricants with air and ethanol. This could have been another contributing factor in a lower resulting wear depth. However, the resulting sludges were not investigated in this study.
6. All aged ZDDP-containing lubricants exhibitedincrease in wear depth at a higher operating temperature. This was in contrast with the results from the

case of non-aged lubricants. It was possible that there was a process of ZDDP depletion during the artificial aging process especially some amount of ZDDP could play an important role as an anti-oxidant to suppress the oxidation reaction. This was supported by the values of viscosity and oxidation number obtained from the aged lubricant samples which were much lower than those aged base stocks without ZDDP. The FT-IR measurements of the test lubricant (with and without ZDDP, aged and non-aged) were also in support of this proposed theory.

As future prospect, further investigations can be carried out comprising a sludge investigation by SEM-EDX, investigation of ZDDP tribofilm formed on rubbed surface by SEM-EDX and further study about physical and chemical properties of aged lubricants.

## REFERENCES


[1] Stachowiak, G., & Batchelor, A. W. (2013). *Engineering tribology*, Butterworth-Heinemann.

[2] Sethuramiah, A., & Kumar, R. (2015).Boundary Lubrication Mechanism and Modeling. In *Modeling of Chemical Wear: Relevance to Practice*(pp. 69-104), Elsevier.

[3] Bowman, W. F., & Stachowiak, G. W. (1996). A review of scuffing models. *Tribology Letters*, *2*(2), 113-131.

[4] Lee, S. C., & Cheng, H. S. (1991). Correlation of scuffing experiments with EHL analysis of rough surfaces. *Journal of tribology*, *113*(2), 318-326.

[5] Lee, S. C., & Chen, H. (1995). Experimental validation of critical temperature-pressure theory of scuffing. *Tribology Transactions*, *38*(3), 738-742.

[6] Ludema, K. C. (1984). A review of scuffing and running-in of lubricated surfaces, with asperities and oxides in perspective. *Wear*, *100*(1-3), 315-331.

[7] Batchelor, A. W., & Stachowiak, G. W. (1995). Model of scuffing based on the vulnerability of an elastohydrodynamic oil film to chemical degradation catalyzed by the contacting surfaces. *Tribology Letters*, *1*(4), 349-365.

[8] Dowson, D. (1965, June). Paper R1: Elastohydrodynamic lubrication: an introduction and a review of theoretical studies. In *Proceedings of the institution of mechanical engineers, conference proceedings* (Vol. 180, No. 2, pp. 7-16), Sage UK: London, England: SAGE Publications.

[9] Hamrock, B. J., & Dowson, D. (1977). Isothermal elastohydrodynamic lubrication of point contacts: part III—fully flooded results. *Journal of Lubrication Technology*, *99*(2), 264-275.

[10] Khruschov, M. M. (1974). Principles of abrasive wear. *wear*, *28*(1), 69-88.

[11] Burwell Jr, J. T. (1957). Survey of possible wear mechanisms. *Wear*, *1*(2), 119-141.

[12] Rabinowicz, E. (1964). Practical uses of the surface energy criterion. *Wear*, *7*(1), 9-22.

[13] Rabinowicz, E., & Mutis, A. (1965). Effect of abrasive particle size on wear. *Wear*, *8*(5), 381-390.

[14] Dwyer-Joyce, R. S., Sayles, R. S., & Ioannides, E. (1994). An investigation into the mechanisms of closed three-body abrasive wear. *Wear*, *175*(1-2), 133-142.

[15] Misra, A., & Finnie, I. (1980). A classification of three-body abrasive wear and design of a new tester. *Wear*, *60*(1), 111-121.

[16] Kayaba, T., & Kato, K. (1979). The analysis of adhesive wear mechanism by successive observations of the wear process in SEM. *Wear of Materials*, 45-56.

[17] Bowden, F. P., & Tabor, D. (1964). *The friction and lubrication of solids. Vol. 2*. OUP.

[18] Vingsbo, O. (1979). Wear and wear mechanisms. *Wear of Materials*, 620-635.

[19] Buckley, D. H. (1981). *Surface effects in adhesion, friction, wear, and lubrication* (Vol. 5). Elsevier.

[20] Suh, N. P. (1973). The delamination theory of wear. *Wear*, *25*(1), 111-124.

[21] Jahanmir, S. N. P. E. P., Suh, N. P., & Abrahamson, E. P. (1974). Microscopic observations of the wear sheet formation by delamination. *Wear*, *28*(2), 235-249.

[22] Bill, R. C. (1983). Fretting wear and fretting fatigue—how are they related? *Journal of Lubrication Technology*, *105*(2), 230-238.

[23] Mutoh, Y. (1995). Mechanisms of fretting fatigue. *JSME international journal. Ser. A, Mechanics and material engineering*, *38*(4), 405-415.

[24] Holweger, W. (2013). Fundamentals of lubricants and lubrication. In *Tribology-fundamentals and advancements*(pp. 3-53). InTech.

[25] Totten, G. E., & Tung, S. (Eds.). (2012). *Automotive lubricants and testing*. ASTM International.

[26] Hutchings, I., & Shipway, P. (2017). Lubricants and lubrication. In *Tribology: friction and wear of engineering materials*(pp. 79-105). Butterworth-Heinemann.

[27] Brown, M., Fotheringham, J. D., Hoyes, T. J., Mortier, R. M., Orszulik, S. T., Randles, S. J., & Stroud, P. M. (2010). Synthetic base fluids. In *Chemistry and technology of lubricants* (pp. 35-74). Springer, Dordrecht.

[28] Ahmed, N. S., & Nassar, A. M. (2011). Lubricating oil additives. In *Tribology-Lubricants and Lubrication*(pp. 249-268). InTech.

[29] Jahanmir, S. (1987). Wear reduction and surface layer formation by a ZDDP additive. *Journal of tribology*, *109*(4), 577-586.

[30] Mang, T., & Dresel, W. (2007). Lubricants and lubrication, 2nd, completely revised and extended edition.

[31] Johnson, D. W. (2016). The Tribology and Chemistry of Phosphorus Containing Lubricant Additives. In *Advance in tribology* (pp. 175-195). InTech.

[32] Besser, C., Schneidhofer, C., Dörr, N., Novotny-Farkas, F., & Allmaier, G. (2012). Investigation of long-term engine oil performance using lab-based artificialageing illustrated by the impact of ethanol as fuel component. *Tribology International*, *46*(1), 174-182.

[33] ASTM D4052-11. (2011). *Standard test method for density, relative density, and API gravity of liquids by digital density meter*. ASTM International.

[34] ASTM D445-65. (1970). *Standard Method Of Test For Viscosity Of Transparent And Opaque Liquids (Kinematic And Dynamic Viscosities)*. ASTM International.

[35] ASTM D664-04. (2011). *Standard test method for acid number of petroleum products by potentiometric titration*. ASTM international.

[36] ASTM D7214-07. (2012). *Standard test method for acid number of petroleum products by potentiometric titration*. ASTM international.

[37] Dwyer-Joyce, R. S. (1997). Tribological Design Data Part 3: Contact Mechanics. *Institution of Mechanical Engineers*.

[38] Costa, H. L., & Spikes, H. A. (2016). Impact of ethanol on the formation of antiwear tribofilms from engine lubricants. *Tribology International*, *93*, 364-376.

[39] Khuong, L. S., Zulkifli, N. W. M., Masjuki, H. H., Mohamad, E. N., Arslan, A., Mosarof, M. H., & Azham, A. (2016). A review on the effect of bioethanol dilution on the properties and performance of automotive lubricants in gasoline engines. *RSC Advances*, *6*(71), 66847-66869.

[40] Morina, A., Neville, A., Priest, M., & Green, J. H. (2006). ZDDP and MoDTC interactions in boundary lubrication—the effect of temperature and ZDDP/MoDTC ratio. *Tribology international*, *39*(12), 1545-1557.

[41] http://www.matweb.com/search/datasheet.aspx?matguid

=d0b0a51bff894778a97f5b72e7317d85

[42] http://www.matweb.com/search/datasheet_print.aspx?matguid

=61e5cbeb3ddc4d76a2b5d3e19cdd0341

[43] Fujita, H., & Spikes, H. A. (2004). The formation of zinc dithiophosphate antiwear films. *Proceedings of the Institution of Mechanical Engineers, Part J: Journal of Engineering Tribology*, *218*(4), 265-278.

[44] Fujita, H., Glovnea, R. P., & Spikes, H. A. (2005). Study of zinc dialkydithiophosphate antiwear film formation and removal processes, part I: experimental. *Tribology transactions*, *48*(4), 558-566.

[45] Parsaeian, P., Ghanbarzadeh, A., Wilson, M., Van Eijk, M. C., Nedelcu, I., Dowson, D., ... & Morina, A. (2016). An experimental and analytical study of the effect of water and its tribochemistry on the tribocorrosive wear of boundary lubricated systems with ZDDP-containing oil. *Wear*, *358*, 23-3

# APPENDIX A

# TISTR TRIBOLOGY TEST REPORTS

วว.TISTR

**THAILAND INSTITUTE OF SCIENTIFIC AND TECHNOLOGICAL RESEARCH (TISTR)**
**MATERIAL PROPERTIES ANALYSIS AND DEVELOPMENT CENTRE (MPAD)**

**Request No. :** S6200340 **Date :** 3 May 2019

**Date of request :** 7 February 2019 **Page :** 1 of 5

**REPORT ON ANALYSIS/ TESTING**
**For**
**NATIONAL METAL AND MATERIALS TECHNOLOGY CENTER**
**114 Thailand Science Park, Phahonyothin Road, Khlong Nueng, Khlong Luang, Pathum Thani 12120**

**Testing/analysis/investigation of** : Disc sample : Grade AISI S2100 (SUJ2)

**Method of testing/analysis/investigation :** Wear test using Pin on Disk Apparatus followed the customer's agreement based on ASTM G 99 – 17

**Result of testing/analysis/investigation :-**

The test results are attached.

**Testing/analysis/investigated by :**

1. R. Nakkanhod

2.

**Approved by**

(Ms. Chalothorn Bhanomsuti)
Director
วว.TISTR
Performance and Safety Inspection Laboratory

**Examined by**

(Ms. Duangporn Ounpanich)

**This report contains 5 pages, all pages must be signed by the authorized person for report approval.**

FS-MPAD-GEN-708-1-09/05/61

**Remark :** The above results are valid exclusively for tested/analysed samples as mentioned in this report. Publication of the results on testing and analysis is prohibited unless written permission is obtained from the governor of TISTR.

สถาบันวิจัยวิทยาศาสตร์และเทคโนโลยีแห่งประเทศไทย (วว.)
Thailand Institute of Scientific and Technological Research (TISTR)
35 Moo 3, Technopolis, Tambon Khlong 5, Amphoe Khlong Luang, Pathum Thani 12120 Thailand
Tel. (66) 0 2577 9000 Fax 0 2577 9009 E-mail : tistr@tistr.or.th Website : www.tistr.or.th

วว.-TISTR

**THAILAND INSTITUTE OF SCIENTIFIC AND TECHNOLOGICAL RESEARCH (TISTR)**
**MATERIAL PROPERTIES ANALYSIS AND DEVELOPMENT CENTRE (MPAD)**

**Request No. :** S6200340 **Date :** 3 May 2019

**REPORT**

**Customer :** NATIONAL METAL AND MATERIALS TECHNOLOGY CENTER **Page :** 2 of 5

NATIONAL METAL AND MATERIALS TECHNOLOGY CENTER has commissioned the Material Properties Analysis and Development Centre, Thailand Institute of Scientific and Technological Research (MPAD/TISTR) to carry out wear test of the disc sample : Grade AISI S2100 (SUJ2) (density 7.718 $g/cm^3$) for 29 pieces using the Pin on Disk Apparatus of Tribometer (UMT TriboLab) followed the customer's agreement based on ASTM G 99 – 17. The test results were reported as coefficient of friction (COF) and volume loss.

The surface appearance of the disc sample : Grade AISI S2100 (SUJ2) before and after test were shown in Fig 1. The wear test of the disc sample : Grade AISI S2100 (SUJ2) in the lubricants at 25°C and 100°C by Tribometer were shown in Fig 2.

**Test conditions and procedures:**

1. The test condition was assigned by the customer:
   - Wear test of the samples in the lubricants (lubricants prepared by customer) at 25°C and 100°C (see Table 1).
2. Test Parameters:
   - Test load : 3 N with ball (as the pin specimen) diameter 6.3 mm and hardness 63.98 HRC (prepared by customer)
   - Wear track radius : 5 mm
   - Speed : 60 rpm
   - Test time : 2 hours
3. Weigh each sample before and after the wear test.
4. Calculation the mass loss and volume loss using the following equation:

$$\text{Volume loss, } mm^3 = \frac{\text{mass (weight) loss, g}}{\text{density, g/cm}^3} \times 1000$$

5. The coefficient of friction (COF) was calculated and reported by the software of Tribometer.

FS-MPAD-GEN-708-2-0905/61

วว.-TISTR

สถาบันวิจัยวิทยาศาสตร์และเทคโนโลยีแห่งประเทศไทย (วว.)
Thailand Institute of Scientific and Technological Research (TISTR)
35 Moo 3, Technopolis, Tambon Khlong 5, Amphoe Khlong Luang, Pathum Thani 12120 Thailand
Tel. (66) 0 2577 9000 Fax 0 2577 9009 E-mail : mst@tistr.or.th Website : www.tistr.or.th

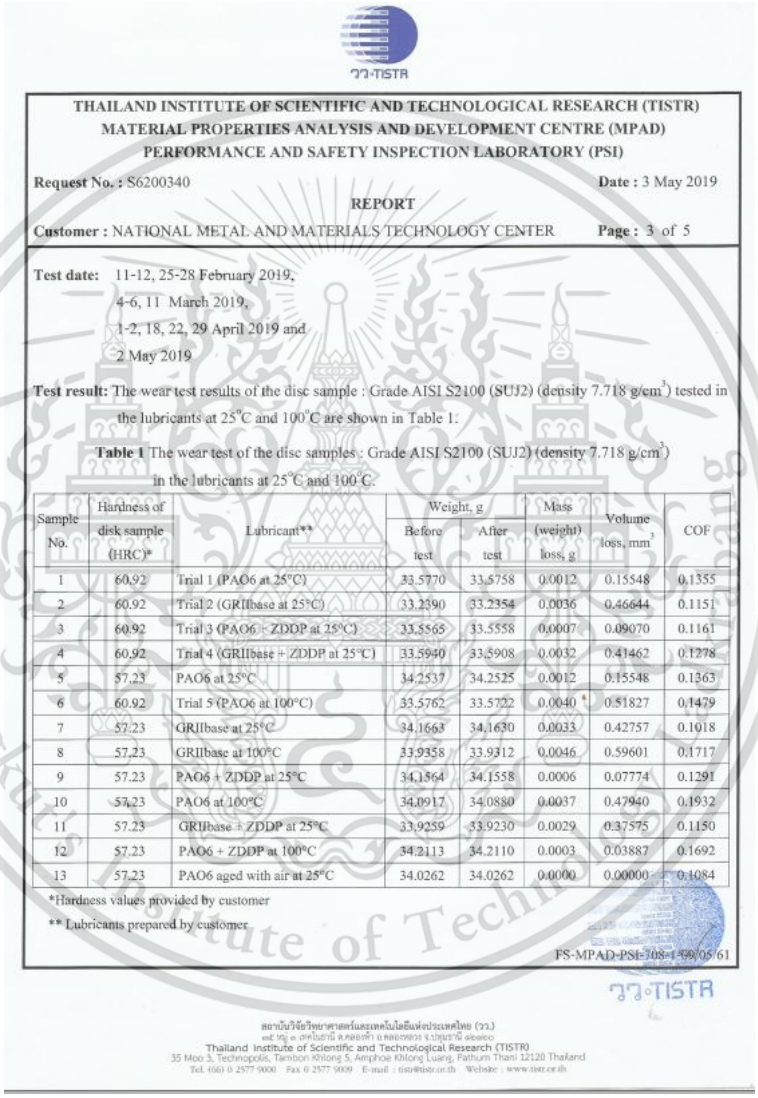

วว.TISTR

**THAILAND INSTITUTE OF SCIENTIFIC AND TECHNOLOGICAL RESEARCH (TISTR)**
**MATERIAL PROPERTIES ANALYSIS AND DEVELOPMENT CENTRE (MPAD)**
**PERFORMANCE AND SAFETY INSPECTION LABORATORY (PSI)**

**Request No. :** S6200340 **Date :** 3 May 2019

**REPORT**

**Customer :** NATIONAL METAL AND MATERIALS TECHNOLOGY CENTER **Page :** 3 of 5

**Test date:** 11-12, 25-28 February 2019,
4-6, 11 March 2019,
1-2, 18, 22, 29 April 2019 and
2 May 2019

**Test result:** The wear test results of the disc sample : Grade AISI S2100 (SUJ2) (density 7.718 g/cm$^3$) tested in the lubricants at 25°C and 100°C are shown in Table 1.

**Table 1** The wear test of the disc samples : Grade AISI S2100 (SUJ2) (density 7.718 g/cm$^3$) in the lubricants at 25°C and 100°C.

| Sample No. | Hardness of disk sample (HRC)* | Lubricant** | Weight, g | | Mass (weight) loss, g | Volume loss, mm$^3$ | COF |
|---|---|---|---|---|---|---|---|
| | | | Before test | After test | | | |
| 1 | 60.92 | Trial 1 (PAO6 at 25°C) | 33.5770 | 33.5758 | 0.0012 | 0.15548 | 0.1355 |
| 2 | 60.92 | Trial 2 (GRIIbase at 25°C) | 33.2390 | 33.2354 | 0.0036 | 0.46644 | 0.1151 |
| 3 | 60.92 | Trial 3 (PAO6 + ZDDP at 25°C) | 33.5565 | 33.5558 | 0.0007 | 0.09070 | 0.1161 |
| 4 | 60.92 | Trial 4 (GRIIbase + ZDDP at 25°C) | 33.5940 | 33.5908 | 0.0032 | 0.41462 | 0.1278 |
| 5 | 57.23 | PAO6 at 25°C | 34.2537 | 34.2525 | 0.0012 | 0.15548 | 0.1363 |
| 6 | 60.92 | Trial 5 (PAO6 at 100°C) | 33.5762 | 33.5722 | 0.0040 | 0.51827 | 0.1479 |
| 7 | 57.23 | GRIIbase at 25°C | 34.1663 | 34.1630 | 0.0033 | 0.42757 | 0.1018 |
| 8 | 57.23 | GRIIbase at 100°C | 33.9358 | 33.9312 | 0.0046 | 0.59601 | 0.1717 |
| 9 | 57.23 | PAO6 + ZDDP at 25°C | 34.1564 | 34.1558 | 0.0006 | 0.07774 | 0.1291 |
| 10 | 57.23 | PAO6 at 100°C | 34.0917 | 34.0880 | 0.0037 | 0.47940 | 0.1932 |
| 11 | 57.23 | GRIIbase + ZDDP at 25°C | 33.9259 | 33.9230 | 0.0029 | 0.37575 | 0.1150 |
| 12 | 57.23 | PAO6 + ZDDP at 100°C | 34.2113 | 34.2110 | 0.0003 | 0.03887 | 0.1692 |
| 13 | 57.23 | PAO6 aged with air at 25°C | 34.0262 | 34.0262 | 0.0000 | 0.00000 | 0.1084 |

*Hardness values provided by customer
** Lubricants prepared by customer

FS-MPAD-PSI-108-1-59/05/61

วว.TISTR

สถาบันวิจัยวิทยาศาสตร์และเทคโนโลยีแห่งประเทศไทย (วว.)
Thailand Institute of Scientific and Technological Research (TISTR)
35 Moo 3, Technopolis, Tambon Khlong 5, Amphoe Khlong Luang, Pathum Thani 12120 Thailand
Tel. (66) 0 2577 9000 Fax 0 2577 9009 E-mail : tistr@tistr.or.th Website : www.tistr.or.th

วว-TISTR

**THAILAND INSTITUTE OF SCIENTIFIC AND TECHNOLOGICAL RESEARCH (TISTR)**
**MATERIAL PROPERTIES ANALYSIS AND DEVELOPMENT CENTRE (MPAD)**
**PERFORMANCE AND SAFETY INSPECTION LABORATORY (PSI)**

**Request No. :** S6200340 **Date :** 3 May 2019

**REPORT**

**Customer :** NATIONAL METAL AND MATERIALS TECHNOLOGY CENTER **Page :** 4 of 5

**Table 1** (Cont.) The wear test of the disc samples : Grade AISI S2100 (SUJ2) (density 7.718 g/cm$^3$) in the lubricants at 25°C and 100°C.

| Sample No. | Hardness of disk sample (HRC)* | Lubricant** | Weight, g | | Mass (weight) loss, g | Volume loss, mm$^3$ | COF |
|---|---|---|---|---|---|---|---|
| | | | Before test | After test | | | |
| 14 | 57.23 | GRIIbase + ZDDP at 100°C | 34.0234 | 34.0210 | 0.0024 | 0.31096 | 0.1722 |
| 15 | 57.23 | GRIIbase aged with air at 25°C | 34.2522 | 34.2521 | 0.0001 | 0.01296 | 0.1206 |
| 16 | 57.23 | PAO6 aged with air at 100°C | 34.0687 | 34.0670 | 0.0017 | 0.22026 | 0.0925 |
| 17 | 57.23 | PAO6 + ZDDP aged with air at 25°C | 34.3386 | 34.3374 | 0.0012 | 0.15548 | 0.1222 |
| 18 | 57.23 | GRIIbase aged with air at 100°C | 34.0552 | 34.0532 | 0.0020 | 0.25913 | 0.1489 |
| 19 | 57.23 | GRIIbase+ZDDP aged with air at 25°C | 34.1791 | 34.1775 | 0.0016 | 0.20731 | 0.1145 |
| 20 | 57.23 | PAO6 + ZDDP aged with air at 100°C | 33.9359 | 33.9338 | 0.0021 | 0.27209 | 0.1546 |
| 21 | 57.23 | PAO6 aged with ethanol at 25°C | 34.1385 | 34.1380 | 0.0005 | 0.06478 | 0.1115 |
| 22 | 57.23 | GRIIbase + ZDDP aged with air at 100°C | 34.3177 | 34.3120 | 0.0057 | 0.73853 | 0.1254 |
| 23 | 57.23 | GRIIbase aged with ethanol at 25°C | 33.9540 | 33.9513 | 0.0027 | 0.34983 | 0.1251 |
| 24 | 57.23 | PAO6 aged with ethanol at 100°C | 34.2237 | 34.2207 | 0.0030 | 0.38870 | 0.0755 |
| 25 | 57.23 | PAO6+ZDDP aged with ethanol at 25°C | 33.6752 | 33.6723 | 0.0029 | 0.37575 | 0.1259 |
| 26 | 57.23 | GRIIbase aged with ethanol at 100°C | 34.0244 | 34.0182 | 0.0062 | 0.80332 | 0.1216 |
| 27 | 57.23 | GRIIbase + ZDDP aged with ethanol at 25°C | 34.1233 | 34.1199 | 0.0034 | 0.44053 | 0.1138 |
| 28 | 57.23 | PAO6 + ZDDP aged with ethanol at 100°C | 34.0645 | 34.0603 | 0.0042 | 0.54418 | 0.1113 |
| 29 | 57.23 | GRIIbase + ZDDP aged with ethanol at 100°C | 34.3098 | 34.306 | 0.0038 | 0.49236 | 0.1351 |

*Hardness values provided by customer

** Lubricants prepared by customer

FS-MPAD-PSI-708-1-09/05/61

สถาบันวิจัยวิทยาศาสตร์และเทคโนโลยีแห่งประเทศไทย (วว.)
๓๕ หมู่ ๑ ตำบลคลองห้า อำเภอคลองหลวง จังหวัดปทุมธานี ๑๒๑๒๐
Thailand Institute of Scientific and Technological Research (TISTR)
35 Moo 3, Technopolis, Tambon Khlong 5, Amphoe Khlong Luang, Pathum Thani 12120 Thailand
Tel. (66) 0 2577 9000 Fax 0 2577 9009 E-mail : tistr@tistr.or.th Website : www.tistr.or.th

วว.TISTR

THAILAND INSTITUTE OF SCIENTIFIC AND TECHNOLOGICAL RESEARCH (TISTR)
MATERIAL PROPERTIES ANALYSIS AND DEVELOPMENT CENTRE (MPAD)
PERFORMANCE AND SAFETY INSPECTION LABORATORY (PSI)

**Request No. :** S6200340 **Date :** 3 May 2019

**REPORT**

**Customer :** NATIONAL METAL AND MATERIALS TECHNOLOGY CENTER **Page :** 5 of 5

Before test After test

**Fig. 1** The surface appearance of disc sample : Grade AISI S2100 (SUJ2) for wear test.

At 25 °C At 100 °C

**Fig. 2** The wear test of the disc sample : Grade AISI S2100 (SUJ2) in the lubricants at 25°C and 100°C by Tribometer.

FS-MPAD-PSI-708-1-09/05/61

วว.TISTR

สถาบันวิจัยวิทยาศาสตร์และเทคโนโลยีแห่งประเทศไทย (วว.)
Thailand Institute of Scientific and Technological Research (TISTR)
35 Moo 3, Technopolis, Tambon Khlong 5, Amphoe Khlong Luang, Pathum Thani 12120 Thailand
Tel. (66) 0 2577 9000 Fax 0 2577 9009 E-mail : tistr@tistr.or.th Website : www.tistr.or.th

# APPENDIX B

## TISTR 3D LASER CONTOUR REPORTS

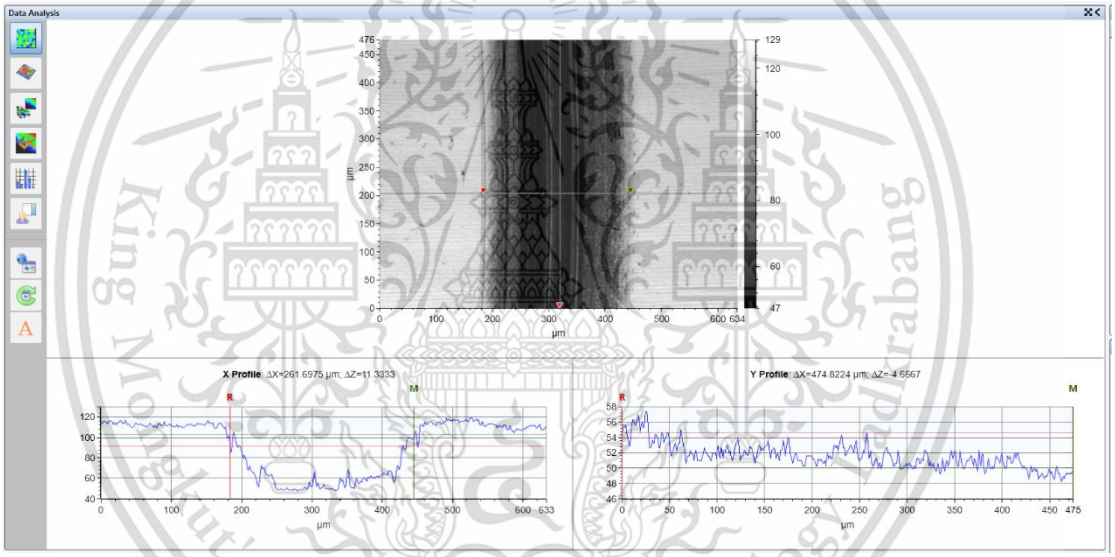

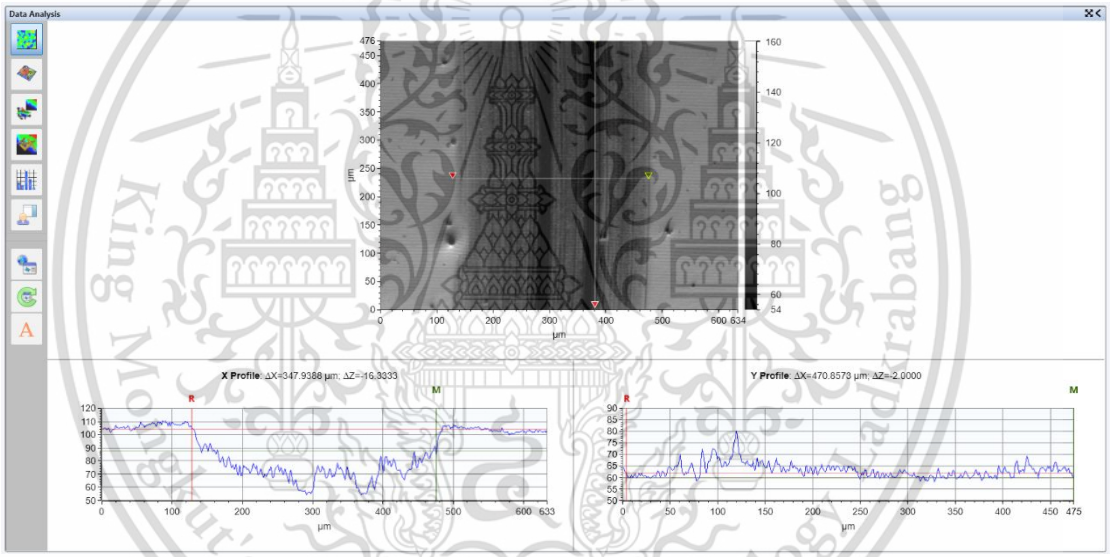

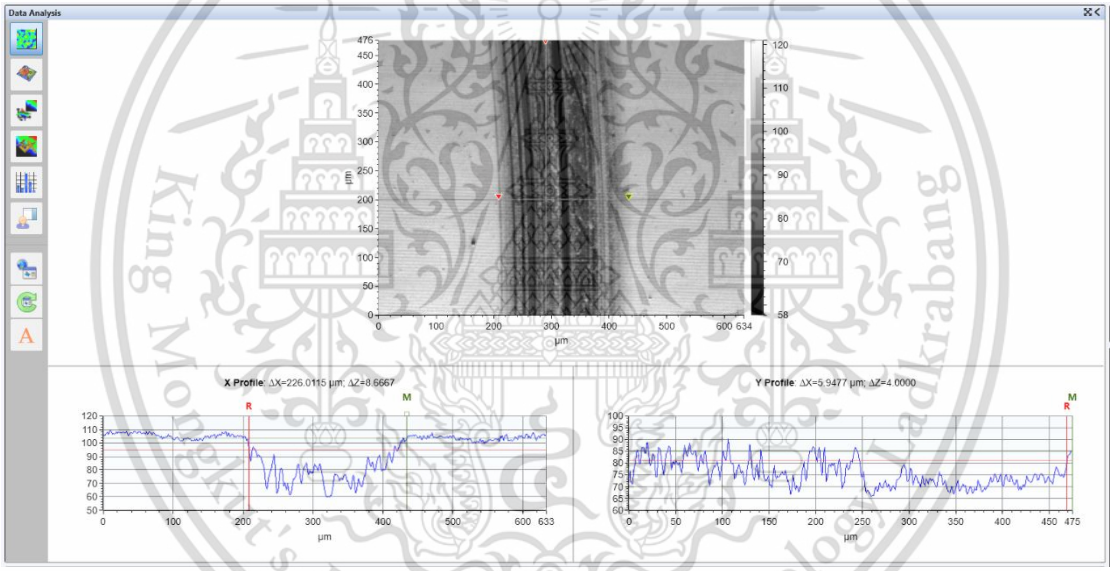

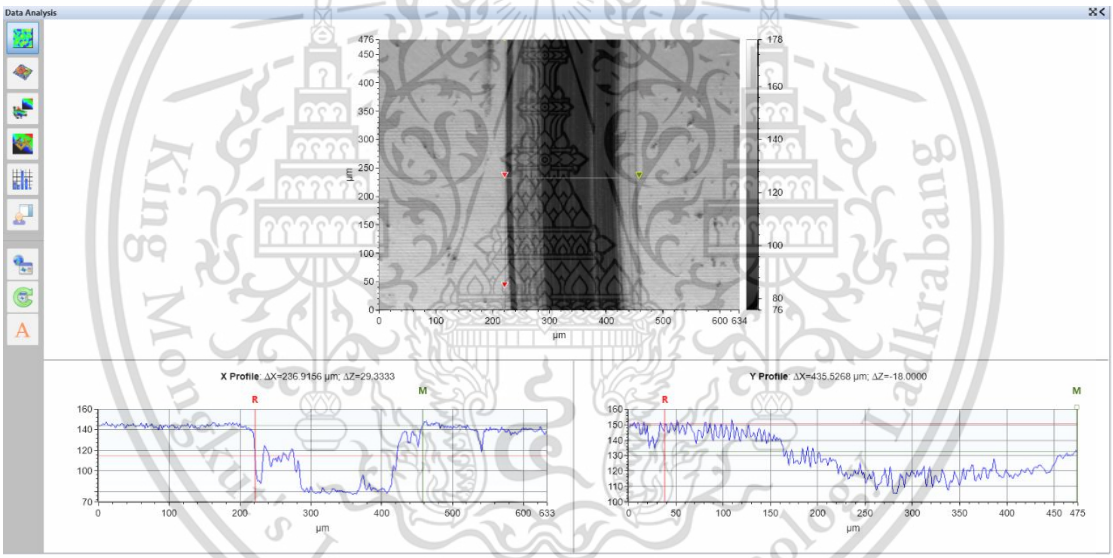

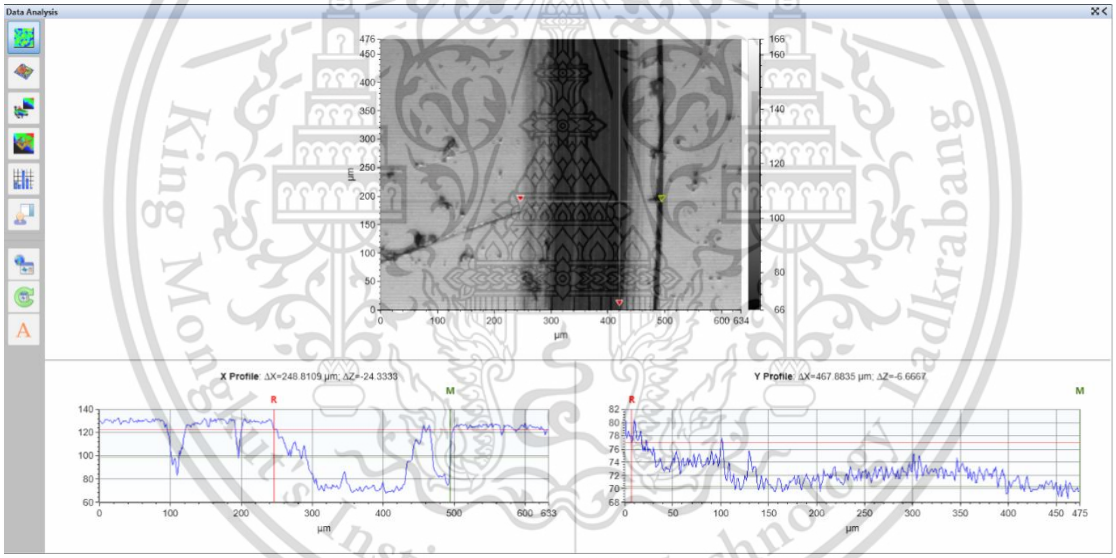

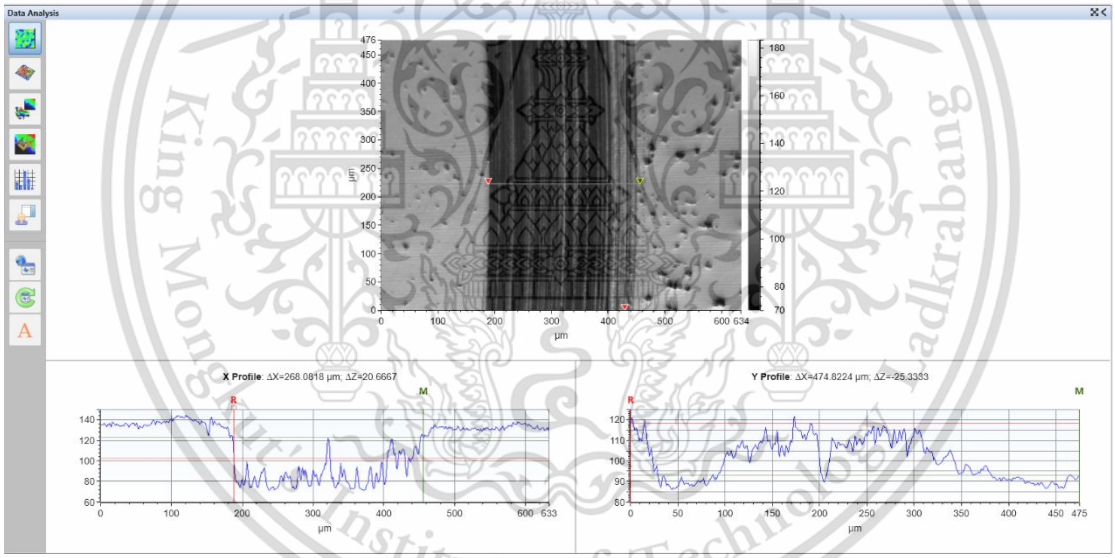

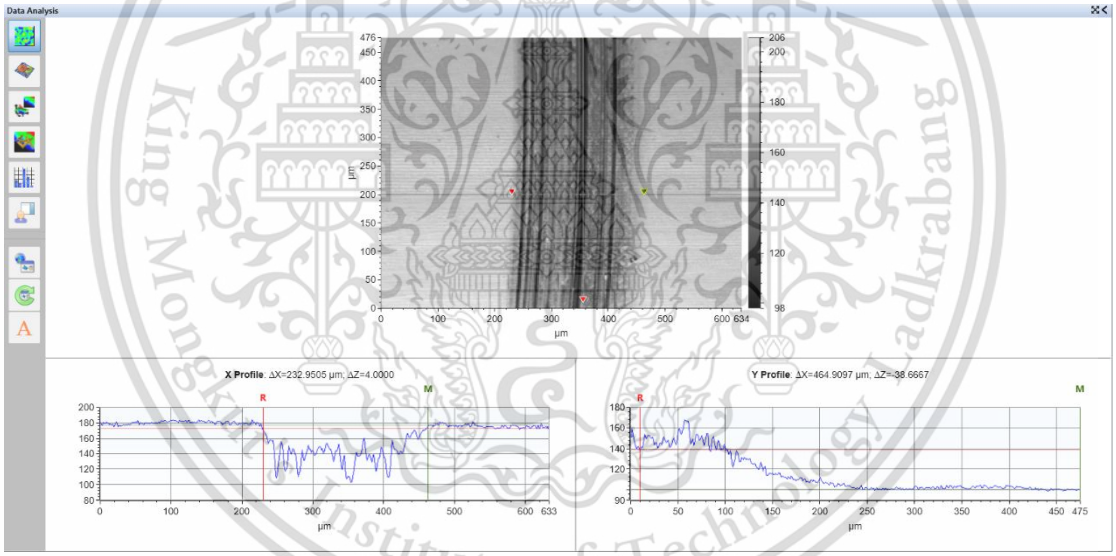

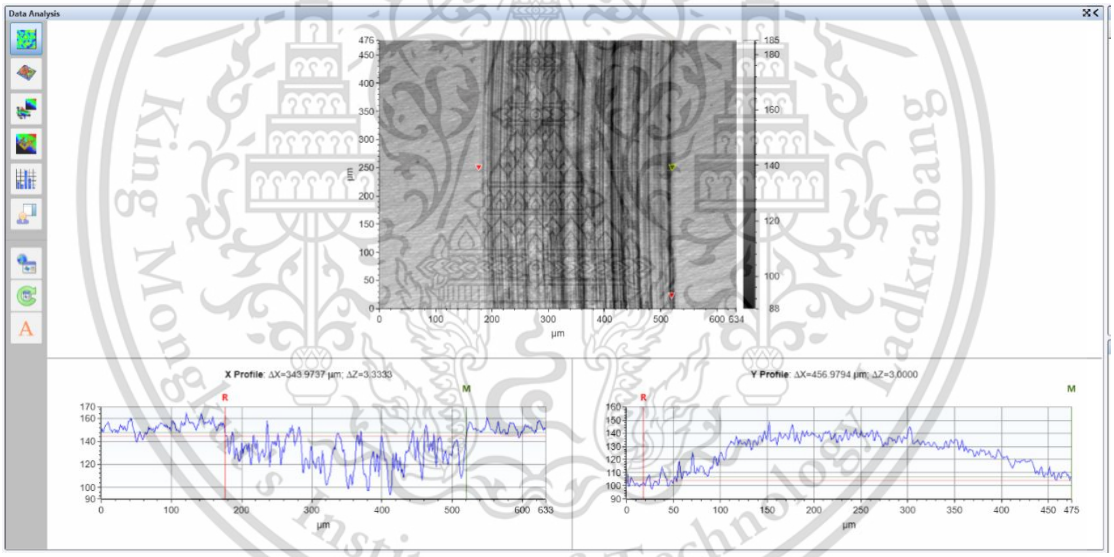

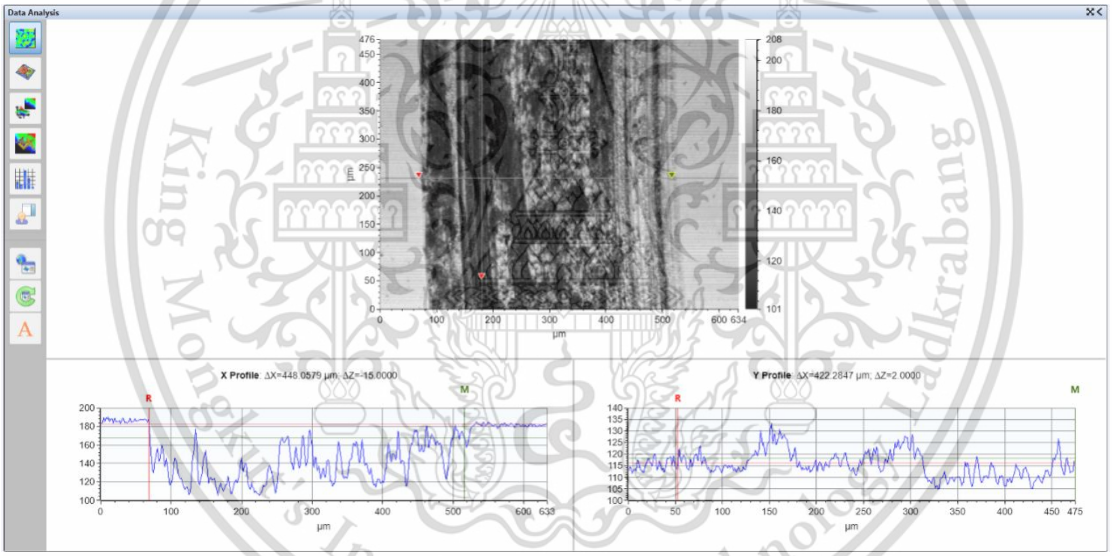

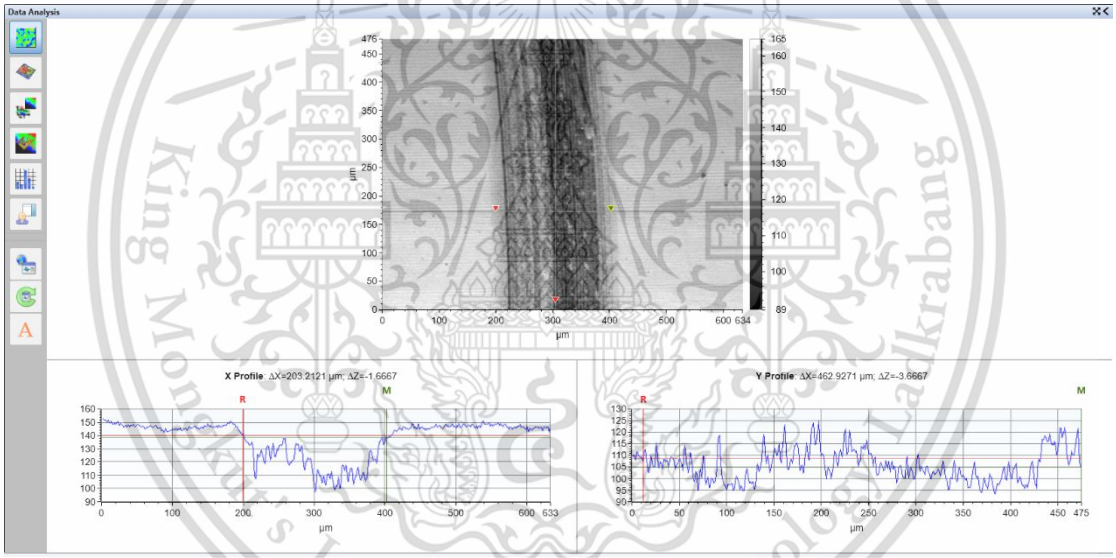

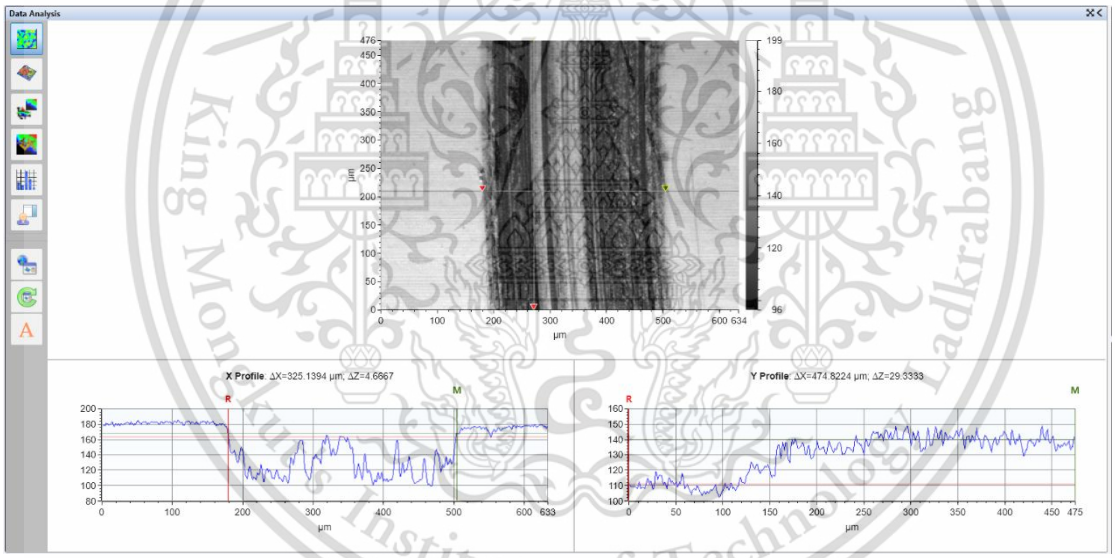

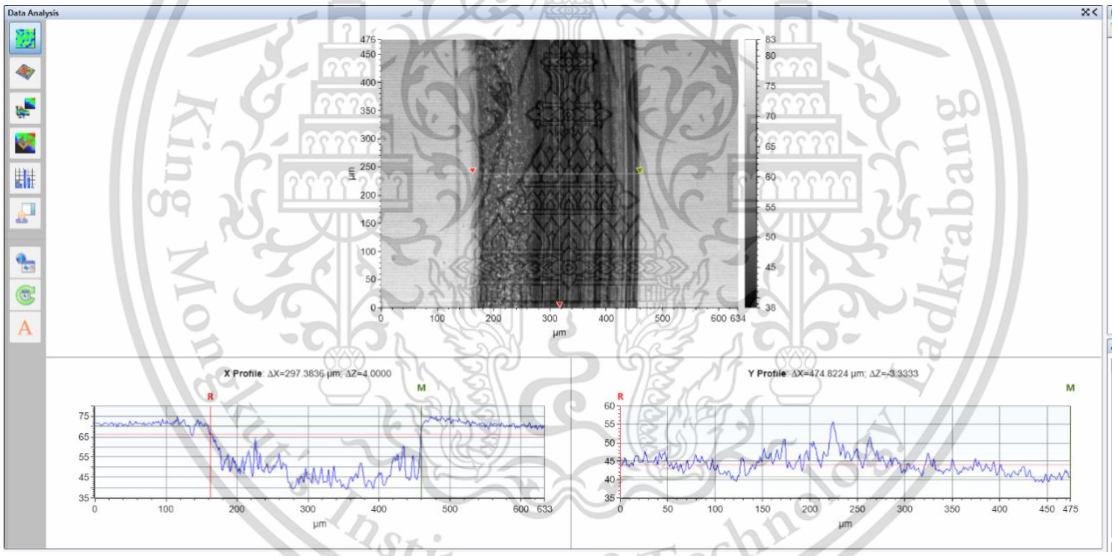

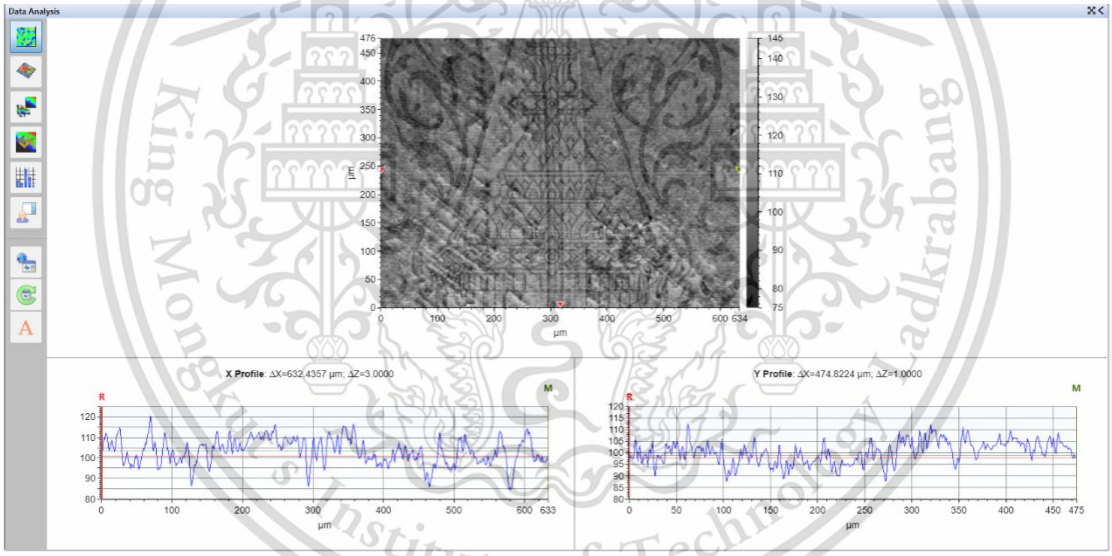

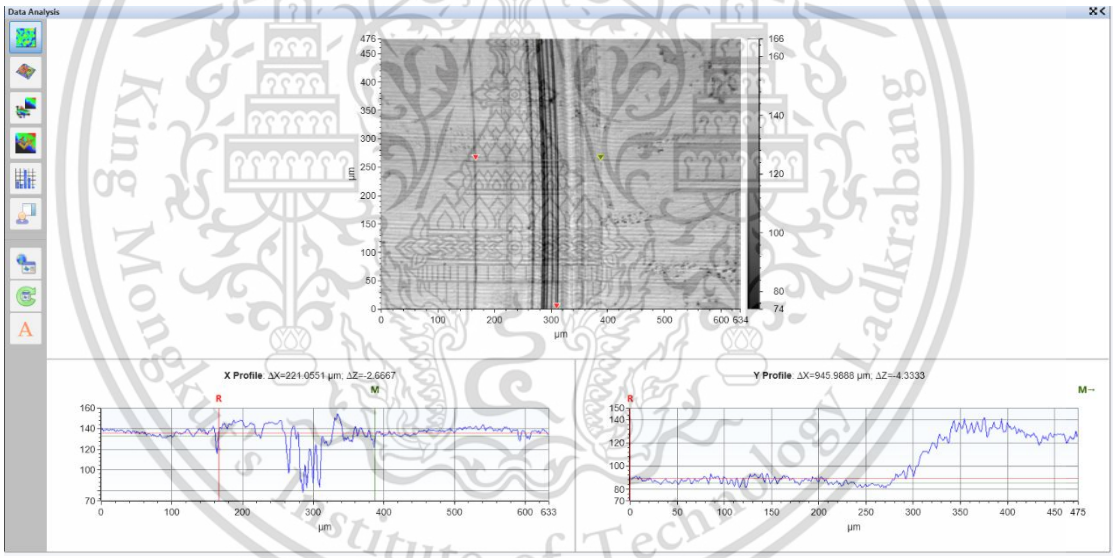

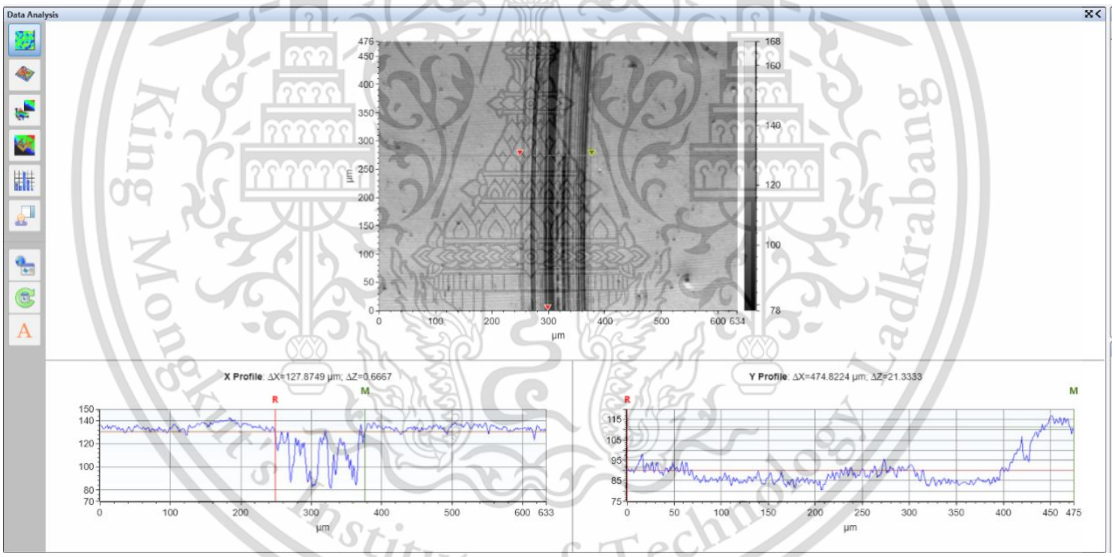

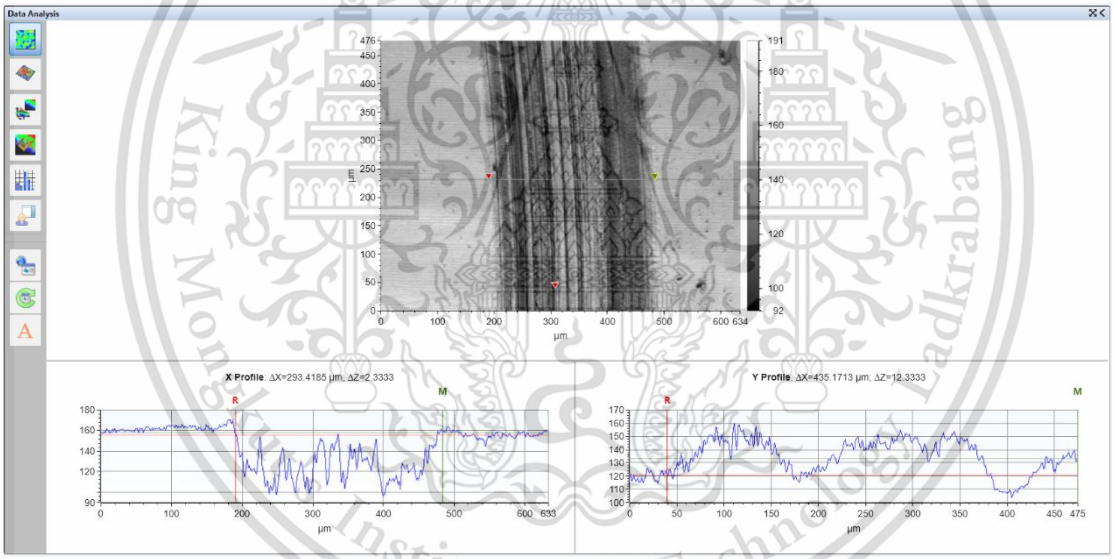

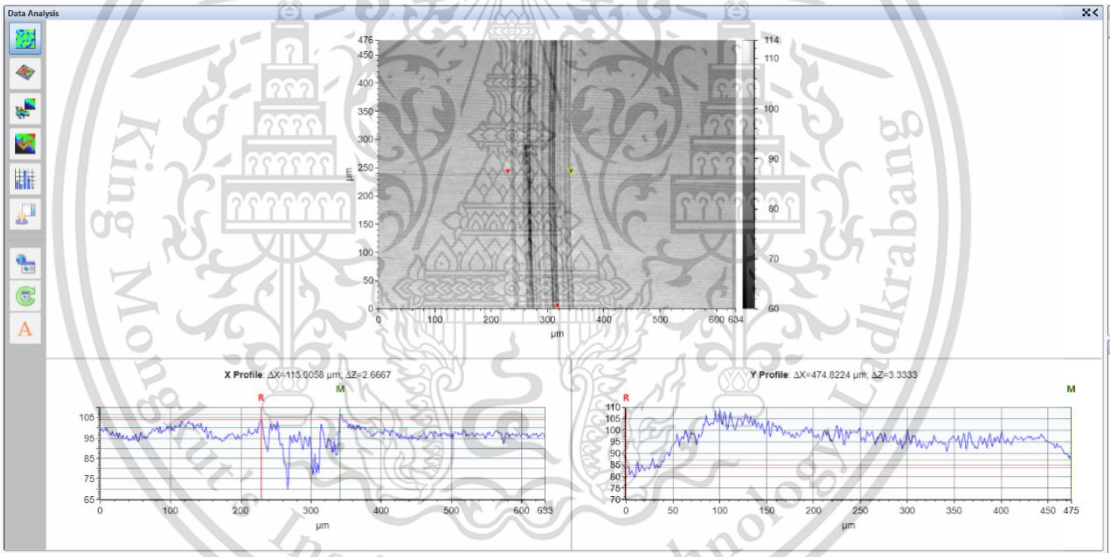

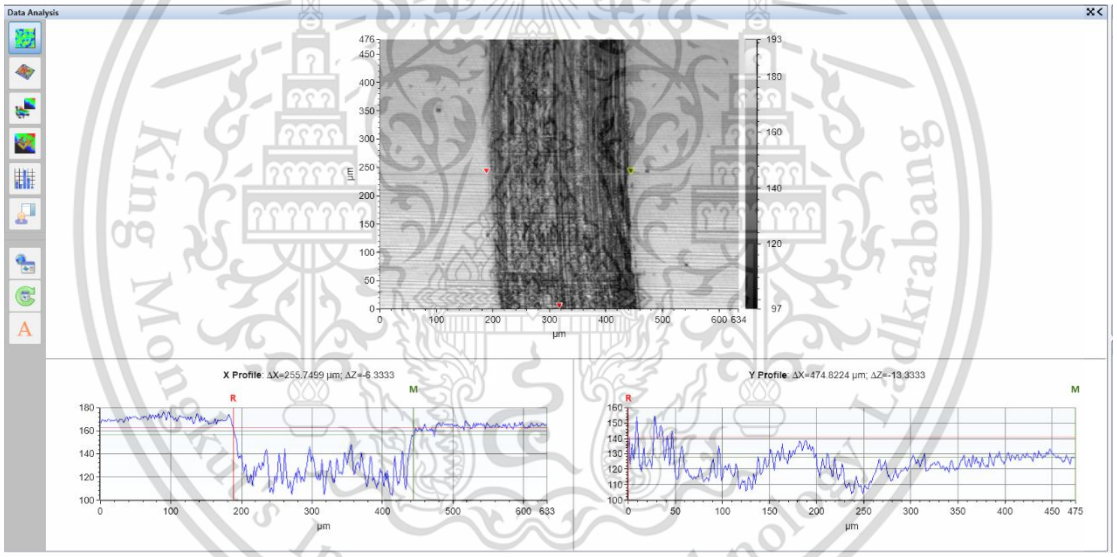

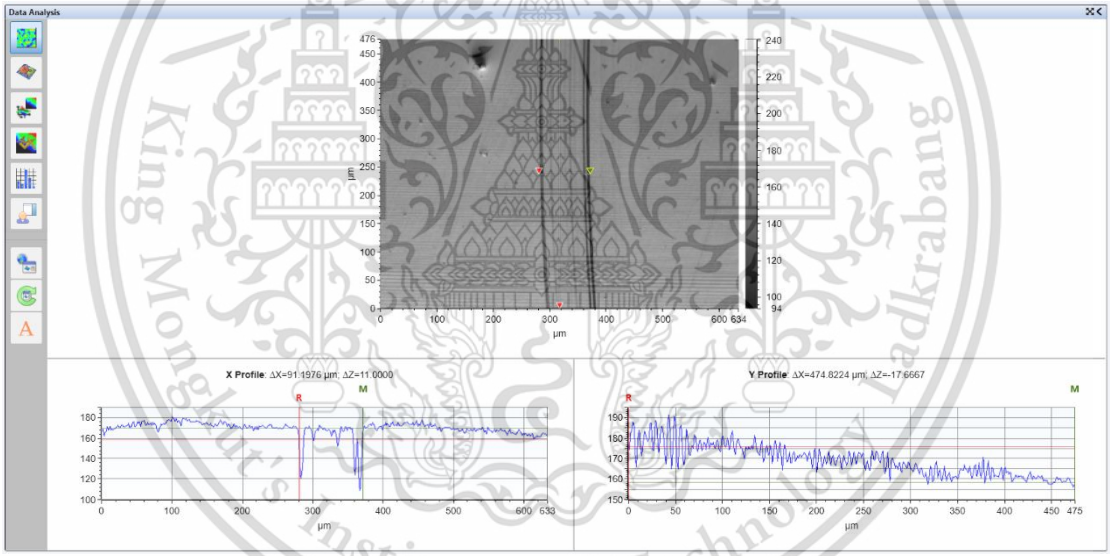

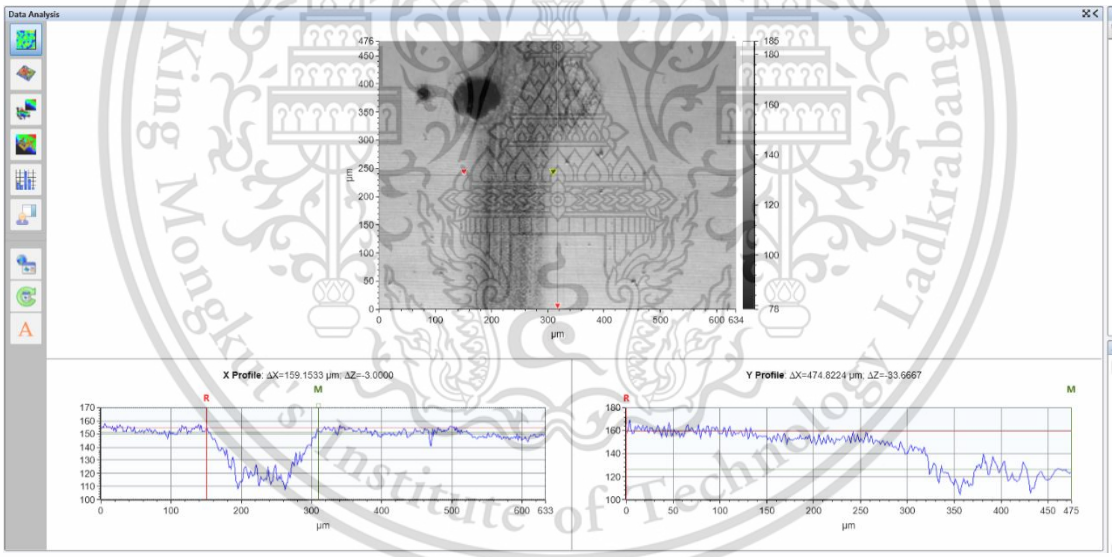

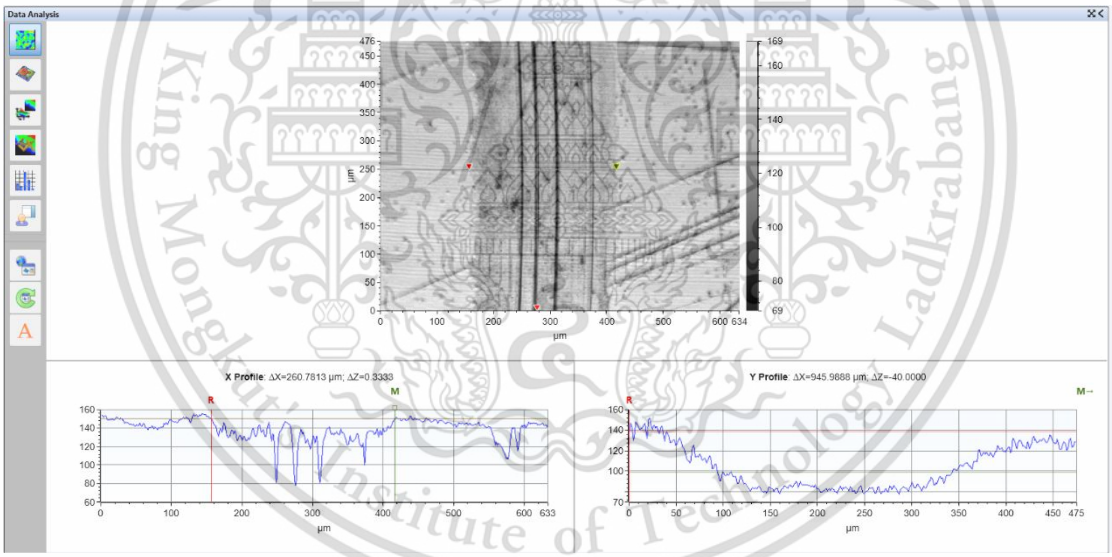

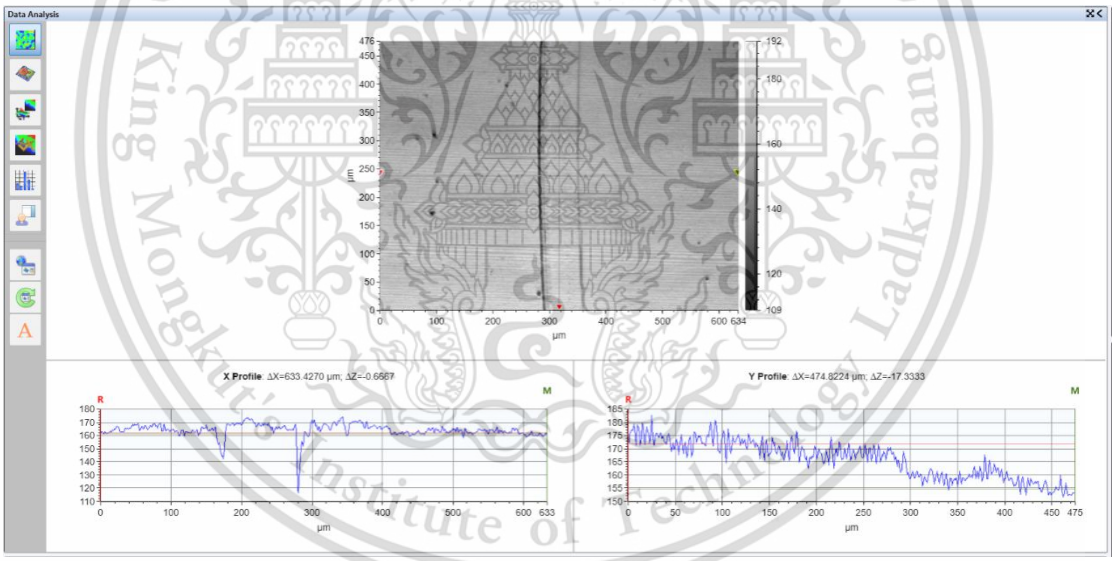

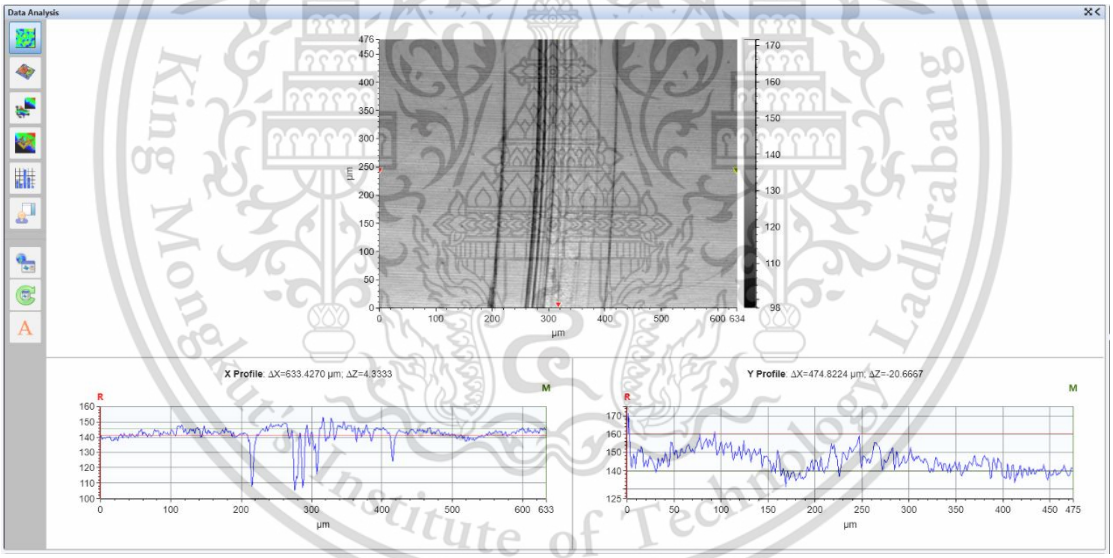

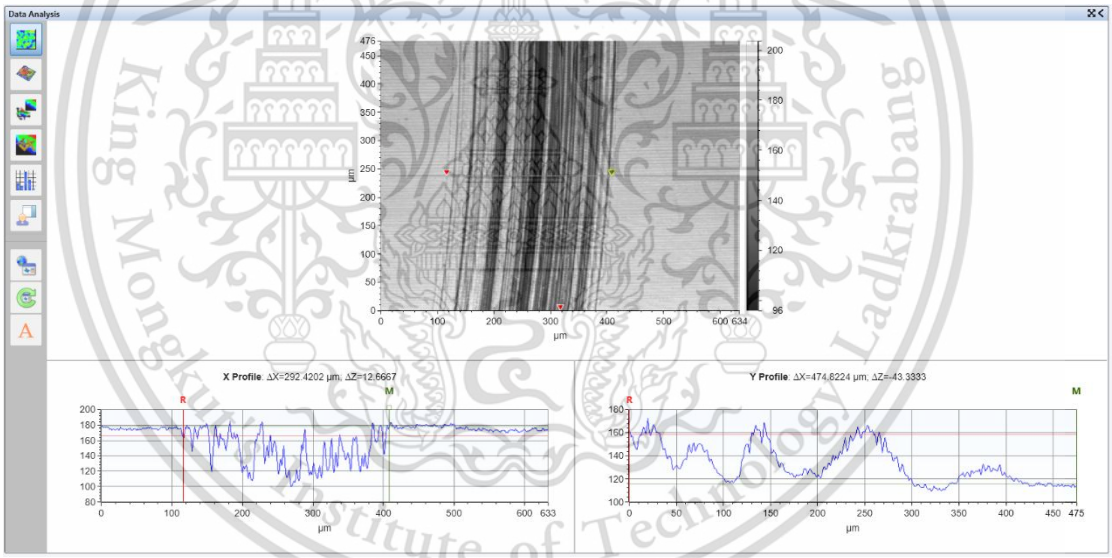

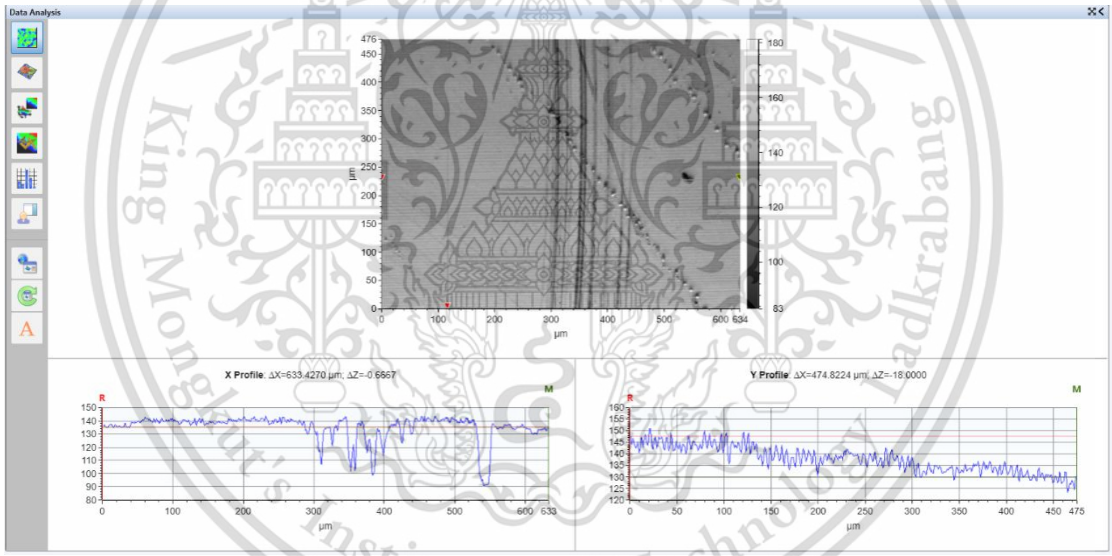

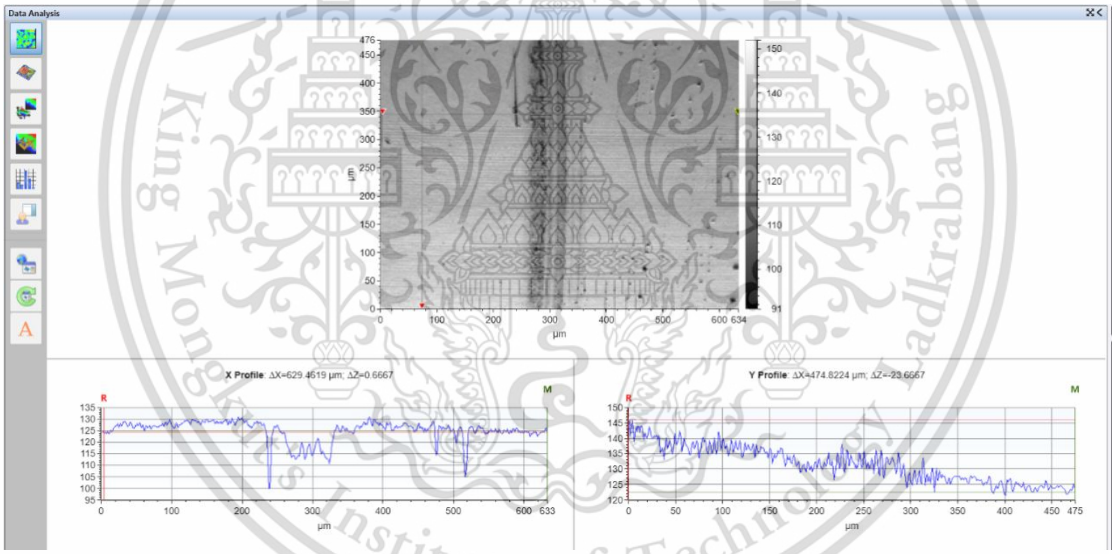

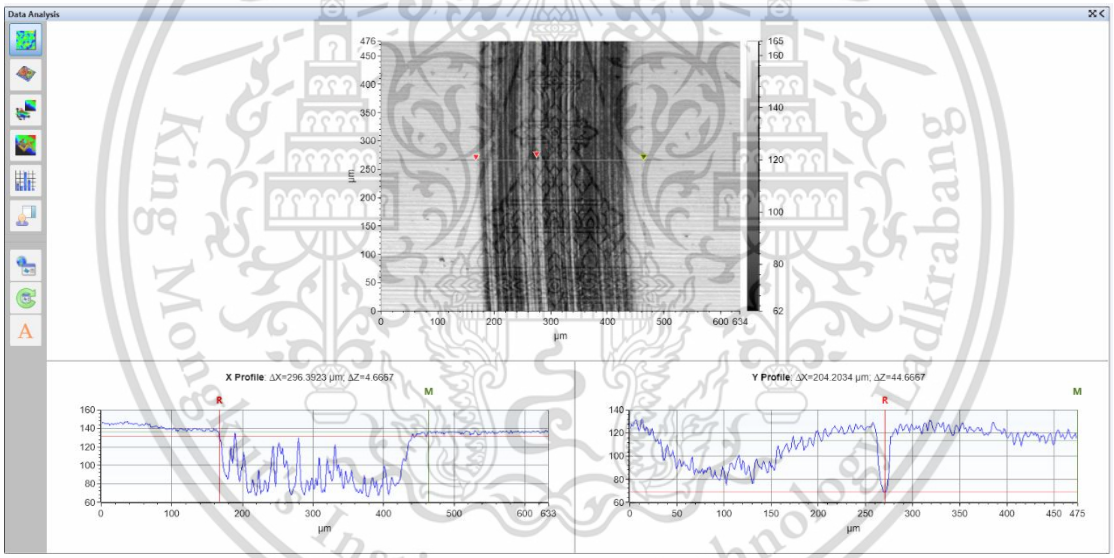

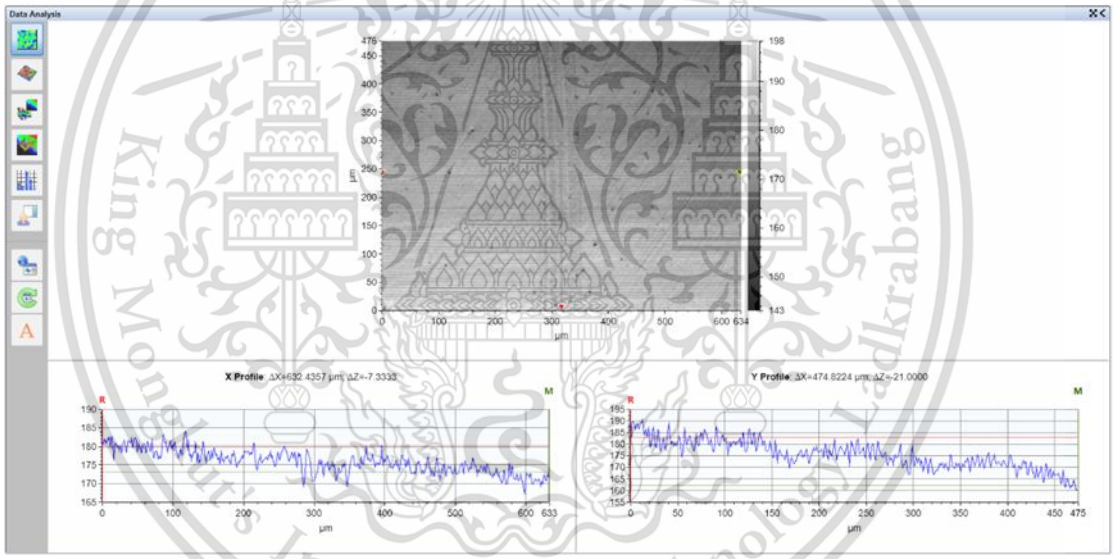

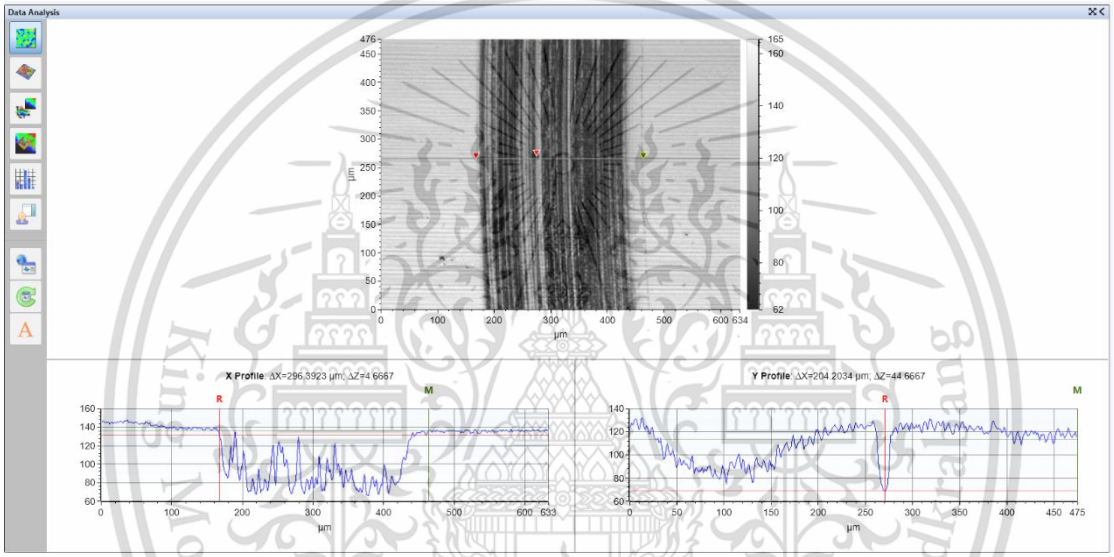

**APPENDIX C**

**PUBLICATION**

The 14th International Conference on Automotive Engineering
April 2-3, 2018,
Challenger, Impact, Muang Thong Thani, Bangkok, Thailand

TSAE-18IC-0701

# Effect of Operating Temperature on Wear Performance of Lubricant

**Kritin Chonvasin[1], Manida Tongroon[2], Preechar Karin[1], Katsunori Hanamura[3] and Chi-na Benyajati[2,*]**

[1] Automotive Engineering, International College, King Mongkut's Institute of Technology Ladkrabang, Chalongkrung Rd., Ladkrabang, Bangkok, 10520, Thailand

[2] National Metal and Materials Technology Center, 114 Thailand Science Park, Phahonyothin Rd., Khlong Nueng, Khlong Luang, Pathum thani, 12120, Thailand

[3] Department of Mechanical Engineering, Tokyo Institute of Technology, Japan

*Corresponding Author: chinab@mtec.or.th, Tel: 02-564-6500, Fax: 02-564-6370

**Abstract**. Lubricant oils generally contain an anti-wear additive that would form into a protective film to protect the rubbed surfaces, resulting in wear reduction. The performance of anti-wear additive has been found to improve when a high operating temperature was applied to the lubricant. This research focused on the effect of operating temperature on the tribological performance and the bulk properties of lubricants with-and-without ZDDP anti-wear additive. In this work, lubricated-sliding wear tests were conducted with different lubricant samples using a tribometer with a ball-on-disc configuration. The test model lubricants were base on, Group II mineral base oil and synthetic PAO6. Furthermore, in order to take into account real engine conditions, test samples were tested with an applied load of 11.71N for AISI 52100 disc specimens and 12.07 N for AISI 1050 disc specimens which corresponded to a maximum Hertzian contact pressure of 0.95 GPa respectively with operating temperatures of 25, 80, 100 °C. The effect of operating temperature on wear performance and post-test properties of lubricants were discussed.

## 1. Introduction

Zinc Dialkyldithiophosphates (ZDDP) is an anti-wear additive that would form a protective film to protect the rubbed surfaces, resulting in wear reduction [1, 2]. The performance of anti-wear additive has been found to improve when a high operating temperature was applied to the lubricant. The effect of operating temperature on wear performance of ZDDP has been studied by many researchers. Fujita [1] studied the effect of rubbing condition on the formation of ZDDP film over a range of operating temperatures. The results showed that a ZDDP thermal film thickness only developed and grew at operating temperatures of 110°C and above this operating temperature but that ZDDP tribofilm was generated on rubbed surfaces even at room temperature. Parsaeian [3] studied the effect of water at

## AUTHOR BIOGRAPHY

| | |
|---|---|
| AUTHOR: | **MR. KRITIN CHONVASIN** |
| DEGREE: | Master of Engineering |
| DATE OF GRADUATION: | 31th July 2019 |
| DATE OF BIRTH: | 21th August1992 |
| PLACE OF BIRTH: | Bangkok,Thailand |

### Undergraduate and Graduate Education:

Master of Engineering inAutomotive Engineering,

King Mongkut's Institute of Technology Ladkrabang, Bangkok, 2019

Bachelor's degree in mechanical engineering,

King Mongkut's Institute of Technology Ladkrabang, Bangkok, 2015

**Major:**Automotive Engineering

### Presentations and Publications:

[1] Kritin Chonvasin, Manida Tongroon, Preechar Karin, Katsunori Hanamura, and Chi-na Benyajati "Effect of Operating Temperature on Wear Performance of Lubricant", 2018, The 14th ICAE International Conference on Automotive Engineering, April 2-3, 2018, Challenger, Impact,Muang Thong Thani, Bangkok, Thailand.